DISSERTATION

STRUCTURAL AND BIOCHEMICAL INSIGHTS INTO THE ROLE OF THE NUCLEOSOME IN TRANSCRIPTIONAL ACTIVATION IN YEAST

Submitted by

Cindy LuAnn Holland White

Department of Biochemistry and Molecular Biology

In partial fulfillment of the requirements

for the Degree of Doctor of Philosophy

Colorado State University

Fort Collins, CO

Fall 2003

COLORADO STATE UNIVERSITY

October 3, 2003

WE HEREBY RECOMMEND THAT THE DISSERTATION PREPARED UNDER OUR SUPERVISION BY CINDY LUANN HOLLAND WHITE ENTITLED "STRUCTURAL AND BIOCHEMICAL INSIGHTS INTO THE ROLE OF THE NUCLEOSOME IN TRANSCRIPTIONAL ACTIVATION IN YEAST" BE ACCEPTED AS FULFILLING IN PART THE REQUIREMENT FOR THE DEGREE OF DOCTOR OF PHILOSOPHY.

Committee on Graduate Work

(Laurie A. Stargell)

(Olve Peersen)

(Paul J. Laybourn)

(Oren P. Anderson)

(Karolin Luger)
Advisor

(Norm P. Curthroys)
Department Head

ABSTRACT OF DISSERTATION

STRUCTURAL AND BIOCHEMICAL INSIGHTS INTO THE ROLE OF THE NUCLEOSOME IN TRANSCRIPTIONAL ACTIVATION IN YEAST

In vivo transcription occurs in the context of highly compacted chromatin. The fundamental repeating element in chromatin and the primary level of DNA compaction is the nucleosome core particle, which comprises 147 base pairs of DNA wrapped around a histone octamer. The extreme compaction of DNA found in the confines of the nucleus has profound implications for our understanding of transcription regulation, since chromatin must allow transcriptional access to specific regions of the DNA molecule while keeping the remaining regions repressed. Approaching these problems by using yeast as a model organism, we determined the three-dimensional structures of the macromolecular complexes in question, and studied nucleosomal dynamics using biochemical and biophysical methods. First, we solved the crystal structure of the nucleosome core particle from the yeast *Saccharomyces cerevisiae*. Compared to higher eukayotes, the structure of the yeast nucleosome suggests a less stable structure, as well as a mechanism for looser nucleosomal compaction, since yeast nucleosome crystals demonstrate an altered packing within the crystal lattice. Biophysical analysis of the stability of yeast nucleosomes confirmed that they are less stable compared to those of *Xenopus laevis*. We then investigated the role of poly (dA·dT) DNA sequence elements, found in many yeast promoter regions, on transcriptional activation within a nucleosome

context. Our results suggest that these rigid DNA tracts form nucleosomes with the same affinity as a strong positioning DNA sequence, and the formed nucleosome is not destabilized by the presence of the poly (dA·dT) tract. We also find that these elements create areas of greater nucleosomal DNA accessibility, which leads to a more efficient binding of a transcription factor. Finally, we show that a transcription factor can bind directly to nucleosomal DNA near the dyad causing partial dissociation of the DNA ends, but does not bring about the dissociation of the underlying histone octamer. Taken together, these studies shed light on the interactions between transcription factors and nucleosomes, and thus allow us to better analyze the interplay between chromatin packaging and transcriptional regulation at the molecular level.

Cindy LuAnn Holland White
Department of Biochemistry and Molecular Biology
Colorado State University
Fort Collins, CO 80523
Fall 2003

ACKNOWLEDGEMENTS

I do not believe that anyone could be to obtain a Doctoral degree without having been truly blessed in this life, and such is the case with me. I first and foremost thank my God and Creator for the tremendous blessings he has given to me. Much thanks, gratitude, and praise goes out to my advisor, Dr. Karolin Luger. Her help and guidance throughout these past five years is greatly appreciated. She was always very willing and able to help me in any way she could, and her love of science and motivation to do great scientific research motivates each and every person in her lab. She has taught me a great deal, and I appreciate her time and efforts during my graduate career. I would also like to thank my committee members: Dr. Laurie Stargell, Dr. Paul Laybourn, Dr. Robert Woody, Dr. Olve Peersen, and Dr. Oren Anderson. Their office doors were always open in me, and their help and suggestions were vital to the completion of my dissertation work. Next, I would like to express my sincerest thanks to the members of the Luger lab. They were absolutely wonderful people to work with, and I could not have done this without their help and encouragement. I will miss them all, and wish each one of them of great and bright future. Finally, I wish to thank my family whose support and love has made me what I am today. I thank my Grandmother, Eva Mae Bray, for all her words of wisdom, encouragement, and love throughout the past twenty seven years. My great love and gratitude also goes out to my husband, Jason White. During the time I have been in graduate school, he has been my very best friend and has helped me through the stress and trials of getting my Ph.D. I am forever indebted to him for his unfailing support. Last but certainly not least, I thank my parents, Charles and Ann Holland. No words can

express what a profound impact their love and care have had on my life. Ever since I first began school, they have dedicated endless hours to help me succeed, and I certainly would not have achieved what I have today without having had two such wonderful parents to guide me through life. My father first instilled in me a love for science, and because of his endless love, encouragement, and belief in me, I dedicate this dissertation to him – *We climbed that mountain!*

TABLE OF CONTENTS

Chapter 1

Review of the Literature

1.1 Chromatin Structure and Function

The nucleosome core particle has been the subject of a vast amount of research from the time that it was first proposed that the basis of chromatin structure was a protein octamer compacting approximately 150 base pairs of DNA (Bram, 1975). Initially, the nucleosome was only seen as a way in which a cell compacted DNA into the nucleus. It was viewed as a very static structure that merely got in the way of nuclear functions such as transcription, repair and replication. However, in recent years, our growing knowledge of chromatin structure and function has allowed us to understand what an important role the histones actually play in a vast number of cellular processes. Chromatin is now viewed as a very dynamic and ever changing entity that plays a key regulatory role in gene expression and cell cycle progression (Vaquero, 2003).

1.1a Nucleosome structure

In the average eukaryotic cell, the DNA is nearly 10^7 times the size of the cell. Thus, DNA must be greatly compacted in order to fit into the confines of the cell nucleus. The cell accomplishes this compaction in the form of chromatin, the basic DNA-protein complex in eukaryotic cells. The basic repeating unit of chromatin is the nucleosome core particle. In this first level of chromatin structure, DNA is compacted five-fold by wrapping 146 base pairs of DNA 1.65 times around a protein octamer. The octamer is composed of two copies each of the four different histone proteins H2A, H2B, H3, and H4. The nucleosome core particle is held together by interactions between the phosphodiester backbone of the DNA and the histone proteins within the octamer.

At the amino acid sequence level, histone proteins are some of the most invariant proteins known, but they are also a very diverse set of proteins. Many isoforms and variants exist. However, all seem to form the same basic structure. Histones have a central domain that forms a histone fold motif as well as an extended tail domain that is very basic and highly modified (Wolffe, 1998). The histone fold is involved both in histone-histone interactions within the nucleosomal core and in histone-DNA interactions. The histone fold exhibits a long central α-helix that is flanked on both sides by shorter helices (Fig. 1.1A) (Arents and Moudrianakis, 1995). The loops between the helices contain residues that interact with the DNA phosphodiester backbone. The H2A/H2B and H3/H4 histone proteins form pairs which make tight dimers that each organize 30 base pairs of DNA, using paired loops or paired helices as DNA binding motifs (Luger and Richmond, 1998). In general, the superhelix path of the DNA is

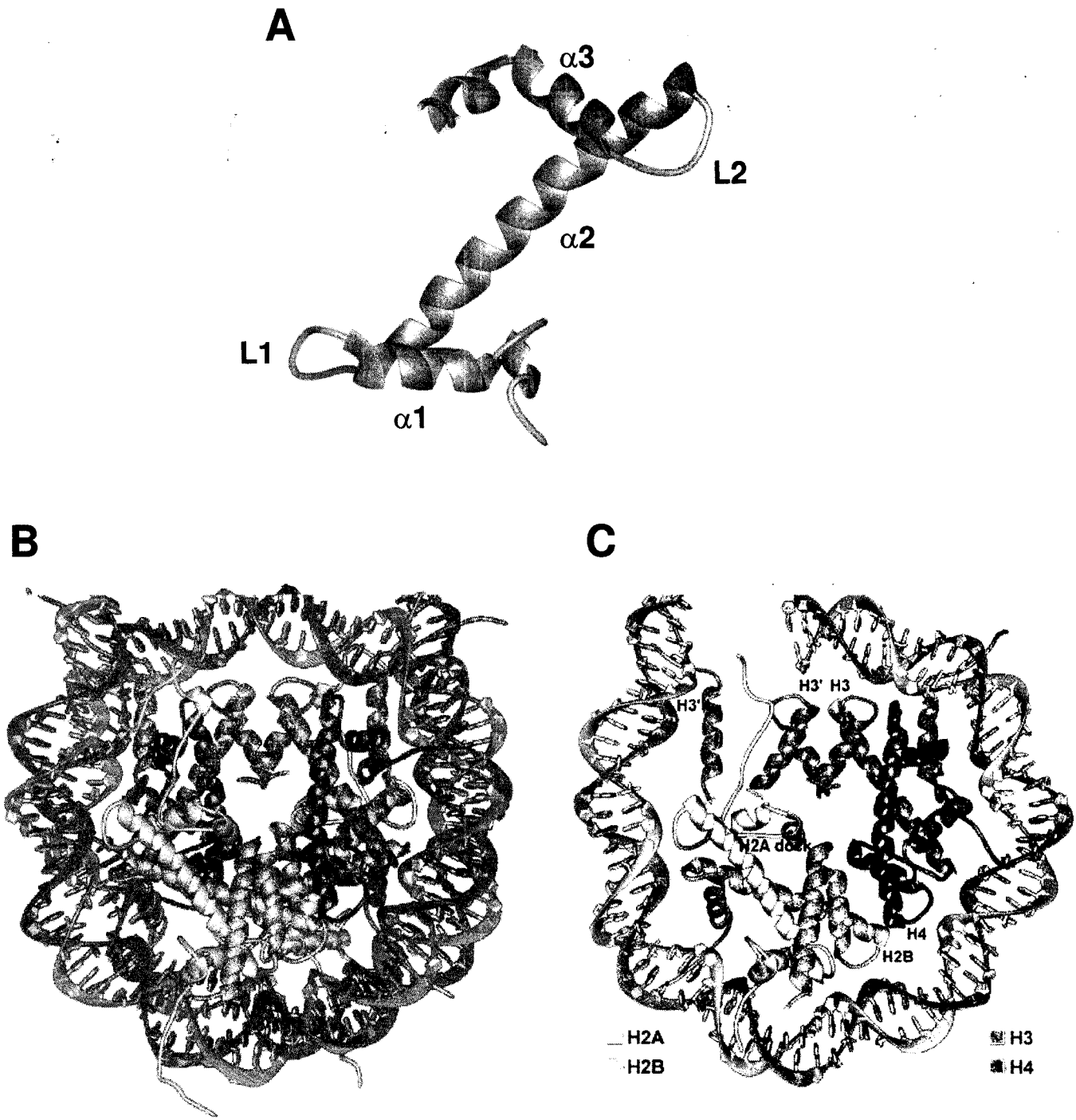

Figure 1.1. The structure of the Nucleosome Core Particle.

(A) The structure of the histone fold of the histone proteins. Histone H2A is shown with the tail regions deleted. **(B)** The crystal structure of the nucleosome core particle from *Xenopus laevis* (Luger et al., 1997) . The structure depicts two copies each of the four histone proteins (the histone octamer) and 146 bp of DNA. The histones are colored as shown in (C) and the DNA double helix is shown in green and brown. **(C)** Diagram of 73 bp of DNA of the nucleosome core particle and associated proteins. Protein-protein and protein-DNA interactions are clearly seen. Each histone is labeled with the colors shown, and the DNA is colored as in (B).

significantly distorted as it travels around the histone core, owing to the local structure of the histone DNA-binding surface. The DNA outwardly buckles as it contacts the underlying histone structures of the H2A/H2B dimers and H3/H4 tetramer. The high-resolution crystal structure of the nucleosome core particle (Fig. 1.1B) shows that protein contacts are made with the inward facing DNA minor groove every 10 base pairs. Protein-DNA interactions include electrostatic interactions, hydrogen bonding, and hydrophobic contacts with the DNA phosphates and deoxyribose sugars (Luger et al., 1997). In order to accommodate any DNA sequence, no contacts are made with the DNA bases. The DNA locations most distant from the superhelical axis show the most bending. The ten base pair segment at each terminus is essentially straight (Richmond, 2003).

The histone tails protrude from the nucleosomal core by passing through the DNA superhelix as well as protruding from the surface of the octamer face. While the H2B and H3 histone tails pass through four of the DNA minor grooves, a significant proportion of the major groove is still accessible as potential binding sites for transcription and replication factors (Luger et al., 1997). The histone tails appear disordered in the crystal structure, although data suggests that the H3 and H4 tails adopt a structured conformation within the nucleosome (Banères et al., 1997). Because the histone tails extend from the core particle, the tails are readily available for modifications as well as interacting with other nucleosomes to function in higher order packing. Tail modifications could promote or disrupt nucleosome-nucleosome contacts, which could lead to the regulation of the transcriptional accessibility of the DNA. Indeed, histone tails are essential for the formation of higher-order chromatin compaction (reviewed in

(Hansen, 2002)). In the crystal structure of the nucleosome core particle from *Xenopus laevis*, the H4 N-terminal tail makes a critical crystal contact with an acidic patch formed on the surface of the H2A/H2B dimer (Luger et al., 1997). It has been speculated that this interaction may mimic interactions in chromatin compaction *in vivo*. The positively charged histone tails can partially neutralize the negatively charged linker DNA, which could also facilitate higher-order nucleosomal packing. Indeed, the histone tails have been shown to be associated with linker DNA (Angelov et al., 2001) as well as with the DNA within a neighboring nucleosome (Zheng and Hayes, 2003). A recent study showed that fully compacted nucleosomal arrays could not be obtained upon deletion of the H4 N-terminal tail (Dorigo, 2003). These results point to a critical role of the histone tails in nucleosomal compaction.

The DNA that extends from between consecutive nucleosome core particles is known as "linker" DNA. Linker DNA length can vary from 10 base pairs to 80 base pairs. In yeast, the average linker length is 10 base pairs, whereas the average in metazoans is 30 to 50 base pairs (Wolffe, 1998). However, linker length can vary depending upon the DNA sequence, cell type, or the presence of regulatory proteins. Thus, even though the histone octamer can accommodate any DNA sequence, nucleosomes often appear at preferred positions along the DNA as governed by the bending constraints of various DNA sequences, as well as by DNA-binding proteins. Nucleosomal positioning can restrict or enhance protein access to gene promoter regions and regulatory elements. Nucleosome positioning can also serve to form more compacted heterochromatin (Eissenberg JC, 2003).

Higher-order chromatin structure is still not well understood. The next level of chromatin compaction beyond the nucleosome core particle is the 30 nm fiber as observed in electron micrographs (Gerchman and Ramakrishnan, 1987). The current most widely accepted model is that the 30-nm fiber is a supercoil of nucleosome core particles also containing the linker DNA and histone H1. Histone H1 is called the "linker histone" because it is associated with the linker DNA. It also binds the two DNA strands at the nucleosomal dyad. In addition to the histone tails, histone H1 has also been shown to facilitate the folding of nucleosomes into the 30 nm fiber and stabilize the compacted structure (Carruthers et al., 1998). Chromatin compaction beyond the 30-nm fiber is relatively less defined. It is thought that loops of 30 nm fibers attach to some sort of scaffolding structure and these structures are then additionally compacted to make the canonical metaphase chromosome. In light of the recent studies that have developed a self-assembly system for nucleosome arrays (Dorigo, 2003; Hansen et al., 1989), future research will surely shed light on these hypotheses and give us a better understanding of higher-order chromatin structure.

1.1b Chromatin and transcription

In vivo, transcription occurs in the context of highly compacted DNA in the form of chromatin. Consequently, this packaging of DNA into chromatin limits protein factor access to cellular genes. Thus, transcription is intimately linked to chromatin. Nucleosomes and higher order chromatin compaction serve an important regulatory role in many nuclear processes. It has been shown that nucleosomes are maintained on the DNA during processes that require DNA access, such as transcription and replication (review in (Wolffe, 1998). However, the packaging of DNA into nucleosomes can act to

repress the initiation of transcription. This transcriptional repression is not merely blockage of access to the DNA by other protein factors involved in the transcription process. The dynamic nature of chromatin works in conjunction with other factors to regulate transcription and other nuclear processes. Two classes of factors exist which work with chromatin to regulate the access of DNA. The first class is ATP-dependent chromatin remodeling factors. The second class comprises factors that covalently modify histone residues, mainly within the histone tails. A discussion of both classes is given below.

Depending on the transcription factor and DNA sequence context, several scenarios are possible for the encounter between DNA binding factors and chromatin. Figure 1.2 gives four of these scenarios. As stated above, nucleosomes are often positioned in distinct regions on DNA promoters. Preset nucleosome structures may provide the architecture for transcription factor access by positioning nucleosomes in such a way as to allow cis-acting DNA-binding sites to be non-nucleosomal (Fig. 1.2A). Preset elements could also position nucleosomes within factor binding regions in which the nucleosome enhances the direct binding of the transcriptional machinery (Fig. 1.2B). However, many DNA binding regions are likely to contain randomly positioned nucleosomes. In these cases, transient exposure of the regulatory regions by nucleosome sliding may allow factor binding (Fig 1.2C) (Polach and Widom, 1996). Finally, many promoter regions are packaged into nucleosomes that are "remodeled" by chromatin remodeling factors that allow facile access of activators (Fig. 1.2D) (Varga-Weisz and Becker, 1998).

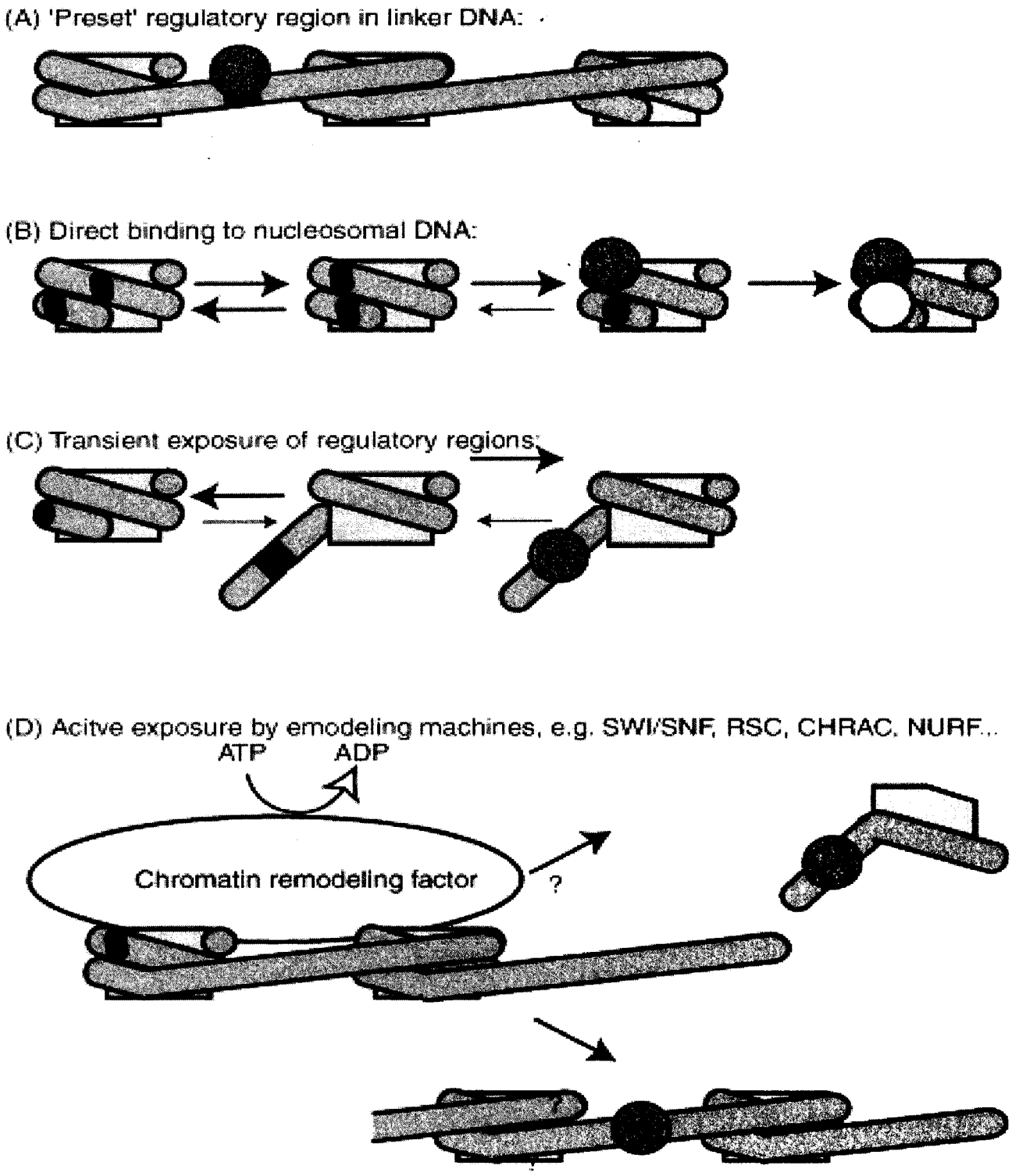

Figure 1.2. Mechanisms for transcription in a chromatin context.

Schematics show different models for the binding of transcription factors within a chromatin context. Transcription factors are depicted by red or yellow circles, the DNA is shown in blue, and the histone octamer is designated by green rectangles. Binding sites are shown on the DNA with black boxes.

Most chromatin remodeling factors act to change the chromatin state in such a way that leads to the "opening up" of DNA sites for transcriptional access. Such an example is the SWI/SNF complex in yeast, which uses energy from ATP-hydrolysis to disrupt nucleosomes to allow the transcriptional machinery to bind to promoter regions (Imbalzano et al., 1994). However, some remodeling factors, such as the NuRD complex, act to form an even more repressive chromatin state (Zhang et al., 1998). The mechanism by which factors alter chromatin is not well understood. Some evidence has shown that ATP-dependent chromatin remodeling complexes, such as RSC, act to transfer the entire histone octamer to another region along the DNA molecule (Lorch et al., 1999). Other experiments have suggested that just the H2A/H2B dimers are repositioned in the histone octamer, creating a destabilized nucleosome and allowing transcriptional activation (Lee, 1999). Many remodeling complexes have been shown to disrupt DNA-histone contacts, demonstrated by the fact that there is an increased accessibility of the DNA to nuclease digestion (Cote et al., 1994). There are two current models for this phenomenon. The first is the hypothesis that remodeling factors promote the sliding of the histone octamer along the DNA, mediated by the simultaneous breaking and annealing of DNA-histone contacts. The ISWI family of ATPases have demonstrated such movement of the histone octamer to adjacent positions of the DNA (Langst et al., 1999). The second hypothesis proposes that remodeling factors cause a loop to be formed in the DNA that protrudes from the face of the histone octamer which would allow the binding of transcriptional machinery (Bazett-Jones et al., 1999). This loop could then be propagated through the nucleosome that would induce mobilization of the nucleosome along the DNA. Whatever the mechanism, nucleosomal changes

induced by chromatin remodeling complexes will probably be subtle, since the loss of a single DNA-histone contact within the nucleosome can overcome defects in the SWI/SNF complex (Kruger et al., 1995), (Muthurjan et al., manuscript submitted).

The second class of factors that regulate transcriptional activation within chromatin act to covalently modify specific residues within the histone proteins. These factors create many different modifications that cause varied effects. Numerous histone tail modifications can exist at the same time, thus making the tail domains a very complex marker for transcriptional activation and repression (reviewed in (Jenuwein and Allis, 2001)). Perhaps the most studied histone tail modification is acetylation, induced by histone acetyltransferase (HAT) activity. HATs transfer an acetyl group from acetyl coenzyme A to tail lysine residues, leading to activated transcription in many, but not all, cases (reviewed in (Grunstein, 1997)). In yeast, transcription is all but eliminated when the lysine residues in some of the histone tails are substituted with arginine residues, which cannot be acetylated (Kuo et al., 1996). Histone tail acetylation results in the neutralization of the positively charged histone tails, thus reducing higher-order folding. In heterochromatin, it has been shown that the histone tails are unacetylated at important lysine residues (Jeppesen and Turner, 1993). In addition, other protein complexes bind to acetylated histone tails and serve to regulate the recruitment of the transcriptional machinery or heterochromatic factors (Deckert and Struhl, 2001). These findings have led to the proposal of a complex histone code, which states that specific tail modifications signal specific cellular events (Rice, 2001).

Conversely, deacetylation of histone tails leads to repression. It has been demonstrated that deacetylation produces a more compacted chromatin structure which

represses the binding of transcription and replication/repair complexes (Wade, 2001). A histone deacetylase in yeast, Rpd3, reverses the action of histone acetyltransferases. Histone deacetylases can be recruited to chromatin by other factors, or they can be complexed to DNA-binding proteins (Struhl, 1998). Histone deacetylases have widespread applications and have been functionally linked to transcriptional repression, DNA repair, recombination, cell cycle progression, DNA replication, chromosome stability, and silencing in telomeres and centromeres (reviewed in (Vaquero, 2003).

Another important histone tail modification is methylation. Methylation occurs by a transfer of a methyl group from S-adenosyl-L-methionine to either arginine or lysine residues on the histone tails as well as within the octamer core. Mono- , di- , or tri-methylation occurs *in vivo* and has varied effects (Zhang, 2001). Only H3 and H4 have been found to be methylated so far. Histone methylation has a large role in transcriptional repression and gene silencing, seemingly acting to form a more compacted and repressive chromatin state by leading to the formation of heterochromatin (Tachibana et al., 2002). However, recent studies have shown that histone methylation can function in transcriptional activation as well (Bannister et al., 2002).

Histone ubiquitination is arising as an important modification involved in transcriptional regulation. This modification occurs when a lysine residue is covalently modified by conjugation to the 76-amino acid protein ubiquitin. Mono- or polyubiquitination can occur and serve varied roles. Even though polyubiquitination of many proteins mark them for degradation, this is not observed for histones, as monoubiquitination of histone proteins in chromatin leads to transcriptional activation (Jason et al., 2002). Even though uH2A is the most abundant species in higher

eukaryotes, lysine 123 in histone H2B is readily ubiquitinated by Rad6 in yeast (Robzyk et al., 2000). It has been shown that ubiquitination of H2A and H2B can destabilize the nucleosome core particle, causing it to dissociate at a lower salt concentration than non-ubiquitinated H2A and H2B (Li et al., 1993). Histone ubiquitination has also been shown to be linked to other covalent modifications such as acetylation and methylation (Seigneurin-Berny et al., 2001; Sun and Allis, 2002). One hypothesis is that the addition of this very large and bulky group onto histone proteins could inhibit nucleosome-nucleosome interactions and thus lead to activated transcription.

Several other histone modifications have been documented. Phosphorylation of serine residues occurs in all four histone proteins. Phosphorylation mainly has been shown to function in nucleosomal compaction leading to chromosome condensation and segregation (Guo et al., 1995). In addition, histone phosphorylation has been linked to transcriptional activation (Cheung et al., 2000). ADP-ribosylation involves the transfer of ADP-ribose molecules to glutamic acids or argine residues. ADP-ribosylation has been directly linked to DNA repair, as well as other cellular processes (Chiarugi, 2002). It seems to function in conjunction with other histone modifications. Experiments have shown that ADP-ribosylation of histones functions in transcriptional silencing, while others have found that the bulky modification leads to a more open chromatin structure leading to activated transcription (Huletsky et al., 1989; Tanny et al., 1999). Finally, all four histones have been found to be biotinylated by the transfer of biotin to lysine residues. The role of this modification is unknown, but some studies point to cell cycle progression, transcription regulation, and chromatin stability (Hymes and Wolf, 1999). In conclusion, it seems that all histone modifications interplay with each other to regulate

many cellular processes. Emerging research also suggests that modifications on the structured regions of histones also play a key role in transcriptional activation or repression (Zhang, 2003). Future research will surely show that each histone modification does not stand alone, but many modifications combine with chromatin remodeling complexes in the regulation of transcription, replication, DNA repair, etc.

Another class of factors that act to change the state of chromatin for cellular processes is the class of histone chaperone proteins. During chromatin assembly, the H3/H4 tetramer is first deposited onto the DNA, followed by the association of the H2A/H2B dimers with the tetramer. *In vitro*, the deposition of the histone octamer onto DNA fragments is often carried out by a salt-gradient reconstitution method. However, *in vivo*, this process is mediated by histone chaperone proteins and ATP-dependent remodeling complexes. The assembly factors work to keep the linker length between nucleosomes somewhat constant and position nucleosomes upstream of genes in order to achieve the regulation of nuclear processes. This causes transcriptionally active or inactive genes to be created in chromatin domains (Hebbes et al., 1994). Some histone chaperones act to add or remove the H2A/H2B dimers or the H3/H4 tetramers from the histone octamer. Cellular factors which work in this capacity include Nap1 (a histone H2A/H2B chaperone), CAF1 (a H3/H4 chaperone protein), and FACT (an RNA Polymerase II transcription elongation factor which has been shown to bind to H2A/H2B) (Adams and Kamakaka, 1999; LeRoy et al., 1998). Other histone chaperones may serve to "mark" transcriptionally active or inactive genes by the deposition of various histone variants.

In recent years, it has been shown that variant histone proteins play a vital role in transcriptional regulation. Most of the histone variants are very similar and only differ by a few amino acids. However, some variants are very different. For example, macro H2A contains an additional ordered domain that protrudes from the nucleosome core. During replication, the major histones are produced in large quantities and are incorporated into chromatin for the replicating cell. Throughout the rest of the cell cycle, replacement histones are synthesized at basal levels. Histone H2A is the most diverse family of histone variants, suggesting a very important role for the H2A/H2B dimer in nucleosomal dynamics. Histone variants are thought to be incorporated into chromatin for varying reasons. Some variants, such as H2A.Z, are associated with transcriptionally active chromatin. H2A.Z has been shown to make subtle changes in the nucleosome structure which in turn has quite large effects on higher order chromatin structure (Fan et al., 2002; Suto et al., 2000). Other histone variants have a role in transcriptional silencing, such as CENP-A which is incorporated in centromeres (Howman et al., 2000). Research has suggested that histone variants can function to provide additional stability or destability to the nucleosome core particle which alters higher order structure, and also that histone variants serve as markers for transcriptionally active or inactive chromatin and DNA damage (reviewed in (Vaquero, 2003)).

1.2 Chromatin in yeast

The yeast *Saccharomyces cerevisiae* is particularly suitable for studies of chromatin structure and function, and thus has been utilized a great deal for this purpose. Some of the properties that make yeast a good candidate for biological studies include rapid growth, dispersed cells, ease of replica plating and mutant isolation, a well-

characterized genome, and a highly versatile DNA transformation system. In addition, yeast contains only two copies of each of the histone proteins, which make them easy to knock out or mutate in order to analyze histone structure and function *in vivo*. Thus, many important experiments that have revealed crucial aspects of chromatin have been performed in yeast.

1.2a Histone sequence and DNA compaction differences in yeast

The amino acid sequence of each histone protein determines how the protein folds in order to form the three-dimensional structure of the histone octamer core. The sequence also encodes the precise location of bond formation between the proteins and contact points with the DNA. Attesting to the vital cellular role that the nucleosome core particle plays in all eukaryotic organisms, the amino acid sequences of the histone proteins are among the most conserved known. In comparing the histone sequences of eukaryotes, the histone sequences from yeast are among the most divergent from mammalian histones, with yeast histones having approximately 79% sequence identity as compared to higher eukaryotes (Baxevanis and Landsman, 1998). In comparison, histone sequences among all mammals share an approximate 97% sequence identity. The sequence differences between yeast and mammals are widely distributed among the histone fold regions as well as the tail domains. Histones H2A and H2B are the most divergent, with each one sharing 72 and 67% identity respectively. Histones H3 and H4 are more conserved, with 84 and 92% identity respectively. Sequence comparisons between *Saccharomyces cerevisiae* and *Xenopus laevis* histones reveal some significant amino acid substitutions at contact points between the histone proteins, as well as amino acids mediating histone-DNA interactions. There is also variations in the histone tail

regions. These amino acid differences are very interesting in light of the DNA compaction variations that exist between yeast and mammals.

Unlike mammals, yeast is a unicellular organism whose entire genome is only ~0.5% the size of that of humans. However, the size of the nucleus is approximately the same. Yeast contains a haploid set of 16 chromosomes, with genes representing 72% of the total DNA sequence. This is much different from higher eukaryotes that contain a lot of "excess" DNA between genes. Because there is not the extent of cell differentiation found in higher eukaryotes, much of the yeast genome is constitutively transcribed, in contrast to the small percentage of actively transcribed genes at any given time in the cells of higher eukaryotes. When yeast cells are in logarithmic growth, 40-60% of the genome is transcribed (Lohr and Ide, 1979). Thus, the need for extensive DNA compaction is less stringent for yeast. The possibility exists that the differences between the yeast histone sequences and those from higher eukaryotes allow the yeast chromatin structure to be more open allowing a larger proportion of the total genome to be expressed.

Indeed, there seem to be differences in nucleosomal compaction in yeast. It has been shown that nucleosomes are very closely spaced in yeast, with an average linker length of just 10 bp compared to 30-50 bp in metazoans (Wolffe, 1998). However, when yeast cells are in logarithmic growth, its chromatin is more rapidly digested by DNase I than the chromatin from the chicken erythrocytes or calf thymus (Lohr and Hereford, 1979). This suggests a more open chromatin structure. In eukaryotes, higher-order chromatin structure is stabilized by the linker histone H1 (Vignali and Workman, 1998). Sequencing of the yeast chromosome XIV in *S. cerevisiae* revealed only one gene,

Hho1p, with regions significantly homologous to histone H1 (Landsman, 1996). The gene has a fairly high rate of transcription and the protein has a nuclear location (Ushinsky et al., 1997). However, deletion of the gene has no effect on cell growth or viability (Escher and Schaffner, 1997). The Hho1p protein has been shown to behave in the same manner as histone H1 *in vitro*, forming a stable ternary complex with di-nucleosomes and producing a 168 bp nucleosomal repeat during MNase digestion (Patterton et al., 1998). However, it has recently been shown that nucleosome positioning in yeast is not dependent on the Hho1p protein (Puig et al., 1999). Thus, it appears that histone H1 does not play an important role in the regulation of chromatin condensation and gene regulation in yeast. This major difference in nucleosomal compaction between yeast and mammals could in part reflect the more open chromatin structure in yeast that is needed for constitutive gene expression.

Previous experimental evidence also suggests that yeast nucleosomes are less stable than those from higher eukaryotes. Yeast mononucleosomes demonstrate an increased molar ellipticity from their circular dichroism spectra as well as a lower melting transition than those from chicken and calf, which suggests that they are less constrained (Lee et al., 1982). Only 30% of plasmid DNA in *S. cerevisiae* is constrained from thermal untwisting *in vivo*, whereas thermal untwisting of DNA is completely suppressed in nucleosomes formed with chicken and monkey histones (Morse et al., 1987). Another study showed that yeast mononucleosomes partially dissociate at 0.5M NaCl, conditions that did not affect chicken nucleosomal cores, indicating a higher susceptibility to ionic strength of the yeast nucleosomes (Pineiro et al., 1991). The same study showed that treatment of yeast nucleosome core particles with the amino group

reagent dimethylmaleic anhydride resulted in the selective release of the H2A/H2B dimer (35% of all H2A and H2B histones were lost) (Pineiro et al., 1991). The authors of this paper concluded that the electrostatic forces holding the nucleosome core particle together might be fewer in yeast than in chicken. These and other studies taken together suggest that nucleosomes from yeast may be less stable than those from higher eukaryotes, and this decreased stability might be due to sequence variations in histones H2A or H2B (Lee et al., 1982; Wallis et al., 1980).

1.2b Histone mutagenesis studies in *Saccharomyces cerevisiae*

A central problem in eukaryotic transcription is how proteins gain access to DNA packaged in nucleosomes. The alteration of several chromatin components can affect transcription through an alteration of the structure of chromatin. In yeast, there have been many factors found that affect transcriptional regulation in relation to chromatin. These regulators can either be positive, acting to open up chromatin structure (such as the SWI/SNF and SAGA complexes), or they can be negative and maintain the repressive chromatin structure (such as histone deacetylases). In order to understand chromatin regulators in more detail, many studies have concentrated on mutations in the four histones. These *in vivo* and *in vitro* studies have shown how histones play a vital role in the dynamic nature of chromatin as well as transcriptional regulation.

Histones repress the transcription of genes by blocking DNA accessibility to the transcriptional machinery in promoter regions, thus interfering with the ability of activation factors to access their DNA binding sites. This hypothesis has been supported by genetic evidence obtained in yeast. The deletion of one or more of the histone genes in *S. cerevisiae* restores transcription to selected repressed promoters (Fassler and

Winston, 1988). However, the repressive role of the histones is gene specific rather than generally repressive, since the deletion of histone H4 in yeast resulted in increased expression of 15% of the genes, decreased expression of 10% of genes, but no effect on 75% of the genes (Wyrick et al., 1999).

A class of mutations that have been identified in *S. cerevisiae* is the SIN (for Switch INdependent) mutations. These mutations were identified as suppressors of the swi/snf phenotype in which the mutations could partially alleviate the defects caused by the inactivation of the SWI/SNF genes (Kruger et al., 1995). These mutations were located in histones H3 and H4, and involved residues which interact directly with the DNA at the central turn at the dyad, or are at or near the surface between the dimer and tetramer subunits. Since all of these mutations lie within one place, it was thought that this region of the histone octamer could act as a negative regulator. In nucleosomes containing the SIN mutations, there is an increased accessibility of the DNA to Dam methyltransferase and micrococcal nuclease. They have also been shown to impair the ability of NCPs to supercoil DNA, as well as disrupt the nucleosomal repression of the PHO5 gene (Wechser et al., 1997). Thus, it is proposed that these mutations disrupt DNA-histone interactions, leading to an increase in the accessibility of nucleosomal DNA.

Nucleosomes isolated from transcriptionally active chromatin appear to be depleted of H2A/H2B dimers and contain histone octamers that have interiors which are more accessible to enzymatic and chemical modifications (Allegra et al., 1987; Hansen and Ausio, 1992; Prior et al., 1983). Histones H2A/H2B also exchange more readily out of transcribed chromatin in yeast (Louters and Chalkley, 1985). Studies have shown that

DNA-tetramer particles are more accessible to DNA-binding proteins and removal of the H2A/H2B dimer facilitates transcription *in vitro* (Boyer et al., 2000). It also has a major influence on chromatin compaction (Hansen and Wolffe, 1994). Using mutation analysis in yeast, it was found that deletion of H4 tyrosine residues that make critical contacts between the H3/H4 tetramer and H2A/H2B dimer is lethal, and mutation of these residues disrupts both gene activation and repression (Santisteban et al., 1997). Therefore, interactions between the tetramer and dimer interfaces within the nucleosome are critical to maintain an intact nucleosome, and an intact nucleosome must be present in order to repress transcription.

Other yeast histone mutations within the histone fold domains have shown dramatic effects as well. Two H2A mutations (S20F and G30D) were isolated which involved residues located on the surface of the nucleosome and in close contact with the DNA. These mutations resulted in increased rates of chromosome loss, defects in traversing the G_2-M phase of the cell cycle, and altered chromatin structure flanking the centromere (Pinto and Winston, 2000). Another study identified 16 mutations in H2A in *S. cerevisiae* that confer a growth defect on media containing raffinose as the carbon source, a phenotype that reflects a defect in the expression of the SWI/SNF dependent SUC2 gene (Hirschhorn et al., 1995). These mutations occurred in several areas of H2A but mostly were clustered toward the N-terminus in a region exposed on the nucleosomal surface but not involved in DNA-histone interactions. The authors also showed that deletion of the H2A N-terminal tail resulted in the same phenotype. Since the mutants did not inhibit the formation of active chromatin, the authors concluded that these mutations affect a step after SWI/SNF remodeling where this region of H2A may be

recognized by a histone binding factor that aids in the dissociation of the H2A/H2B dimer (Hirschhorn et al., 1995). In conjunction with these experiments, another study revealed that isolated H2B mutants that suppressed phenotypes associated with the absence of the SWI/SNF complex occur at residues involved in H2A/H2B dimer formation and dimer-tetramer association (Recht and Osley, 1999).

Small deletions and point mutations that alter the flexible N-terminal tails of different yeast histones have been shown to result in specific transcriptional changes. Deletions of the N-terminus of H4 that removed much of the conserved basic region led to the derepression of the yeast silent mating-type cassettes, and certain point mutations in the same region abolished the silencing of the HMLα loci (Ravindra et al., 1999). A set of systematic deletions and mutations in the histone tails of H3 and H4 revealed that histone tails function both in gene activation and repression. H3 deletions increase GAL1 mRNA levels, while similar deletions in the H4 tail decrease them (reviewed in (Perez-Martin, 1999)). In fact, mutations of the lysine residues within the H4 tail caused transcriptional defects that in many cases were stronger than deletion of these residues (Durrin et al., 1991). These studies suggest that tail domains are required for nucleosomal array condensation in yeast. The N-termini also mediate transcriptional activation and repression by the binding of specific chromatin associated proteins or receiving post-translational modifications.

As can be seen, many studies have investigated transcriptional regulation within a chromatin context in yeast. However, no structural information exists which can allow these studies to be better understood. Structural information elucidating the mechanisms involved in such processes is very limited, and an understanding of the exact structural

changes that are incorporated in yeast nucleosomes that allows access of the transcriptional machinery is needed. Solving the crystal structure of the yeast nucleosome core particle would allow us to see genetic data in a structural manner, thus achieving a better understanding of the transcriptional processes involved.

1.3 The role of homopolymeric poly (dA·dT) elements in yeast promoters

Nucleosomal positioning in yeast promoter regions appears to be influenced by a combination of several factors. These factors include the inherent properties of the DNA sequence, anisotropy of the DNA structure, chromatin boundary elements, chromatin compaction and the interactions of trans-activating factors with nucleosomes, chromatin remodeling complexes, and histone tail modifications. The positioning of nucleosomes along promoter elements regulates their access by transcription factors, and thus gene expression. Transcription factor access to promoter areas is governed by many factors and elements. One element that has been proposed to stimulate transcription through an effect on chromatin structure is the homopolymeric poly (dA·dT) elements found in many yeast promoter regions. Experimental data suggests that these elements cause a predisposition to promoter accessibility that is required for activated transcription of many yeast genes.

1.3a Poly (dA·dT) adopts an unusual DNA structure which may perturb nucleosomal formation

Homopolymeric poly (dA·dT) elements are found in many yeast promoter regions. These DNA regions differ in structure from canonical B-form DNA. Poly (dA·dT) tracts form a very rigid and straight DNA structure that is different to two sugar-phosphate geometries (Nelson et al., 1987). These tracts have a narrowed minor groove

and a short helical repeat of 10 bp per turn, compared to 10.5 bp per turn for typical B-form DNA (Alexeev et al., 1987), (Peck and Wang, 1981). Crystal structures of poly (dA) · poly (dT) tracts shows additional bifurcated hydrogen bonds and a base-pair propeller twist that is higher than expected (Coll et al., 1987; Dickerson et al., 1982). Because of the above structural properties, it was previously speculated that poly (dA·dT) tracts would not be able to conform to bending around the histone octamer, and thus could not be incorporated into nucleosomes.

Indeed, early studies of these DNA elements affirmed this hypothesis, as these elements showed an inherent resistance to nucleosome formation (Kunkel and Martinson, 1981; Rhodes, 1979; Simpson and Kunzler, 1979). More recently, however, it has been shown that poly (dA·dT) can be incorporated into nucleosomes. Losa et. al. found that a poly (dA·dT) tract which is nucleosome free *in vivo* can be incorporated into nucleosomes *in vitro* (Losa et al., 1990). Additional studies have supported the conclusion that poly (dA·dT) can be incorporated into nucleosomes, and competitive assays have demonstrated that the homopolymer reconstitutes into core particles with about the same affinity as heterogeneous DNA sequences (Puhl et al., 1991). In fact, it has been shown that poly (dA·dT) forms nucleosomes more strongly as the temperature of the exchange mixture is increased, so that poly (dA·dT) outcompetes heterogeneous sequence DNA for histone association at elevated temperatures (Puhl and Behe, 1995). Thus, the DNA conformation adopted by these elements at higher temperatures facilitates nucleosome formation.

These elements are also incorporated into nucleosomes *in vivo*. The chromatin structure of the *S. cerevisiae* DNA topoisomerase I promoter has been shown to contain a

29 bp-long poly (dA·dT) element within a stably positioned nucleosome core particle (Rubbi et al., 1997). Prunell et. al. demonstrated that nucleosomes will form on a 20 bp poly (dA·dT) element inserted into plasmid DNA *in vivo*, but that the tract shows a marked preference for the edges of the particle (Prunell, 1982). Other studies have supported the idea that poly (dA·dT) regions are excluded from the center of nucleosomes (Satchwell et al., 1986). Short poly (dA·dT) tracts demonstrate inherent DNA curvature in the human estrogen receptor gene, which is predicted to be ~30 bp from the nucleosomal dyad by computer analysis (Wada-Kiyama et al., 1999). It seems as though the T-tract structure characteristic of poly (dA·dT) is partially lost upon folding into nucleosomes, demonstrating that the structural constraints of nucleosome core particles dominate over those of poly A tracts (Schieferstein and Thoma, 1996).

However, many promoter regions which contain poly (dA·dT) elements have been shown to be nucleosome free. For example, the *HIS3*, *URA3*, and *DED1* promoters of *S. cerevisiae* contains poly (dA·dT) elements that are within nucleosome free regions *in vivo* (Filetici et al., 1998; Lascaris et al., 2000; Tanaka et al., 1996). In fact, many promoter regions that contain poly (dA·dT) tracts of 4-11 bp in length have been found to be nucleosome free (Suter et al., 2000). Because of these results, it was thought that, due to their rigid structure, poly (dA·dT) elements destabilized nucleosomes *in vivo* and thus led to the exclusion of nucleosomes on promoter regions. However, other results suggest that nucleosomal placement on promoter regions is due to structural characteristics common to promoter regions and not to specific sequence elements (Mai et al., 2000). DNA sequence plays a major role in determining nucleosomal positions, since nucleosomes form on the same DNA positions both *in vivo* and *in vitro* (Shen and Clark,

2001). DNA sequences that have lower affinities for histone octamers have been identified. However, the fact that poly (dA·dT) can be incorporated into nucleosomes both *in vitro* and *in vivo* suggests that nucleosome free promoter regions are not established merely by poly (dA·dT) mediated exclusion. Thus, whether poly A tracts form nucleosomes can depend on their length, flanking sequences, and reconstitution conditions.

1.3b The role of poly (dA·dT) elements in transcriptional activation

A common feature of many yeast promoter regions is the presence of poly (dA·dT) DNA sequences, and poly A elements >10 bp occur at much higher frequencies than expected in the genome (Dechering et al., 1998). In *S. cerevisiae*, poly (dA·dT) tracts >10 bp were found in 2495 sites, 1760 of which were located within 500 bp upstream of an open reading frame (ORF), and poly (dA·dT) tracts >20 bp were found in 130 sites, 98 of which were located upsteam of an ORF (Shimizu et al., 2000). These elements thus appear to play a key role in rapid transcriptional activation.

Studies into genes which contain poly (dA·dT) regions revealed that they are required for activated transcription. In the yeast *HIS3*, *DED1*, and *URA3* genes, poly A tracts act as upstream promoter elements necessary for wild-type levels of transcription (Filetici et al., 1998; Lascaris et al., 2000; Tanaka et al., 1996). These studies showed that transcriptional activation depended on the length of the poly A tract, as longer stretches were more effective activators. In the *ILV1* promoter, nucleosomes are positioned to exclude two poly (dA·dT) elements and the Reb1p binding site (Moreira et al., 2002). Deletion of the poly (dA·dT) elements diminishes *ILV1* expression, but does not cause reconfiguration of the *ILV1* chromatin structure. Thus, the poly A element is

not responsible for the nucleosome exclusion observed in the promoter, which may be due to other activator proteins or complexes (Moreira et al., 2002).

The effect of other activator complexes on poly (dA·dT) function is under debate. In the *HIS3* promoter, a poly (dA·dT) element required for activated transcription is incompased within a nucleosomal-free region. Transcription of the *HIS3* gene is highly dependent on *GCN5*. But upon *GCN5* disruption, a nucleosome is formed encompassing the poly (dA·dT) element (Filetici et al., 1998). This suggests that *GCN5* is responsible for creating the nucleosome free regions around the poly A element. However, another group found that the poly A structure of the *HIS3* promoter is not dependent on *GCN5* and that no *GCN5*-dependent nucleosome remodeling of the poly A region is occuring (Suter et al., 2000). A study of the yeast *NHE1* promoter revealed that removal of a 20 bp poly (dA·dT) element resulted in a much greater reduction in promoter activity, and that the element can activate a foreign gene (Yang et al., 1996). Gel shift analysis revealed a protein binding to the region, and mutation of a few of the adenosine residues resulted in reduced protein binding to the element, although the identity of the protein was not determined (Yang et al., 1996). Thus, it appears as though other proteins or complexes may act to recognize poly (dA·dT) regions in order to activate transcription.

However, most poly A tracts are not associated with proteins and therefore participate in transcription regulation by virtue of their intrinsic DNA structure (Suter et al., 2000). The only known poly (dA·dT) binding protein in yeast is the product of the *DAT1* gene - datin. Datin recognizes poly A tracts >9-11 bp in length *in vitro*, and it appears to be able to affect transcription both negatively and positively (Winter and Varshavsky, 1989). Certain yeast promoters containing a poly (dA·dT) tract, including

the *ILV1* promoter, are dependent on datin for efficient basal level expression (Moreira et al., 2002). However, most poly A elements function independent of datin. Thus, it appears that the element's function is dependent on its intrinsic DNA structure, instead of recruitment of transcription factors.

Studies have suggested that poly (dA·dT) tracts alone are not sufficient to disrupt nucleosome formation, but might lead to a local distortion of the nucleosomal DNA. A study by Shimizu et. al. showed that poly (dA·dT) tracts disrupt local nucleosome structure in a length-dependent manner (Shimizu et al., 2000). A tract of 34 bp in length excluded nucleosome formation, but a tract of 15-29 bp in length only showed partial nucleosomal disruption when digested with MNase, and a tract 12 bp in length produced no disruption. They saw that when length is moderate, the DNA region near the poly (dA·dT) element is more accessible to MNase within the nucleosome. Thus, they concluded that the dynamic changes of the poly A element between T-tract structure and the usual B-form conformation may distort the local DNA structure within the nucleosome (Shimizu et al., 2000). The fact that it is possible to form triple helices on a nucleosomal poly (dA·dT) element, whereas nucleosomes inhibit triplex formation with random sequence DNA, suggests that the DNA has locally moved away from the histone octamer (Brown and Fox, 1998). A 16 bp poly (dA·dT) element located within the Amt1 gene promoter in the yeast *Candida glabrata* has been shown *in vivo* to create areas of increased Dnase I hypersensitivity within a nucleosome (Zhu and Thiele, 1996). Therefore, some poly (dA·dT) elements may function by disturbing nucleosomal DNA to protrude away from the octamer surface, enhancing the binding of transcription factors.

1.4 Transcriptional regulation of the Amt1 gene in *Candida*

glabrata

Metals and oxygen play important roles in enzymatic reactions by acting as cofactors for many enzymes. However, metals and oxygen can react to form highly toxic free radicals. Thus, the cell must keep metal concentrations at safe and effective levels. Copper is a very important metal found in all species. It is required for normal cellular growth, development, and function. Copper has to be transported into cells, correctly distributed, and made available to enzymes to act as a cofactor for many enzymatic reactions. However, copper must be removed from cells when present at toxic levels. Since copper can create hydroxyl radicals that can cleave DNA and damage proteins, eukaryotes sense copper levels and respond to high copper by activating the transcription of a class of genes encoding components of the copper homeostasis machinery. The metallotheioneins (MTs) are a class of small, cysteine-rich metal-binding proteins that sequester metal ions and protect the organism from metal toxicity. In yeast, MT genes are regulated by changes in copper concentrations. A set of regulatory proteins bind copper and transmit the signal directly to the transcriptional machinery to activate the MT genes (Liu and Thiele, 1997).

In the opportunistic pathogenic yeast *Candida glabrata*, the transcription factor Amt1 is one such copper sensory molecule that monitors intracellular copper levels and induces MT expression when the accumulation of copper exceeds sufficient levels. Amt1 is required for copper detoxification in the *C. glabrata*, and shares sequence homology with the copper regulatory protein *ACE1* found in *S. cerevisiae* (Liu and Thiele, 1997). Amt1 binds to DNA as a monomer and contains two domains: a basic N-terminal domain and an acidic C-terminal domain. The C-terminal domain plays a role in transcriptional

activation, and the N-terminal domain is responsible for binding DNA and copper (Zhou and Thiele, 1993). The N-terminal domain, which encompasses the first 115 amino acids out of a total of 265 amino acids in the protein, contains several cysteine residues that form a metal binding motif which binds four coppers and one zinc [Thorvaldsen, 1994 #1696]. Bound copper ions are essential for Amt1 DNA binding, but not for zinc site binding (Farrell et al., 1996).

The NMR structure of part of the N-terminal domain of Amt1 (residues 1 to 42) consists of a three-stranded anti-parallel β-sheet with two short helices that project from one end (Turner et al., 1998). Conserved residues form a basic patch that may be important for DNA-binding. Copper ions form a tetracopper cluster, and both the zinc and tetracopper domains participate in DNA binding (Turner et al., 1998). Amt1 binds to DNA in the minor groove where the amino acids are deeply buried in an extended conformation. An arginine residue, embedded within a region similar to other known minor groove binding motifs, plays a critical role in high-affinity DNA binding and normal copper detoxification (Koch and Thiele, 1996). The copper and zinc atoms contact bases separated by one and a half turns of the DNA helix, and the role of the metal ions is clearly to bind DNA (Turner et al., 1998).

When copper binds to Amt1, Amt1 binds to its own MRE and activates transcription of the Amt1 gene (Liu and Thiele, 1997). This rapid production of high levels of Amt1 allows the cell to quickly respond to toxic copper levels by having more transcription factor present to activate the MT genes. The Amt1 gene is induced 15 to 20 fold in response to copper via this transcriptional autoactivation mechanism that requires Amt1 and a single MRE (metal responsive element) in the Amt1 promoter. The

conserved Amt1 binding sequence is TNNNGCTG, and the protein makes critical interactions with the major and minor grooves. The conserved threonine residue in the minor groove of the Amt1 binding site plays a critical role in DNA binding, and mutations of these residues results in a much reduced affinity (Koch and Thiele, 1996).

It has been found that a homopolymeric (dA·dT) element located adjacent to the MRE within the Amt1 gene plays a critical role in its rapid transcriptional activation. The poly (dA·dT) element contains 16 contiguous adenosine residues, and this element is essential for rapid Amt1 binding and autoregulation (summarized in Figure 1.3) (Zhu and Thiele, 1996). However, there is no DNA-binding factor which binds to this element which would act to recruit Amt1 to the promoter. Using *in vivo* micrococcal nuclease sensitivity, Zhu and Thiele showed that the poly (dA·dT) element and MRE are embedded within a stably positioned nucleosome (Zhu and Thiele, 1996). This nucleosome is not disrupted upon Amt1 binding and gene transcription. The poly (dA·dT) element confered localized DNA distortion in the nucleosome since the flanking sequences around the element showed DNase I hypersensitivity. They concluded that the role of the poly (dA·dT) element is to make the DNA around the nucleosome more accessible for transcription factor binding. In a later study, Koch and Thiele showed that the activation of the Amt1 gene is impaired when the poly (dA·dT) element is positioned downstream of the MRE within the nucleosome, implicating that the placement of the poly (dA·dT) element is essential in order to obtain transcriptional activation (Koch and Thiele, 1999). These results suggest that the positioning of homopolymeric (dA·dT) elements adjacent to cis-acting regulatory sites may play a key role in providing

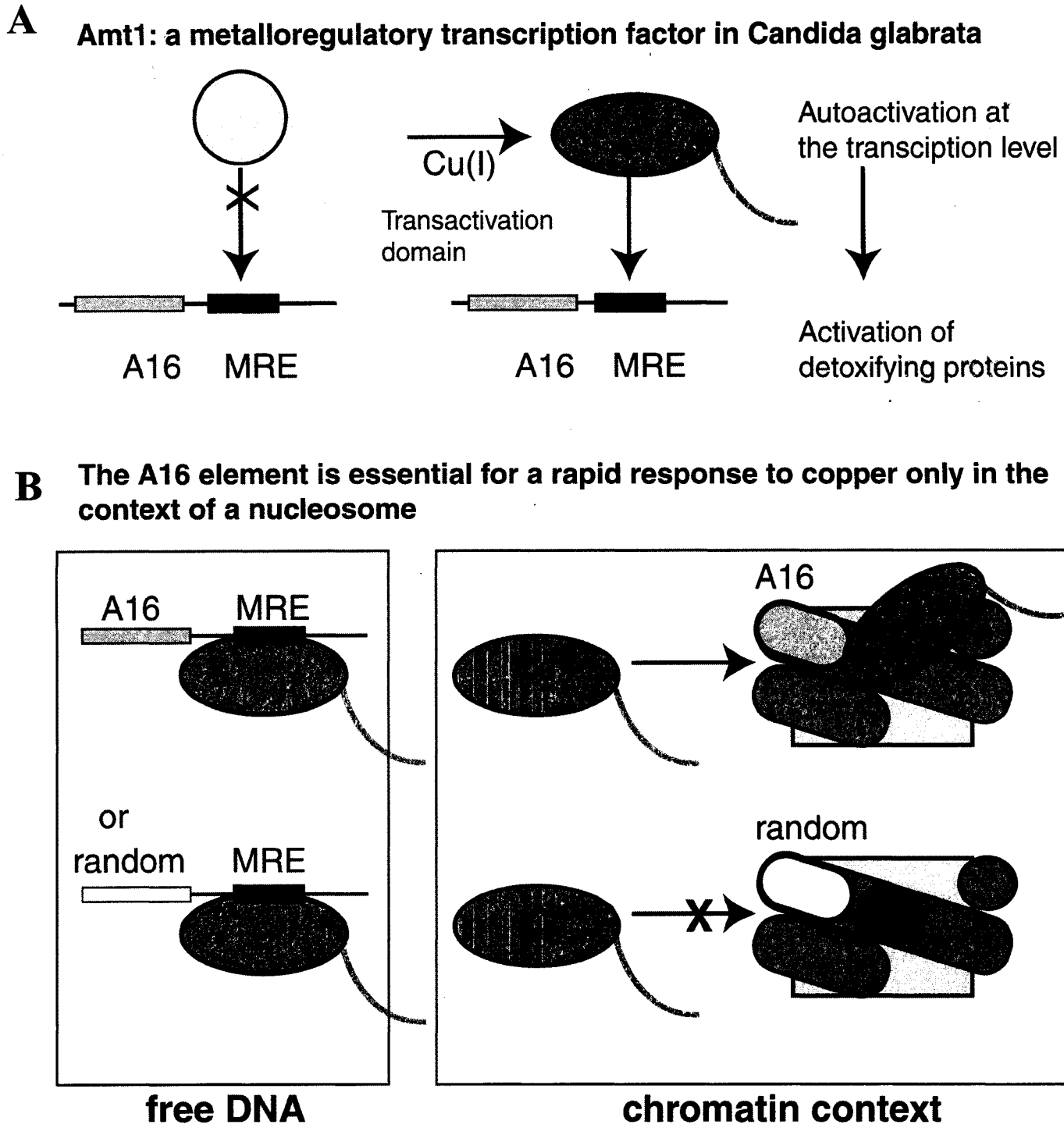

Figure 1.3. Mechanism of Amt1 autoactivation.

(A) Schematic depicting the requirement of bound copper in order for the Amt1 transcription factor to be activated and thus bind to its MRE. Amt1 with unbound copper is given in yellow, and copper-bound Amt1 is shown in red. The critical elements present in the Amt1 gene promoter in order to achieve transcriptional activation is given. **(B)** Representation showing that the poly (dA·dT) element is essential in order to get rapid Amt1 binding and transcriptional activation in the context of a positioned nucleosome core particle. Amt1 is shown in red, DNA is purple, the histone octamer is depicted in green, and the A_{16} and MRE DNA elements are shown in gray and black, respectively.

transcription factor accessibility via the formation of specific nucleosomal structures which weaken the interactions between core histone proteins and DNA.

1.5 Specific Aims of Thesis

The scope of the work outlined in this thesis investigates the structural context of transcriptional regulation in yeast. The current hypothesis is that structural changes imparted on the histone octamer, either due to changes within the histone sequence, incorporation of histone variants, action of chromatin remodeling factors, or the presence of DNA sequences that do not easily fold around the histone core, decrease the stability of the nucleosome core particle. Consequently, this enhances transcription factor access to chromosomal DNA. I test this hypothesis in a structural context by first determining the structure of the yeast nucleosome core particle, followed by testing the stability of yeast nucleosomes compared to those of higher eukaryotes. I then investigate the stability of nucleosomes incorporating a homopolymeric (dA·dT) DNA sequence, proven to stimulate transcription. Various biophysical techniques are employed to see if these rigid DNA tracts create areas of greater DNA accessibility within the nucleosome core particle, which would allow for activated transcription. I then study the binding of the transcription factor Amt1 to the nucleosome, and determine if binding affects underlying interactions within the histone octamer as well as the DNA molecule. Finally, I attempt to determine the crystal structure of a nucleosome containing a 16 bp poly (dA·dT) element. With these studies, we can better understand the detailed interaction between transcription factors and the nucleosome core particle in yeast. This allows us to better comprehend transcriptional regulation in a chromatin context.

Chapter 2

Crystal Structure of the Yeast Nucleosome Core Particle Reveals Fundamental Differences in Inter-Nucleosome Interactions

This chapter was published in *The EMBO Journal*. The text of this manuscript and the figures are presented as they appeared in this journal. The reference for this chapter is shown below. Robert Suto gave support and technical advice during the completion of this project.

White, C.L., Suto, R.K., and Luger, K. 2001. Structure of the yeast nucleosome core particle reveals fundamental changes in internucleosome interactions. *EMBO Journal.* **20** (18), 5207-5218.

2.1 Abstract

Chromatin is composed of nucleosomes, the universally repeating protein-DNA complex in eukaryotic cells. The crystal structure of the nucleosome core particle from *Saccharomyces cerevisiae* reveals that the structure and function of this fundamental complex is conserved between single-cell organisms and metazoans. However, yeast nucleosomes are likely to be subtly destabilized as compared to nucleosomes from higher eukaryotes. Importantly, minor sequence variations lead to dramatic changes in the way in which nucleosomes pack against each other within the crystal lattice. This has important implications for our understanding of the formation of higher-order chromatin structure and its modulation by post-translational modifications. Finally, the yeast nucleosome core particle provides a structural context by which to interpret genetic data obtained from yeast. Coordinates have been deposited with the Protein Data Bank under accession number 1ID3.

2.2 Introduction

The packaging of DNA in the eukaryotic nucleus is achieved by a hierarchical scheme of folding and compaction into protein-DNA assemblies collectively called chromatin (Widom, 1998). At the first level of organization, two tight superhelical turns of 147 base pairs of DNA are wrapped around a histone octamer to form the nucleosome core particle. In higher eukaryotes, the addition of linker histone H1 to linker DNA forms the nucleosome, the basic repeating unit of chromatin. Hundreds of thousands of nucleosomes are further compacted into multiple higher organizational levels. Because of DNA packaging in chromatin, the structure and accessibility of nucleosomal DNA

deviates dramatically from that of linear, 'naked' DNA, as seen in the high-resolution X-ray structure of the nucleosome core particle from *Xenopus laevis* [Luger, 1997 #343]; (Luger et al., 2000). Depending on the structural context, chromatin can both promote and impede transcription, replication, recombination, and DNA repair. Thus, chromatin plays a central role in the regulation of these vital processes. Eukaryotic cells have developed elaborate mechanisms to modulate the inherently dynamic chromatin structures in a regulated manner (Workman and Kingston, 1998).

The histone octamer consists of two copies each of the four histone proteins H2A, H2B, H3, and H4. Two histone pairs, composed either of H2A and H2B, or H3 and H4, form tight dimers that each organize 30 base pairs of DNA (Luger and Richmond, 1998). Two H3-H4 dimers form a tetramer that organizes the central 60 base pairs of the nucleosomal DNA. By structurally similar interactions, one (H2A-H2B) dimer is tethered to one half of the histone $(H3\text{-}H4)_2$ tetramer. The (H2A-H2B) dimer organizes 30 base pairs towards either end of the DNA. The penultimate 10 base pairs of nucleosomal DNA are organized by a region of H3 that does not form an integral part of the $(H3\text{-}H4)_2$ tetramer, and is most likely not able to bind DNA in the absence of the (H2A-H2B) dimer (Luger et al., 1997; Luger and Richmond, 1998). The massive distortion of the DNA is brought about mainly by the tight interaction between the structured regions of the histone proteins and the minor groove of the DNA at fourteen independent DNA binding locations, either using L1L2 loops or $\alpha_1\alpha_1$ DNA binding motifs (Luger and Richmond, 1998). At the molecular level, the interaction of the histone octamer with the DNA is formed mainly by tight hydrogen bonds between the main chain amide and the phosphate oxygen of the DNA, assisted by electrostatic

interaction with basic side chains. In the context of a mononucleosome, the flexible histone tails do not contribute to the stability of the complex (Luger *et al.*, 1997). Other nucleosome structures containing chicken histone proteins (Harp et al., 2000) or the histone variant H2A.Z (Suto et al., 2000) have confirmed this basic design.

Many groundbreaking studies that address the complex interplay between chromatin structure and transcription regulation in the living cell stem from yeast genetics (reviewed by (Gregory, 2001); and (Hartzog and Winston, 1997). These studies were made possible by the obvious suitability of yeast for genetic studies, and by the fact that the *S. cerevisiae* genome contains only two genes for each of the four core histone proteins. Many of the characteristics of chromatin in higher organisms are seen in yeast. For example, *S. cerevisiae* contains histone variants, such as the histone H2A variant H2A.Z (HTZ1) (Santisteban et al., 2000); (Jackson and Gorovsky, 2000) and the centromere-specific H3 variant CenpA (cse4) (Glowczewski et al., 2000). *S. cerevisiae* also uses targeted ATP-dependent chromatin remodeling factors (Aalfs and Kingston, 2000) and reversible modification of histone tails, such as acetylation, de-acetylation (Vogelauer et al., 2000), methylation (Strahl et al., 1999), phosphorylation (Hsu et al., 2000), and ubiquitination (Robzyk et al., 2000), in order to regulate the level of DNA accessibility in a chromatin context.

However, fundamental differences between the yeast genome and that of higher organisms suggest that chromatin might be organized in a different manner in yeast. Yeast is a unicellular organism whose entire genome is only ~ 0.5 % the size of that of higher eukaryotes. Much of the yeast genome is constitutively open for transcription, as opposed to the small percentage of actively transcribed genes at any given time in the

cells of higher eukaryotes. Yeast nucleosomes are very closely spaced, with a repeat length of 162 ± 6 base pairs (Horz and Zachau, 1980), resulting in a linker length of only 15 to 20 base pairs. In contrast, the repeat length in metazoans ranges from 175 to 240 base pairs, with an average of approximately 190 base pairs. No linker histones have been found to be associated with yeast chromatin in a stoichiometric manner. Recently, the presence of a gene (HHO) encoding a protein with linker histone homology (Hho1p) has been identified, and it has been suggested that this gene product may function as a linker histone. However, deletion of this gene has neither growth nor mating defects, suggesting that this protein does not play an important role in chromatin organization in yeast (Patterton et al., 1998).

Histone proteins are highly conserved among eukaryotic organisms, with yeast histones being among the most divergent from mammalian histones (Baxevanis and Landsman, 1998). The differences are distributed throughout the length of the amino acid sequence, with many of the more divergent sequence changes clustered in the flexible histone tails. The distinct sequence divergence between the histone proteins of *S. cerevisiae* and metazoans may well reflect the different requirements for DNA compaction between unicellular and multicellular organisms.

Here we present the crystal structure of the *Saccharomyces cerevisiae* nucleosome core particle. Analysis of the structure suggests that subtle sequence variations may affect the overall stability of the core particle in this organism, as well as lead to differences in the interaction between neighboring nucleosomes. This may be a reflection of differences in nucleosome organization *in vivo*. In addition, the structure is now available to analyze the numerous genetic studies from yeast in a structural context. In

particular, our data suggest a straightforward mechanism by which the recently described ubiquitination of a specific residue in H2B (Robzyk et al., 2000) may affect chromatin compaction *in vivo*.

2.3 Materials and methods

2.3a Expression, Purification, and Reconstitution of Yeast NCP

Yeast histone expression plasmids (pet28a) were a kind gift from Dr. Xuetong Shen. Proteins were over-expressed in BL21 (DE3) CodonPlus RIL- plysS (Stratagene) and purified using previously published protocols (Luger et al., 1999). The histone proteins were refolded to a histone octamer, and reconstituted into nucleosome core particles using a 146-base pair palindromic DNA fragment derived from human α-satellite regions [Luger, 1997 #343]. Milligram amounts of yeast nucleosome core particles were subjected to heat shifting, followed by subsequent purification using preparative gel electrophoresis (Luger et al., 1999).

2.3b Crystallographic procedures

Crystals of *Sce*-NCP were obtained by vapor diffusion at a protein concentration of 4 mg ml^{-1} with 70 mM KCl, 76 mM $MnCl_2$, and 10mM potassium cacodylate (pH 6.0) in the drop equilibrated against 35mM KCl, 38 mM $MnCl_2$, and 5mM potassium cacodylate (pH 6.0). Macro-seeding of sitting drops increased crystal size. For data collection, the crystals were transferred into cryo-protectant and were flash frozen in liquid propane at -130°C before transferring to the cryo-stream at -180°C, as previously described [Luger, 1997 #343]. Data were collected at beamline 5.0.2 at the Advanced Light Source in Berkeley. Data from two crystals were processed using Denzo and Scalepack (Otwinowski and Minor, 1997).

Molecular replacement, with PDB entry 1AOI as the search model, was used to obtain initial phases. Refinement was performed using CNS (Brunger et al., 1997) and model building into the $|2F_o - F_c|$ and $|F_o - F_c|$ electron density maps was done in O (Jones et al., 1991). The entire model was checked using SA-OMIT maps during the early stages of model building to eliminate model bias. PROCHECK analysis (Laskowski et al., 1993) of the final model shows that the model has good overall geometry, with no residues falling in the disallowed regions of the Ramachandran map. Figures were prepared using MOLSCRIPT (Kraulis, 1991), BOBSCRIPT (Esnouf, 1999), MIDAS (Ferrin et al., 1988) and O (Jones et al., 1991).

2.4 Results

2.4a Structure determination

Crystals of the nucleosome core particle from *Saccharomyces cerevisiae* (*Sce*-NCP) were obtained under similar conditions as the previously published crystal structure of the nucleosome core particle containing *Xenopus laevis* histone proteins (*Xla*-NCP, (Luger et al., 1997). We have found previously that crystallization conditions and diffraction quality are highly dependent on the DNA fragment being used. Despite the fact that the same palindromic DNA sequence derived from human α-satellite repeats was used to reconstitute yeast nucleosomes, *Sce*-NCP crystals behaved rather differently. They took much longer to grow, exhibited a different morphology, were extremely fragile, and diffracted to a significantly lower resolution at a synchrotron source (3.1 Å as opposed to a routinely obtained 2.2 Å resolution for *Xla*-NCP; (Luger et al., 2000). Furthermore, although the original space group was maintained, the longest crystallographic axis deviated significantly in length (Table 1).

Table 2.1. Summary of Crystallographic Analysis

Data Collection Statistics

Space group	a=, b=, c=	Resolution (Å)	Reflections (Total/Unique)	Completeness (%)	R_{sym}[a]
$P2_12_12_1$	104.9, 110.4, 192.6	50 –3.1	517,812 (39,551)	99.5 (99.9)[b]	0.056 (0.299)[c]

Refinement Statistics[c]

			Root-Mean-Square Deviations		Average B-factors (Å^2)		
Resolution (Å)	Reflections	R_{cryst}/R_{free}[d]	Bonds (Å)	Angles(Å)	Protein	DNA	Solvent
40 – 3.1	38,264	0.223/0.292	.0069	1.14	62.05	132.93	56.7

[a] $R_{sym} = \Sigma \left| I_h - \langle I_h \rangle \right| / \Sigma I_h$, where $\langle I_h \rangle$ is the mean of measurements for a single hkl.
[b] Value in parentheses is for the highest resolution shell: 3.15 – 3.1 Å.
[c] Atomic model: 757 amino acids (H2A: 15-124, H2A': 12-119, H2B: 30-122, H2B': 29-124, H3: 38-134, H3': 38-134, H4: 24-102, H4':18-102), 60 water molecules and 17 manganese ions (a total of 12129 atoms). The remainder of the histone tails was too disordered to be included in the final model.
[d] $R_{cryst} = \Sigma \left| F_{obs} - F_{calc} \right| / \Sigma F_{obs}$

Phase information was obtained using the previously published nucleosome core particle structure from *X. laevis* (pdb entry 1AOI) as a search model. Data collection and refinement statistics are given in Table 1. Sequence differences between *S. cerevisiae* and *X. laevis* were clearly visible in the original $2F_o$-F_c electron density map. As in *Xla*-NCP, the histone fold regions, as well as the extensions that are responsible for the main protein-protein and protein-DNA interactions in the yeast nucleosome core particle, are highly ordered. However, the histone tails become quickly disordered as they extend past the DNA superhelix. Slightly less of the flexible histone tails is visible in the *Sce*-NCP structure as compared to *Xla*-NCP (Table 1).

2.4b The structures of nucleosome core particles from *S. cerevisiae and X. laevis* are very similar

Amino acid sequence alignments between *S. cerevisiae* and *X. laevis* histones show that H2A and H2B are more divergent (72% and 67% identity) than H3 and H4 (84% and 92% identity) (Figure 1A). Although changes are more numerous in the flexible histone tails (especially in those of H2A and H2B), the folded regions of all four histone proteins are also divergent. The overall structure of the nucleosome core particle from *Saccharomyces cerevisiae* (Figure 1B and C) is very similar to that of the previously reported structure of the nucleosome core particle from *Xenopus laevis* (Luger et al., 1997). This shows that the function of the histone octamer is identical at the level of histone-DNA interaction, despite the differences in sequence and chromatin organization between yeast and higher eukaryotes. The Cα atoms of the histone octamers of *Sce*-NCP and *Xla*-NCP superimpose with an overall root mean square deviation (RMSD) of 1.14Å, and the phosphates of the two DNA strands align with an RMSD of 1.15 Å. The two

Figure 2.1

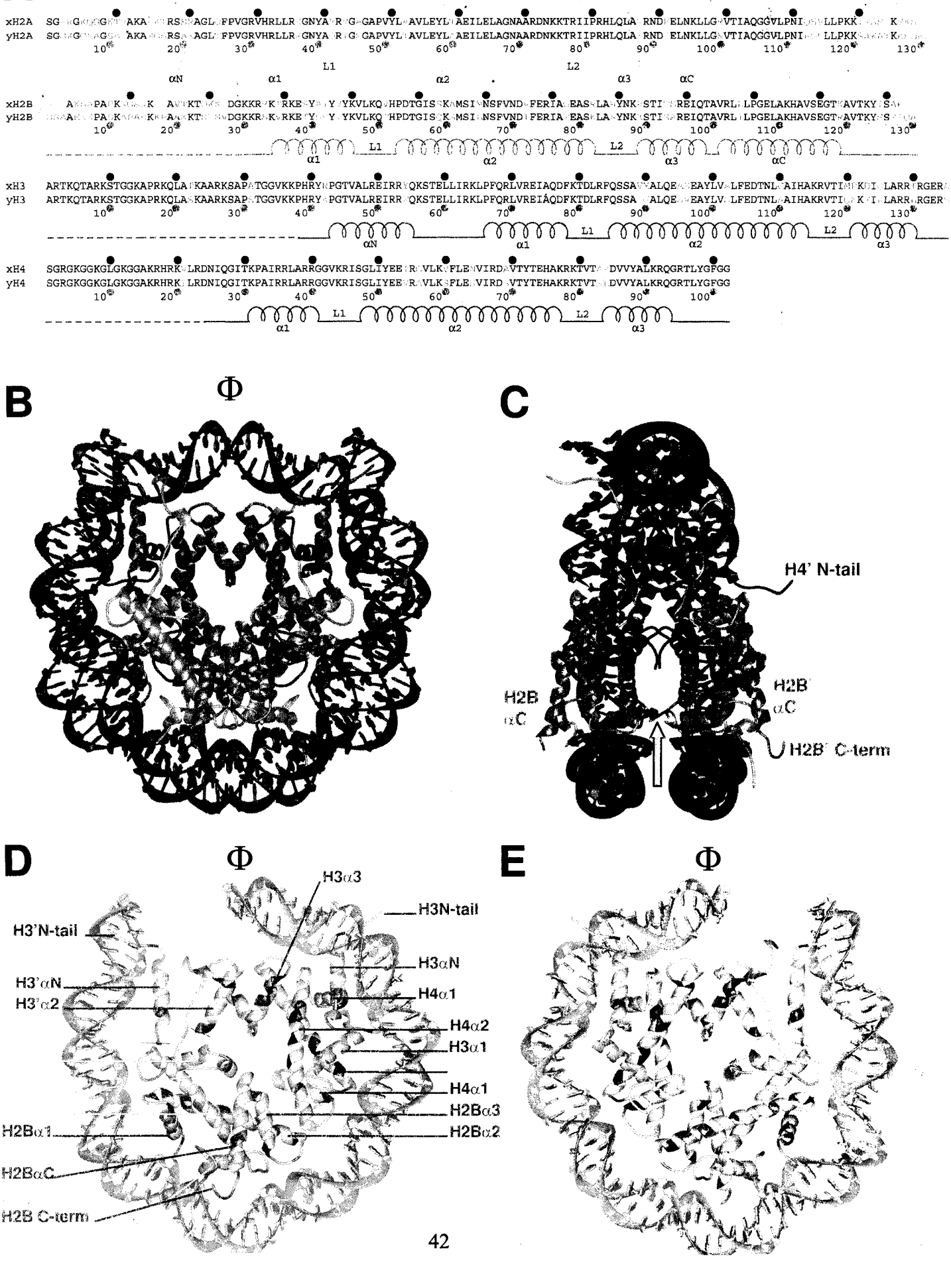

Figure 2.1. Secondary and tertiary structure of the yeast nucleosome core particle. (**A**) Sequence alignment of *Xenopus laevis* (top line) and *Saccharomyces cerevisiae* histone proteins (bottom line). Amino acid differences are colored in magenta. Intervals of 10 amino acids for *X. laevis* (black circles) and *S. cerevisiae* (magenta circles) are indicated. The α-helices and loops located within the structured regions are labeled; the flexible histone tails are indicated by dashed lines. (**B**) The crystal structure of the yeast nucleosome core particle, viewed down the superhelical axis. Histone chains are colored yellow for H2A, red for H2B, blue for H3, and green for H4. The DNA is shown in turquoise. The position of the molecular dyad axis is indicated (ϕ). (**C**) Side view of the yeast nucleosome core particle, obtained by rotation of 90° around the axis of non-crystallographic symmetry, with part of the DNA removed for clarity. The arrow denotes the location of the L1 loop. (**D**) Amino acid differences in the yeast octamer are colored according to histone coloring scheme given above. The conserved amino acids and DNA are shown in gray. Only 73 base pairs of the DNA and associated proteins are shown. The solvent-exposed surface view of one half of the nucleosome is shown. **(E)** The same half of the nucleosome viewed from the interior surface between the two gyres of the DNA supercoil.

Table 2.II: Structural alignment of *Sce*-NCP and *Xla*-NCP. RMS deviations between the *Saccharomyces cerevisiae* and *Xenopus laevis* structures[a, b].

		H2A	H2B	H3	H4	DNA
Chain #1:	All[c]	1.06 (0.51)	1.23 (0.76)	1.44 (0.47)	0.83 (0.47)	1.23 (1.15)
	Δtail[d]	0.89 (0.46)	1.20 (0.71)	1.43 (0.47)	0.81 (0.43)	
Chain #2:	All[c]	1.85 (1.06)	1.20 (0.80)	1.07 (0.59)	3.53 (2.77)	1.11 (1.14)
	Δtail[d]	1.08 (0.56)	1.18 (0.79)	1.07 (0.59)	1.04 (0.58)	

[a] Values given in Å.
[b] Values given include all sidechains (values in parenthesis are for the α-carbon backbone or phosphate atoms only).
[c] All: Includes all residues of the entire model.
[d] Δtail: Includes only the structured regions of the model, as defined by [Luger, 1997 #343]

structures (including side chains and DNA bases) superimpose with an RMSD of 1.57Å. The most striking deviations in the Cα trace of the two structures are found in the C-terminal tail of the second copy of histone H2A (H2A') as well as in the N-terminal tail of histone H4' (Table 2, compare lanes 'All' with lanes 'Δtail'). These tails take completely different paths in the two structures as a result of variations in their structural environment (see below).

The regions of the histone proteins that are responsible for protein-protein and protein-DNA interaction are structurally much more conserved than the histone tails. Analysis of the RMSD for each chain, based on the same alignment (Table 2, lane 'Δtail'), and a distance plot for each Cα atom (not shown), shows that both copies of histone H2B are the most structurally divergent. This is expected from the relatively high degree of sequence divergence between *X. laevis* and *S. cerevisiae* for this particular histone. However, the L1 loops and C-terminal helix of H2B, where the sequence is very similar (Figure 1A), also exhibit noticeable structural deviations (~2.4 Å RMSD) compared to the corresponding regions in *Xla*-NCP. In *Sce*-NCP, both H2B L1 loops are involved in crystal contacts, whereas they are not involved in any inter-nucleosome contacts in *Xla*-NCP (see below). These structural differences in L1 loop conformation lead to local deviations (~2.5 Å RMSD) in the nearby DNA phosphates.

The overall architecture of the histone octamer, as well as all of the residues that are involved in direct protein-DNA interactions, is unchanged between *S. cerevisiae* and *X. laevis* (Figure 1D and 1E). Thus, the general mechanism by which the histone octamer distorts linear DNA into a tight superhelix is maintained between yeast and higher eukaryotes. The path of the DNA around the histone octamer is conserved between the

two structures, with only local deviations between the positions of the phosphates in regions of high B-factors. This is indicated by the relatively low RMSD values for the superposition of the DNA in the *Xla*-NCP and *Sce*-NCP structures (Table 2).

2.4c Sequence differences cause changes in molecular surface and in histone-histone interaction

Sequence differences in the histone fold regions and extensions (Figure 1A) are not limited to amino acid residues on the surface of the nucleosome core particle, but equally affect residues that are buried deep within the histone octamer core. This is demonstrated in Figures 1D and 1E, which show the location of amino acid differences on one half of the yeast nucleosome core particle, viewed from the outside (Figure 1D), and from between the two gyres of the DNA superhelix (Figure 1E). Sequence differences that change the molecular surface of the yeast histone octamer (Figure 1D) could reveal how inter-particle interactions are altered in yeast *in vivo*. Evidence for this is seen in the dramatic differences in the packing of yeast nucleosomes within the crystal lattice (see below). In addition, interactions with other cellular factors may be affected by surface variations. In contrast, amino acid differences that are buried within the histone octamer (Figure 2E) may locally affect the stability of histone – histone interactions, thus contributing to an overall change in nucleosome stability.

The main signature of the molecular surface of *Xla*-NCP is a large acidic patch formed by seven amino acids from the structured regions of H2A and H2B (Luger et al., 1997). Several basic regions that create a favorable interaction interface for DNA surround this area. Both features are maintained in *Sce*-NCP, but there are subtle changes in the charge distribution and shape of the yeast histone octamer surface as compared to

that of *Xenopus laevis*. Additional positively charged amino acids are located on the surface, and thus render it slightly more basic (supplemental figure 1).

In all nucleosome core particle structures reported to date (Harp et al., 2000; Luger et al., 1997; Suto et al., 2000), the two H2A-H2B dimers interact through a small but significant interface formed by the L1 loops of two adjacent H2A molecules, indicated by an arrow in Figure 1C. In *Xla*-NCP, two hydrogen bonds and two salt bridges stabilize this interface (Figure 2A and B). *Xla*-H2A Asn-38 forms tight bonds with *Xla*-H2A' Glu-41 and *Xla*-H2B' His-79. Owing to non-crystallographic symmetry, these interactions are mirrored between *Xla*-H2A'-Asn-38 and *Xla*-H2A/H2B (Figure 2A and B). Although the path of the main chain within the L1 loop is almost identical in the yeast structure, the corresponding residues are changed, resulting in a loss of all interactions at this interface (Figure 2C and D). In yeast, Glu-41 is changed to a glutamine, and His-79 is changed to an alanine (H2A Glu-42 and H2B Ala-85 in yeast, Figure 1A). In order to avoid steric clashes between the two amino groups of the asparagine and glutamine residues, the two glutamine residues point downward towards the DNA (Figure 2C). As a result, no stabilizing interactions exist between the two H2A/H2B dimers in this region, and the buried surface is reduced to 90 $Å^2$ in *Sce*-NCP, compared to 150 $Å^2$ in *Xla*-NCP. Together, these findings strongly suggest a significantly weaker interaction at this particular interface in the *S. cerevisiae* core particle as compared to that of *X. laevis*.

Most of the amino acid sequence differences are found in the N-terminal tails of H2A and H2B, and in the C-terminal tail of H2A. However, it is the N-terminal tail of H4' that shows the largest deviations between the two structures (Table 2). This particular tail is directly involved in transcription regulation and gene silencing, and its

Figure 2.2

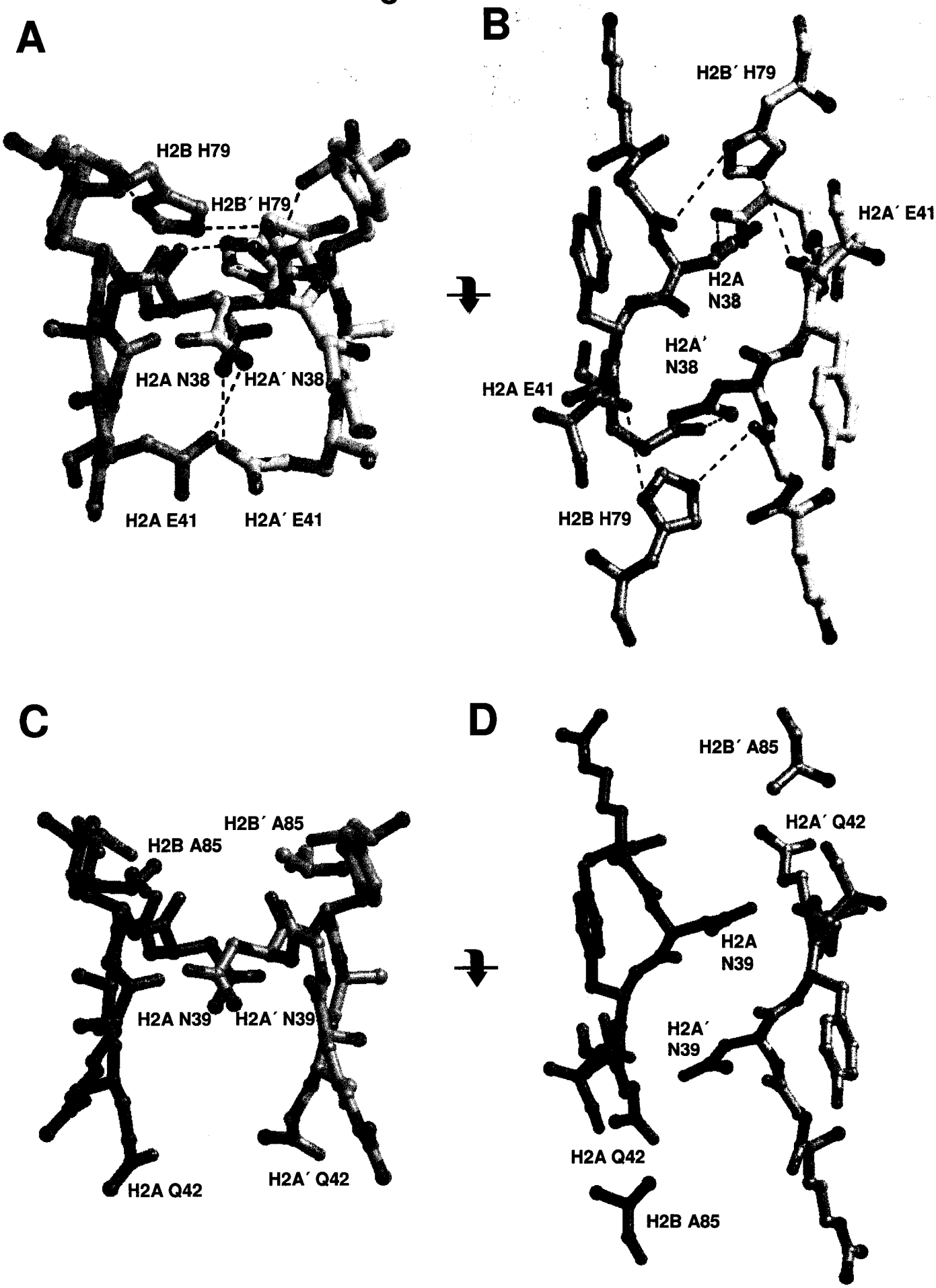

Figure 2.2. Interactions between two (H2A-H2B) dimers within a nucleosome. (**A**) The side chain interactions of the H2A and H2A' L1 loops in *Xla*-NCP, in the same orientation as shown in Figure 1C. *Xla*-H2A and H2A' are colored in purple and gray, respectively. Dashed lines indicate hydrogen bonds. (**B**) The same region is shown in a view obtained by a 90° rotation around the horizontal axis (as indicated). (**C** and **D**) The equivalent region in *Sce*-NCP, viewed in the same orientation as in (A) and (B), respectively. Note the total absence of inter-molecular hydrogen bonds.

importance is demonstrated by the fact that the sequence of this region is almost completely conserved between *S. cerevisiae* and *X. laevis* (Figure 1A). In *Xla*-NCP, the H4 N-terminal tail forms essential crystal contacts with the acidic patch on the surface of a neighboring nucleosome (Luger and Richmond, 1998). No such contact is made in *Sce*-NCP (see below), which allows the H4 tail to adopt an alternative conformation that is completely different from that observed in either chain in *Xla*-NCP. Similar differences are seen for the C-terminal tail of H2A. This confirms that histone tails can indeed assume different conformations that depend on the structural context.

2.4d Sce-NCP and Xla-NCP crystals are held together by different types of interactions

Perhaps the most striking difference between the *S. cerevisiae* and *X. laevis* structures is the way in which the nucleosome core particles pack within the crystal lattice. It should be noted that the packing of nucleosomes within a crystal does not necessarily reflect the way in which particles are organized in condensed chromatin. The most obvious difference is that individual nucleosomes are located on long contiguous DNA in the cell, whereas they exist as individual, unconnected particles in the crystal. However, we believe that similar rules apply to *in vivo* packing and to packing within the crystal lattice, for the following reasons. First, crystallization of nucleosome core particles is performed at relatively low ionic strength and at very high (micromolar) nucleosome concentrations. Second, and more importantly, crystallization is the result of the tight packing of particles into a regular arrangement, and is driven by the search for an energetically favorable mode of interaction between the surfaces of two neighboring

particles. It is believed that these same constraints also apply to chromatin condensation *in vivo.*

Three types of major interactions drive the formation of *Xla*-NCP crystals into staggered layers of nucleosome cores. First, the end-to-end stacking of nucleosomal DNA is the major driving force in forming one plane of the crystal lattice (green particles in Figure 3A). Second, the histone octamers contact one another through a series of interactions between the basic H4 tail of one nucleosome and the acidic patch region of a neighboring particle (Fig. 4B; and (Luger and Richmond, 1998). These contacts are essential for crystallization, as has been shown by the mutation of *Xla*-H4 Lys-20 to Cys (K. Luger, unpublished results). Third, a Mn^{+2} mediated crystal contact directly chelates the base of H3 α1 to the H2B L1 loop of the neighboring particle (Figure 4A and B). These areas of protein-protein interaction connect two consecutive layers of nucleosome core particles (Figure 3B). Additional protein-protein and DNA-DNA interactions further stabilize the crystal lattice. Importantly, each of the involved residues listed above is conserved in yeast.

The DNA end-to-end crystal contacts are essentially maintained in *Sce*-NCP, with only minor differences in stacking geometry. However, the protein-protein interactions between nucleosomes are completely different. The result is that nucleosomes in neighboring planes stack on top of each other with their superhelical axes almost superimposed (Figure 3C), whereas the arrangement in *Xenopus laevis* is more staggered (Figure 3B). Despite this fact, the total surface area that is actually buried upon crystal formation is very similar (~4000 $Å^2$) between the two structures. One consequence of this arrangement is that individual layers are more tilted with respect to each other in *Sce*-

Figure 2.3

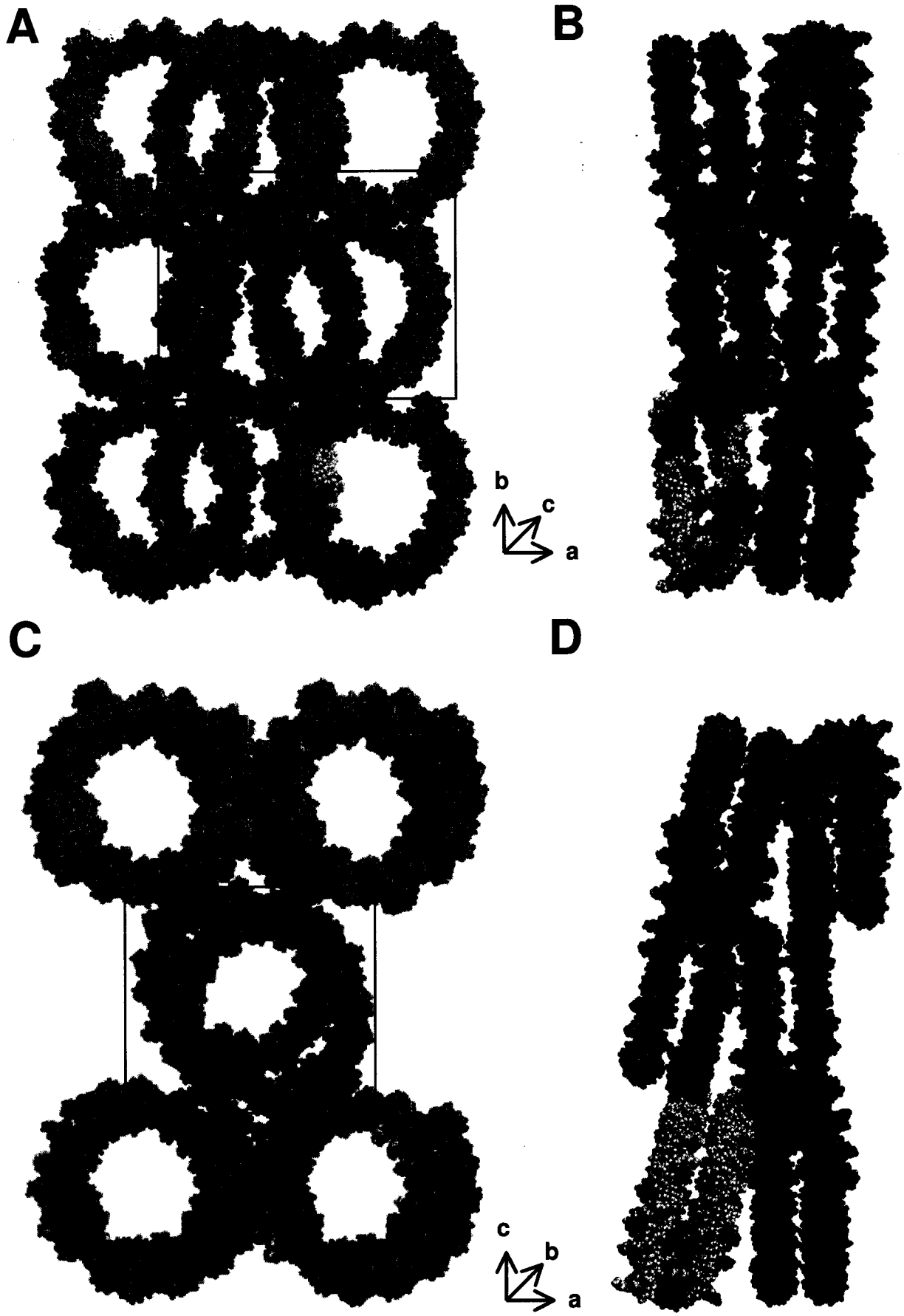

Figure 2.3. Crystal packing of *X. laevis* and *S. cerevisiae* nucleosome core particles. (**A**) *Xla*-NCP crystal packing viewed approximately down the superhelical axis. Short arrows show the approximate location of the three crystallographic axes. Only the DNA is shown for clarity; like colors denote nucleosomes which lie within the same plane. (**B**) The same arrangement of molecules is rotated by 90° around the crystallographic b-axis. (**C**) and (**D**) *Sce*-NCP crystal packing in the same views as (A) and (B), respectively. The discrepancy in the notation of the crystallographic *b*- and *c*- axes stems from the fact that the previous study used different programs to index the data (Luger et al., 1997). Particles whose molecular interaction is shown in Figure 4 are boxed.

NCP (compare Figure 3B and 3D). The different contacts between the histone octamers in *Sce*-NCP pulls the adjacent nucleosome upward, which causes the loss of the back-to-back crystal packing between nucleosomes within the same layer. This leads to the observed increase in the length of the crystallographic *c*-axis from 181 Å in *Xla*-NCP to 193 Å in *Sce*-NCP. The loss of this contact is evident when comparing the interaction of the central green particles with the neighboring red particles in Figure 3A and Figure 3C. As a practical consequence of these changes in crystal packing, *Sce*-NCP crystals were extremely fragile and would often shatter at the slightest touch.

The dramatic changes in nucleosome – nucleosome interactions seen in yeast is a result of contacts involving the C-terminal helix (αC) of H2B. This extremely well ordered helix lies exposed on the surface of the histone octamer, and plays an important role in defining the surface (Figure 1C). In *Xla*-NCP, it is involved in some minor contacts with the DNA of a neighboring particle. In contrast, the entire helix is involved in forming essential crystal contacts in *Sce*-NCP (Figure 4C and D). Within one region, a manganese coordination site is formed by two histidine and two glutamate residues from two neighboring nucleosomes. Glu-65 on α2 of H2A and His-52 on the L1 loop of H2B chelate a manganese ion that is held in turn by H2B' Glu-108 and H2B' His-112 at the base of αC of the adjacent nucleosome (Figure 5A). If such a contact was made in vivo (and we emphasize that the involvement of these residues in in vivo nucleosome packing is not supported by any experimental evidence), zinc would probably replace manganese.

The C-terminal region of H2B αC is also crucial in producing crystal interactions. Sequence alignment shows that this region is quite divergent between yeast and higher

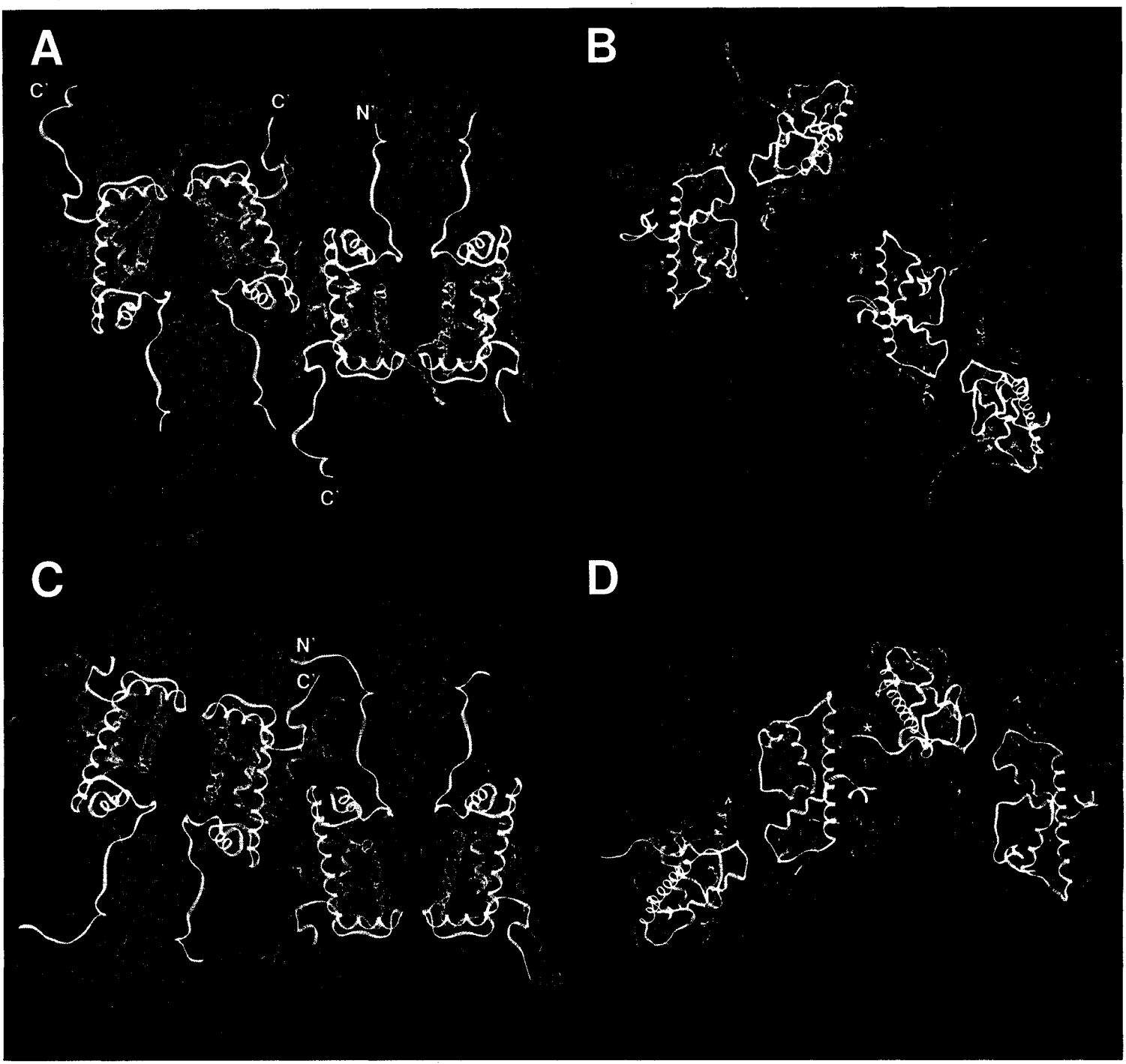

Figure 2.4: Protein-protein interactions within the crystal lattice.

(A) Crystal contacts between two neighboring nucleosomes in *Xenopus laevis* in a view that places the superhelical axis in a horizontal orientation (as seen in Fig. 1C). **(B)** The same *Xla*-NCP packing as shown in (A), but viewed down the molecular two-fold axis. This view is achieved by a 90° rotation around the superhelical axis (horizontal). In both views, the nucleosome core particle to the left of the pair corresponds to the center green particle in Figure 3A, whereas the right-hand particle corresponds to the blue particle in Figure 3A (boxed in Figure 3A and C, respectively). Histones are colored as in Figure 1. The location of the H2A and H4 histone tails is indicated. The position of the Mn^{2+} ion that is crucially involved in forming crystal contacts is shown (*). **(C and D)** Two yeast nucleosome core particles shown in the same orientation as seen in (A) and (B), respectively. With respect to Figure 3C, the same two particles are depicted as for *Xla*-NCP.

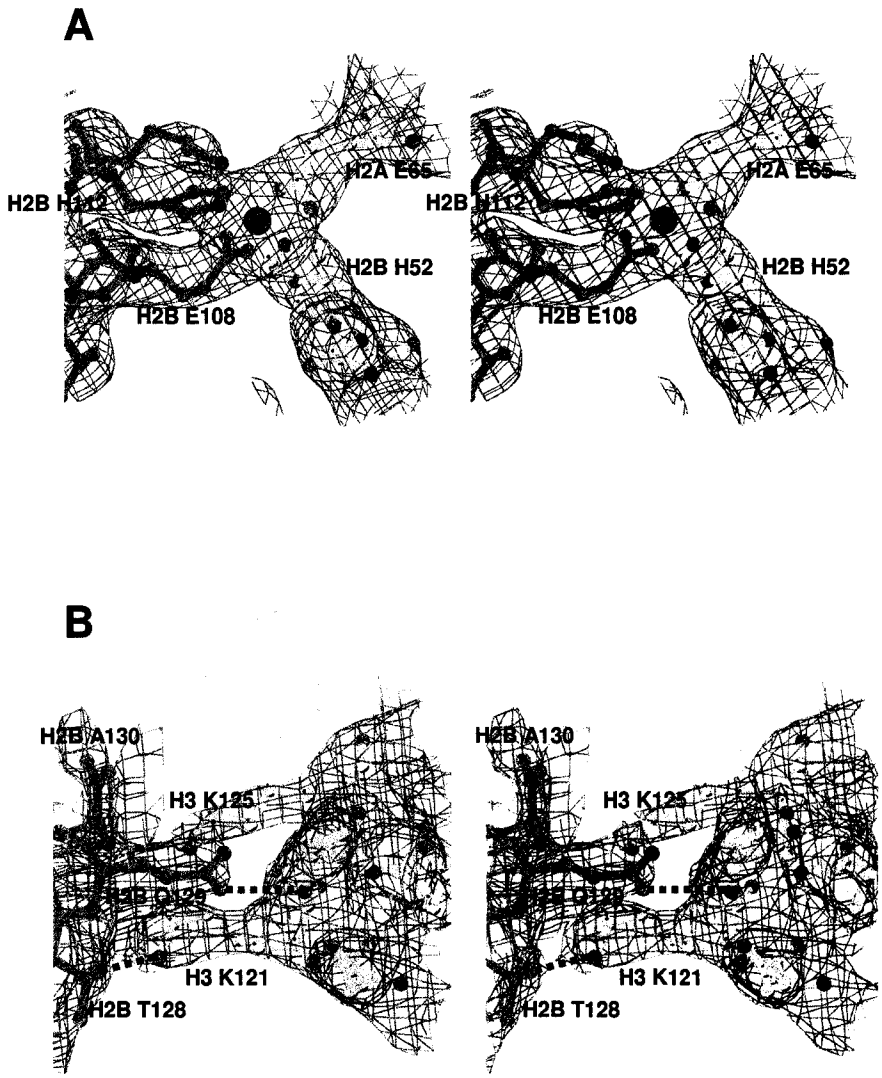

Figure 2.5. Details of nucleosome – nucleosome interactions in yeast NCP.

(A) Stereo view of a section of the $|2F_o - F_c|$ electron density map, calculated at 3.1Å and contoured at 1σ, showing a Mn^{+2} mediated crystal contact between H2A Glu65 and H2B His52 of one nucleosome (dark red) and H2B' Glu108 and H2B' His112 of the neighboring nucleosome (gold). **(B)** Stereo view of the hydrogen bonds between the H2B C-terminal end of H2B αC (dark red) and residues in histone H3 of a neighboring nucleosome core particle (gold), showing a section of the $|2F_o - F_c|$ electron density map calculated at 3.1 Å and contoured at 8-1σ.

eukaryotes. *Saccharomyces cerevisiae* contains two additional amino acids along with other changes on the C-terminus of H2B (Figure 1A). H2B Thr-128 and Gln-129 form hydrogen bonds with Lys-121 and Lys-125 of the H3 chain of the neighboring nucleosome (Figure 5B). None of these residues are present in *Xenopus laevis* (Figure 1A). We propose that the contacts located along the H2B αC helix are responsible for the alternate crystal packing observed in yeast.

As a result of the change in the relative position of neighboring nucleosomes within the crystal lattice (best viewed by comparing Figure 4B and D), the yeast H4 N-terminal tail is no longer able to interact with the acidic patch of the neighboring nucleosome. In fact, the H4 N-terminal tail is not involved in any crystal contacts and takes a completely different path. This results in the large RMS deviation of histone H4' (Table 2). Consequently, neither acidic patch is involved in any crystal contacts. Instead, both regions tightly coordinate a manganese ion, using the side chains of H2A Asp-90, Glu-92, and Glu-61. The altered arrangement of nucleosomes within the yeast crystal lattice brings the N-terminal tail of H2A into close proximity with the C-terminal tail of H2A of a neighboring particle (Figure 4C). Although the electron density in this region is rather weak, these tails are positioned to cross over and make crystal contacts. One contact between *Sce*-H2A Lys-120 and *Sce*-H2A Thr-12 in the neighboring nucleosome is clearly observed in the crystal structure. Incidentally, the long H3 N-terminal tail from yet another nucleosome core particle is headed into the same direction (data not shown). These observations further support the involvement of histone tails in inter-particle contacts.

2.5 Discussion

The crystal structure of the yeast nucleosome core particle shows that the overall principles of DNA organization in the nucleosome are maintained between lower and higher eukaryotes. The path of the DNA as well as the overall conformation of the structured regions of the histone proteins are conserved, as is the location of many critical structural water molecules and divalent ions (K. Luger, manuscript in preparation). Sequence variations between yeast and higher eukaryotes are distributed throughout the histones, and are located both on the surface of the histone octamer as well as buried deep within the nucleosome structure. The latter could be collectively responsible for a subtle destabilization of the yeast nucleosome core particle. This finding is consistent with a more open chromatin structure in yeast. None of the residues that are critically involved in the organization of the DNA is affected by these changes. Importantly, the structure presented here allows us to study mutations that have been isolated in the structured regions of yeast histone proteins by *in vivo* screens in a structural context (for example, (Hirschhorn et al., 1995; Kruger et al., 1995; Kurumizaka and Wolffe, 1997; Recht and Osley, 1999; Santisteban et al., 1997; Wechser et al., 1997).

2.5a Sequence variations are distributed throughout the nucleosome structure and may result in subtle destabilization of the yeast nucleosome

The most significant changes in protein-protein interactions within the yeast nucleosome core particle, compared to nucleosomes from higher organisms (Luger and Richmond, 1998); (Suto et al., 2000); (Harp et al., 2000), are located in the H2A L1 loops where the two H2A-H2B dimers interact. We found a complete absence of all stabilizing interactions (including hydrophobic interactions) in this area in yeast. This is in contrast to four strong hydrogen bonds and salt bridges located in this region in the structures of

metazoan nucleosome core particles (Harp et al., 2000; Luger et al., 1997). How much does this relatively small interface contribute to nucleosome stability? We are currently investigating this question using fluorescence energy transfer to compare the relative stability of nucleosomes containing *Xenopus laevis* and *Saccharomyces cerevisiae* histones. Considering that this region is seemingly involved in holding together the two gyres of the DNA superhelix (Figure 1C), even a subtle destabilization could have a relatively large effect on overall nucleosome stability during transcription. The same set of residues that we have shown to be prohibitive for the formation of a stable interface is also seen *Schizosaccharomyces pombe* and in sea urchins. Similarly prohibitive combinations of amino acids are found only in Euglena, Leishmania, and slime molds. Generally, this region is rather divergent both among species and among histone variants (Baxevanis and Landsman, 1998). We have speculated earlier that the L1 loops could provide a mechanism to ensure that the gene product from one particular H2A gene is incorporated into a single nucleosome (Suto et al., 2000). The results presented here suggest a more general role of this region in modulating nucleosome stability.

2.5b Histone tails can assume various distinct conformations

The role of the histone N-terminal tails in the regulation of transcription, exerted mainly by reversible post-translational modification of conserved lysine and serine residues is undisputed (see (Strahl and Allis, 2000), for a recent review). The N-terminal tails have also been shown to be involved in the condensation of the chromatin fiber (Carruthers and Hansen, 2000), and in the formation of silent chromatin regions by interaction with other factors (Grunstein, 1997). The detrimental effects of N-terminal tail deletions *in vivo* suggest that they have many different, yet partially redundant, functions

(Grunstein et al., 1995); (Grunstein, 1997); (Hansen et al., 1998). We show that the H4 and H2A N-terminal tails, and the H2A C-terminal tail can assume completely different conformations depending upon the structural context. We have evidence that this holds true for all histone tails. This structural heterogeneity, which might be potentiated by post-translational modifications (Wang et al., 2000) might allow the histone tails to interact with a variety of different protein factors and to perform a large number of different functions (Hansen et al., 1998).

2.5c Sequence variations lead to changes in nucleosome-nucleosome interactions

It is reasonable to suggest that *S. cerevisiae*, which maintains a relatively open chromatin structure and lack histone H1, organize nucleosomes into higher order structures that differ significantly from that found in higher eukaryotes. The folding of nucleosomal arrays into compact fibers involves, by definition, the close packing of nucleosome cores in an energetically favorable manner. Regardless of the source of histones, this process is not dependent on linker histone H1 *in vitro*. However, it does depend on the presence of the N-terminal tails (Carruthers and Hansen, 2000). This is reflected in the crystal packing of nucleosome core particles of both *Xenopus laevis* and *S. cerevisiae*, although the *in vivo* interactions at the molecular level are likely to be different. In yeast, nucleosome-nucleosome interactions are mainly governed by the C-terminal α-helix of H2B, with contribution from the H2A C- and N-terminal tails. The packing also seems to take advantage of basic residues that are clustered along the protein-DNA interface to pack against the DNA of the neighboring nucleosome (Figure 3A). This is in marked contrast to the crystal packing in nucleosomes from higher

eukaryotes, where the H4 N-terminal tail interacts with an acidic region on the surface of the histone octamer. Our data confirms that the role of histone tails in the formation of higher order structure is highly redundant, as suggested earlier (Tse and Hansen, 1997); [Schuster, 1986 #1360]; (Ling et al., 1996). We also note a conspicuous absence of protein-DNA interaction in forming inter-nucleosome contacts in both crystal structures.

We demonstrate that nucleosomal interactions may be completely altered by relatively minor amino acid changes (such as the addition of two amino acids to the C-terminal end of H2B αC), while maintaining the contacts that are mediated by DNA. This shows that there are indeed several ways in which nucleosomes may be packaged in an energetically favorable way, and that small changes in the histone surface are sufficient to provoke these changes. This finding has important implications for our understanding of the formation of higher order structure. The role of the flexible histone tails in the formation of higher order structure and crystal packing is well established (Moore and Ausio, 1997); (Carruthers and Hansen, 2000). Thus, it is tempting to speculate that changes imparted by the reversible modification in histone tails provides a means to switch between different modes of nucleosome-nucleosome interactions *in vivo*. Furthermore, methylation of lysine residues in the structured regions of the histones could have similar effects. We are careful to point out that the precise molecular mechanism by which nucleosomes pack together in the context of a chromatin fiber may not directly be reflected in crystal packing. However, it has been recently shown in the crystal structure of bacterial flagellin that protein crystals can indeed mimic reality (Samatey et al., 2001).

The crucial involvement of the C-terminal helix of H2B in inter-nucleosomal contacts is of particular interest in light of the recent discovery that H2B Lys-123 is ubiquitinated *in vivo* by Rad6 in yeast. Ubiquitination is predicted to disrupt these contacts and lead to local or global effects on chromatin folding. Consistent with this idea, mutation of Lys-123 in yeast leads to defects in mitioic cell growth and meiosis (Robzyk et al., 2000). Additional *in vivo* studies also support the notion that ubiquitination of the H2B C-terminus has an effect on chromatin accessibility. Ubiquitinated H2B has been found to have a role in activated transcription that partially overlaps with that of the nucleosome remodeling factors Swi/Snf and SAGA (M. A. Osley, personal communication). This suggests that inter-nucleosomal contacts that are mediated by H2B αC may indeed be involved in forming inhibitory chromatin structures *in vivo*, and that the degree of chromatin compaction may be regulated by Rad6-dependent ubiquitination in yeast.

In summary, our findings confirm that the overall structure of the nucleosome core particle is conserved between yeast and higher eukaryotes. However, localized sequence variations, particularly in the L1 loop of H2A, may serve to fine-tune nucleosome stability. Importantly, we have shown that there are different ways to form stable inter-particle contacts. We have verified that the major driving force in the formation of such contacts is interactions made between the protein moiety of nucleosomes. We further show that packing is altered in response to subtle sequence variations. This has important implications for our understanding of how the reversible modification of histone tails and structured regions may be employed to alter higher order chromatin structure.

2.6 Acknowledgements

We would like to thank Drs. Carl Wu and Xuetong Shen (Laboratory of Molecular Cell Biology, NCI, NIH) for yeast histone expression plasmids, and Drs. T. Earnest and Gerry McDermott at the Advanced Light Source in Berkeley for support. We are particularly grateful to Dr. M. A. Osley for critical reading of the manuscript and for the kind permission to cite some of her unpublished data. This work was supported in part by the NIH (GM61909-01), by a Searle Scholar Award to K.L., by the Cancer League of Colorado, and by grant RG0059/2000-M from the Human Frontiers Science Program.

2.7 Protein Data Bank Coordinates

Coordinates have been deposited with the Protein Data Bank under accession number 1ID3.

Supplemental Figures for Chapter 2

The following figure was cited as "supplemental figure 1" in the text.

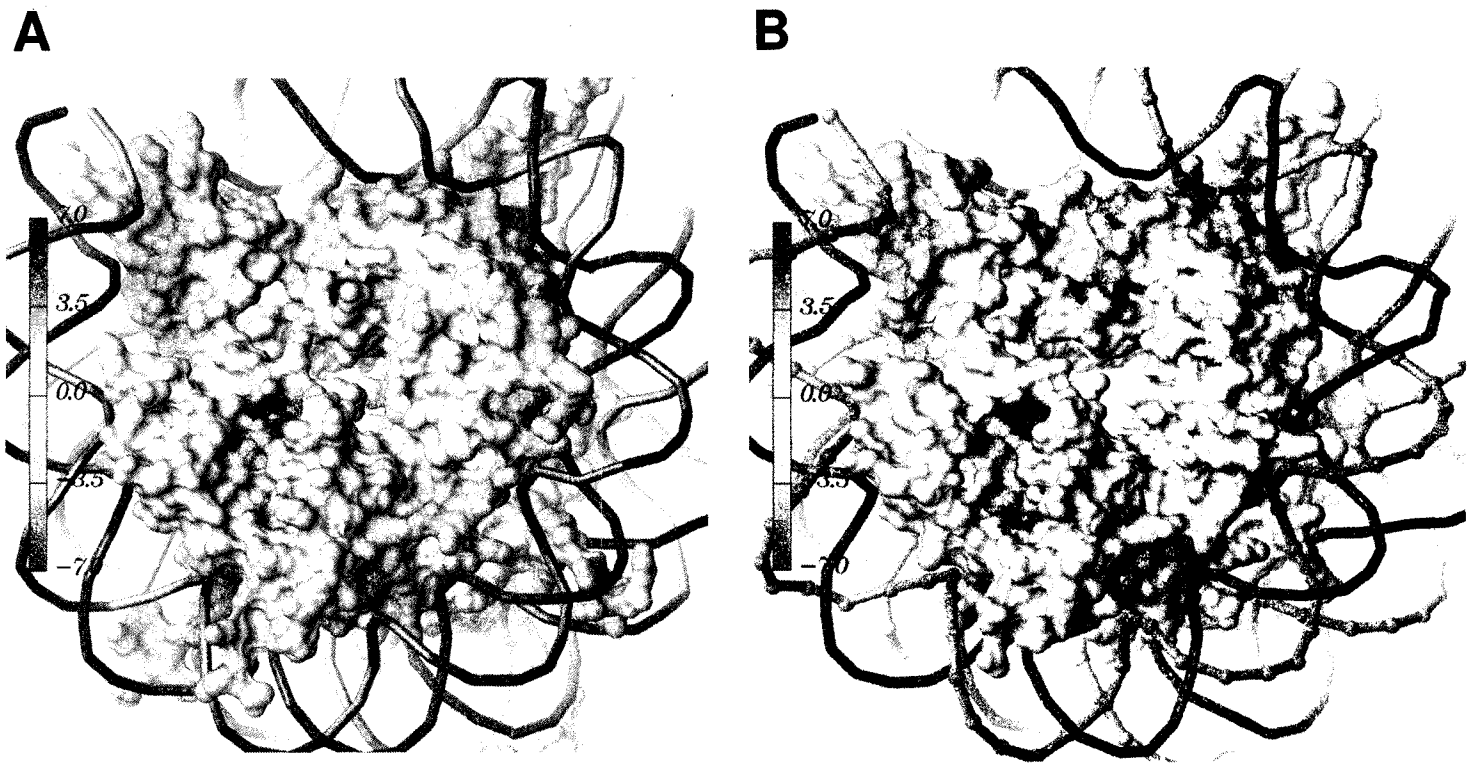

Figure 2.6. Molecular surface of *X. laevis* and *S. cerevisiae* nucleosome core particles.

(A) Molecular surface representation of the crystal structure of the nucleosome core particle from *X. laevis*. A scale showing the coloring scheme of the acidity or basicity of the surface charge is shown. **(B)** Molecular surface representation of the nucleosome core particle from *S. cerevisiae*.

Chapter 3

The Yeast Nucleosome Core Particle Displays a Decreased Stability That Is Due, In Part, to Structural Changes Within the H2A L1 loops

In the crystallographic studies outlined in the previous chapter, we found evidence to support the idea that the yeast nucleosome core particle is less stable than that of higher eukaryotic organisms due to a complete loss of interactions between the H2A L1 loops. To test this hypothesis, we set out to determine the relative stability of the yeast nucleosome core particle compared to that of *Xenopus laevis*. The *X. laevis* L1 loop was mutated to match that of *S. cerevisiae* in order to verify the hypothesis that the L1 loops are the exact regions responsible for the decreased stability of the yeast nucleosome. This data will be written up for submission to the journal *Biochemistry* as referenced below.

White, C.L., Mellett, A., Daley, S., and Luger, K. The yeast nucleosome core particle displays a decreased stability that is due, in part, to structural changes within the H2A L1 loops.

3.1 Abstract

The fundamental repeating element in chromatin and the primary level of DNA compaction is the nucleosome core particle, which comprises 146 base pairs of DNA wrapped around a histone octamer core. The histone proteins are some of the most conserved proteins known, indictive of the critical role of packaging DNA into nucleosomes in eukaryotes. Yeast histones contain the greatest sequence variation among eukaryotes, with *Saccharomyces cerevisiae* having 79% sequence identity as compared to the higher eukaryotic organism *Xenopus laevis*. The crystal structure of the *S. cerevisiae* nucleosome core particle suggests it is a less stable complex as compared to the previously solved structure from *X. laevis*. In the study outlined here, we have set out to test this hypothesis by determining the stability of the yeast nucleosome core particle relative to the *X. laevis* core particle using biophysical methods. Using mutational analysis, we determined a region within the yeast structure that is at least partly responsible for the altered stability. Our results show that the *S. cerevisiae* nucleosome is indeed less stable than that from *X. laevis*, and that this decreased stability is due to differences within the L1 loop.

3.2 Introduction

The first level of DNA compaction in eukaryotes is the nucleosome core particle, which involves wrapping 147 base pairs of DNA around a histone octamer core. The three-dimensional structure of the histone octamer is determined by the amino acid sequence of each histone protein. The sequence also encodes the precise location of bond formations between the proteins and contact points with the DNA. Because of the fact

that the nucleosome core particle plays such a vital cellular role in all eukaryotic organisms, the amino acid sequences of the histone proteins are among the most conserved known. In comparing histone sequences, the histones from yeast are among the most divergent from mammalian histones, with yeast having approximately 79% sequence identity as compared to higher eukaryotes (Baxevanis and Landsman, 1998).

Yeast is a unicellular organism whose entire genome is only ~0.5% the size of that of humans. However, the size of the nucleus is approximately the same. Yeast contains a haploid set of 16 chromosomes, with genes representing 72% of the total DNA sequence. This is much different from higher eukaryotes, which have five times more genes than yeast, but contain three hundred times more DNA. 40-60% of the yeast genome is constitutively transcribed during logarithmic growth, in contrast to the small percentage of actively transcribed genes at any given time in the cells of higher eukaryotes (Lohr and Ide, 1979). Thus, the need for extensive DNA compaction is less stringent for yeast. The possibility exists that the differences between the yeast histone sequences and those from higher eukaryotes allow the yeast chromatin structure to be more open to larger proportions of the total genome being expressed. This is supported by the fact that when yeast cells are in logarithmic growth, its chromatin is more rapidly digested by DNase I than the chromatin from chicken erythrocytes or calf thymus (Lee et al., 1982). In addition, it appears that histone HI does not play an important role in the regulation of chromatin condensation and gene activation in yeast (Puig et al., 1999). This major difference in nucleosomal compaction between yeast and mammals could in part reflect the more open chromatin structure that is needed for constitutive gene expression.

One way in which the more open chromatin structure in yeast is maintained could be due to a decreased stability of the yeast nucleosome core particle. This would allow easier nucleosomal dissociation in order to rapidly activate transcription. Previous experimental evidence supports the conclusion that yeast nucleosomes are less stable than those from higher eukaryotes. Yeast mononucleosomes demonstrate an increased molar ellipticity and a lower melting transition than those from chicken and calf, which suggests that the DNA is less constrained (Lee et al., 1982). Only 30% of plasmid DNA in *S. cerevisiae* is constrained from thermal untwisting *in vivo*, whereas thermal untwisting of DNA is completely suppressed in nucleosomes formed with chicken and monkey histones (Morse et al., 1987). Another study showed that yeast mononucleosomes partially dissociate at 0.5M NaCl, conditions that did not affect chicken nucleosomal cores, indicating a higher susceptibility to ionic strength of the yeast nucleosomes (Pineiro et al., 1991). The same study showed that treatment of yeast nucleosome core particles with the amino group reagent dimethylmaleic anhydride resulted in the selective release of histones H2A and H2B (Pineiro et al., 1991). The authors of this paper concluded that the electrostatic forces holding the nucleosome core particle together might be weaker in yeast than in chicken. These and other studies taken together suggest that nucleosomes from yeast may be less stable than those from higher eukaryotes, and this decreased stability could be due to sequence variations in histones H2A or H2B (Lee et al., 1982), (Wallis et al., 1980).

The crystal structure of the nucleosome core particle from the yeast *Saccharomyces cerevisiae* revealed that sequence variations in histones H2A and H2B cause a loss of interactions within the H2A L1 loops where the two H2A-H2B dimers

interact (White et al., 2001). All nucleosome structures solved from higher eukaryotes reveal that the H2A L1 loop contains a number of strong hydrogen bonds and salt bridges that hold the two H2A-H2B dimers together and thus acts to stabilize the two gyres of the DNA superhelix (Luger et al., 1997), (Harp et al., 2000), (Davey et al., 2002). However, two amino acid differences in yeast (H2A Glu42 and H2B Ala85) result in a complete loss of interactions at this interface (White et al., 2001). The H2A L1 loop is also the site of major changes in all histone variant structures solved to date (Suto et al., 2000) (Chakravarthy et al, unpublished data). Therefore, due to this suggested importance of the H2A L1 loop interactions, which seemingly stabilizes the interactions between the H2A/H2B dimers and thus the DNA superhelix, these structural differences suggest a destabilization of the yeast nucleosome core particle as compared to nucleosomes from higher eukaryotes. It is speculated that this decreased stability could result in the easier depletion of the H2A-H2B dimers from the nucleosomal core (White et al., 2001).

In the study presented here, we have investigated the overall stability of the yeast nucleosome core particle compared to that from higher eukaryotic organisms. Utilizing fluorescence resonance energy transfer as a tool to study nucleosomal stability, we have found that the nucleosome from *Saccharomyces cerevisiae* is less stable than that from *Xenopus laevis* in response to salt-induced disassembly. Temperature-dependent shifting assays and nucleosome dilution dissociation experiments confirm these results. However, our current data suggests that this decreased stability is not only due changes in the H2A L1 loop. However, our results support the idea that yeast can maintain a more open chromatin structure in order to keep most of its genes constitutively transcribed.

3.3 Materials and Methods

3.3a Expression, purification, and reconstitution of yeast nucleosomes

Recombinant yeast histone proteins were overexpressed in BL21 (DE3) CodonPlus RIL- (Stratagene) from pet28a expression plasmids, and histones from *Xenopus laevis* were expressed from plasmids grown in Bl21 (DE3) plysS cells. The proteins were isolated in inclusion bodies and purified according to published protocols (Luger et al., 1999). Histone octames were refolded by mixing the four histone proteins in eqi-molar ratios and dialyzing against a 2M salt buffer as described (Dyer et al., 2003). Nucleosome core particles were reconstituted by salt gradient dialysis of histone octamers and an asymmetric146 bp DNA fragment derived from 5S DNA (Dyer et al., 2003).

3.3b Mutagenesis of the *Xenopus laevis* L1 loop

The residues involved in the formation of the H2A L1 loop from *Xenopus laevis* were mutated to match the residues found in *Saccharomyces cerevisiae*. This involved mutating H2A E41 to a glutamine, and H2B H79 to an alanine. Site-directed mutagenesis of the *Xenopus laevis* histone expression plasmids was completed using the QuikChange Site-Directed Mutagenesis Kit from Stratagene. Forward and reverse complementary primers were synthesized that contained the desired mutations, and PCR was carried out according to kit directions. To confirm the presence of the desired mutations and to ascertain that no other mutations had occurred, the complete coding regions of the mutated DNAs were sequenced. Protein expression, purification and octamer refolding of the mutated histone proteins were completed as described above.

3.3c Nucleosome Dilution Experiments

Nucleosomes used in the dilution experiments were reconstituted by mixing *Saccharomyces cerevisiae* or *Xenopus laevis* octamer with 146 bp α-satellite DNA which was radiolabeled at its 5' ends with T4 polynucleotide kinase (Roche) and [γ-^{32}P]ATP using standard protocols. Nucleosome reconstitution was performed by a stepwise dilution protocol as described in (Gottesfeld et al., 2001), using steps of 2M, 1M, 0.8 M, 0.67 M, and 0.2 M NaCl. Incubations were carried out at room temperature, and the final NCPs were heat shifted at 37°C for one hour. The nucleosomes were then subjected to serial dilution in a buffer containing 100mM NaCl, 10mM Tris/HCl pH 7.6, 10% glycerol, 0.1% NP-40, 0.95 μg/μl glycogen. Dilutions were carried out in a 21 μl reaction volume, and NCPs were allowed to equilibrate at room temperature for three hours in order to obtain equilibrium at the following nucleosome concentrations: 16.7 nM, 5.6 nM, 1.9 nM, 0.62 nM, 0.21 nM, 0.07 nM, and 0.02 nM. The samples were then run on 6% native-PAGE gels in a 1X TBE buffer, and the gels were analyzed by phosphorimage analysis.

3.3d Fluorescent Labeling of DNA ends

In order to achieve labeling of the ends of the DNA with different fluorescent chromophores, the two strands of an asymmetric 146 bp 5S DNA fragment were separated by incubating the DNA in 500 mM NaCl and 10mM NaOH for 15 minutes at room temperature. The separated strands were loaded onto a DEAE-TSK ion exchange column in a buffer containing 10mM NaOH and the two separate strands were eluted with a gradient from 0.35 M to 1.0 M NaCl. A cystaminedihydrochloride/EDC (1-ethyl-3,3-dimethylaminopropylcarbodiimide) reaction was carried out in order add cystaminedihydrochloride onto the 5' ends of each of the separate DNA fragments. The

strands were then purified over an ion-exchange column in order to remove any excess linker. The strands were then incubated with either the donor chromophore 7-diethylamino-3-(4'-maleimidylphenyl)- 4-methylcoumarin (CPM) or the acceptor chromophore fluorescein-5-maleimide (FM) overnight in the presence of TCEP. The excess dye was purified away by spin columns of Sephadex G-25 resin. The strands were ethanol precipitated and resuspended in TE in order to achieve high concentrations, followed by reannealing the two labeled strands together. This is accomplished by mixing the two strands together in equal ratios in a 500mM NaCl buffer, and then heating at 90°C for 3minutes, cooling at 4°C for 5 minutes, and then heating again at 75°C for 15 minutes. The DNA was allowed to cool to room temperature slowly, followed by several cycles of heating at 37°C and cooling on ice. The DNA was finally analyzed by gel electrophoresis in order to make sure that the strands were properly labeled and complete re-annealing occurred.

3.3e Fluorescence Resonance Energy Transfer (FRET) Experiments

FRET experiments were carried out as described in detail in Park et al. (publication in progress). In short, nucleosomes containing non-labeled histone octamers and double-labeled 5S DNA (donor chromophore FLU on one DNA end and acceptor chromophore CPM on the other end) were mixed with 0.1 M NaCl to a final protein concentration of 20 μg/ml and incubated for 30 minutes at 20°C. The distance dependent fluorescence emission of the chromophores was monitored to distinguish the steps of NCP disassembly. As the ends of the DNA begin to dissociate, the distance between the two chromphores increases which reduces the ability to obtain fluorescence transfer, and thus the donor signal increases. The excitation wavelength was set at 385nm and the acceptor

emission was observed at 520nm in order to obtain the initial fluorescence spectrum. 5.0 M NaCl was then added stepwise to a final concentration of 1.5 M. The increase in donor fluorescence was monitored at 475nm during all steps of salt addition. All experiments were carried out at 20°C, and the data was corrected for dilution before analysis.

3.3f Temperature-dependent shifting assays

Heat shifting assays were performed by heating aliquots of reconstituted nucleosomes (0.7 mg/ml) for the time points indicated in a PCR thermal cycler at 37°C. Shifting was arrested by rapid cooling to 0°C, and 1.75μg of each sample was loaded onto a 5% native-PAGE gel (in a 0.2x TBE buffer) after adding sucrose to a final concentration of 5% (w/v). Gels were run at 4°C, and the gels were first stained with ethidum bromide, followed by staining in Coomassie blue.

3.4 Results

3.4a Nucleosome dilution experiments reveal that nucleosomes from *S. cerevisiae* dissociate more readily than those from *X. laevis*

Previous biophysical data suggests that nucelosomes from yeast are less stable than those from higher eukaryotic organisms (Lee et al., 1982), (Morse et al., 1987), (Pineiro et al., 1991). The crystal structure of the nucleosome core particle from *S. cerevisiae* also suggests that yeast nucleosomes could have a decreased stability (White et al., 2001). The differences that imply this altered stability of yeast NCPs are found in the region of the H2A L1 loops. The two H2A-H2B dimers interact through the L1 loops, and this interaction contributes to the stability of the histone octamer and thus the DNA

helix (Fig. 3.1B). Only two amino acids are different in the yeast L1 loop as compared to *X. laevis* (H2A Glu42 and H2B Ala85) (Fig. 3.1A). However, these changes lead to a total loss of hydrogen bonding in the L1 loop of the *S. cerevisiae* NCP (Fig. 3.1C). The loss of these interactions, therefore, could lead to the destabilization of the H2A/H2B dimers, and thus the entire nucleosome structure. Studies have shown that nucleosomes dissociate into free DNA and histones upon dilution (Cotton, 1981), (Yager, 1984). A dilution method has previously been described which enables one to determine the apparent binding affinities of a particular histone octamer to DNA (Gottesfeld and Luger, 2001). We chose this method to compare the affinity of the *S. cerevisiae* histone octamer to free DNA compared to the octamer from *X. laevis*. To perform the experiment, the 146 bp α-satellite DNA fragments were radiolabeled with P^{32} and then reconstituted into nucleosomes containing either the *S. cerevisiae* or *X. laevis* histone octamer. Serial dilutions of the nucleosomes were prepared in a buffer containing 100 mM NaCl. The nucleosomes were allowed to equilibrate for 3 hours at room temperature, and then analyzed by native-PAGE electrophoresis. As seen in Fig. 3.2, under the conditions used, yeast nucleosomes dissociate more readily than those from *X. laevis*. Therefore, the histone octamer from yeast has a slightly lower affinity for DNA than does the *X. laevis* octamer.

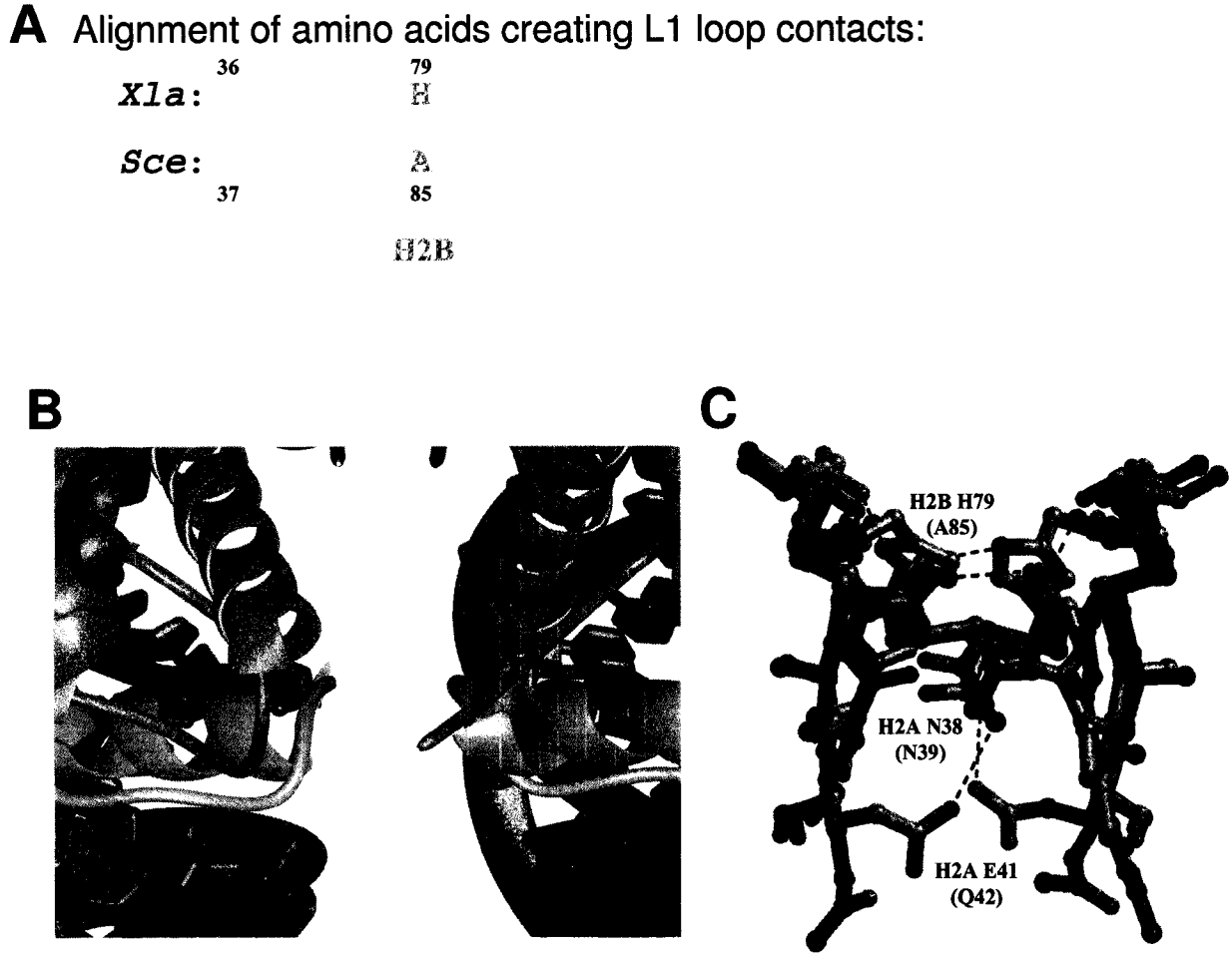

Figure 3.1 The location and structure of the L1 loop in the *S. cerevisiae* nucleosome core particle.

(A) Sequence alignment of the L1 loops from *X. laevis* (*Xla*) and *S. cerevisiae* (*Sce*). The amino acids are colored as to the histone each is contained in as shown. The first residue number of the H2A amino acids and the number of the H2B amino acid is indicated for each type. **(B)** A close-up view of the H2A L1 loop viewed using a ribbon diagram of the crystal structure of the *S. cerevisiae* nucleosome core particle, viewed between the two DNA gyres with parts of the DNA removed for clairty. Histone colors are the same as in (A), with the DNA colored in teal. **(C)** An overlay of the specific side-chain structures of the H2A L1 loops from *X. laevis* (purple) and *S. cerevisiae* (green) shown in the same view as in (B). The *X. laevis* amino acids are labeled with the cooresponding residues of *S. cerevisiae* shown in parentheses. Hydrogen bonding in the *X. laevis* structure is shown by black dashed lines. Note the complete lack of hydrogen bonding in the yeast structure.

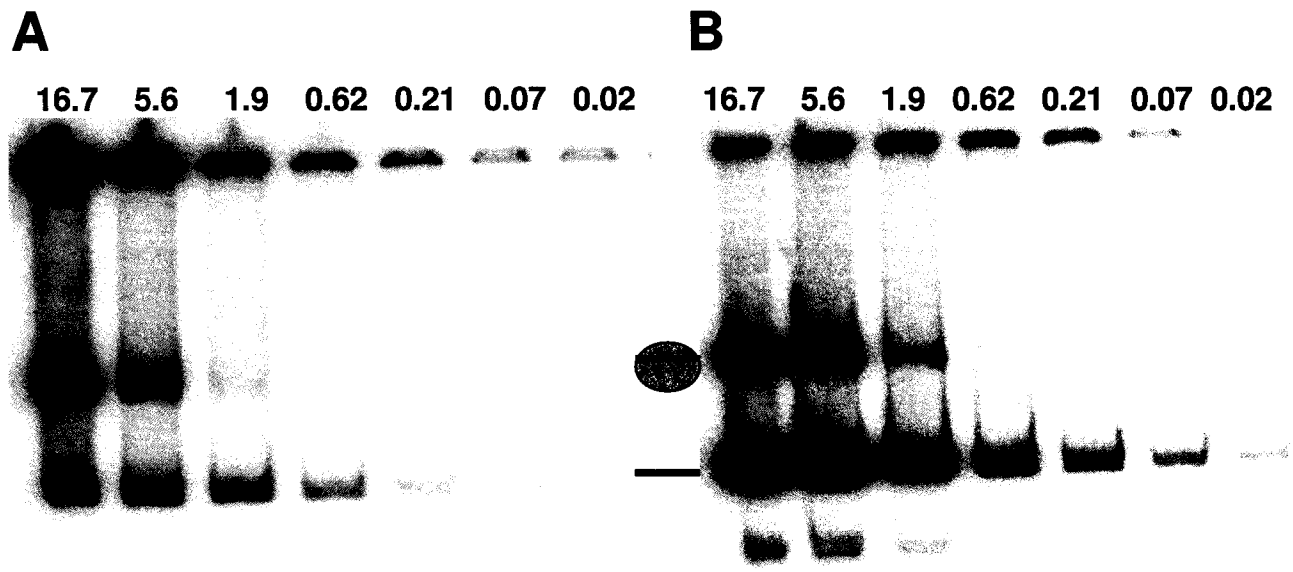

Figure 3.2 Dilution studies of the yeast nucleosome core particle

(A) 6% Native-PAGE gel showing the sequential dilution of the *S. cerevisiae* nucleosome core particle. The nucleosome concentration for each lane is given in mM. The upper band is the nucleosome core particle, with the lower band being free DNA as shown schematically. The lowest band seen in some lanes is free 73mer DNA. The gel was analyzed by phosphorimage detection. **(B)** Dilution of the *X. laevis* nucleosome core particle, with nucleosome concentration in each lane given in mM. Gel conditions and analysis are the same as in (A).

3.4b FRET experiments show that *S. cerevisiae* nucleosomes are less stable than those from *X. laevis*

To further test the hypothesis that yeast nucleosomes are destabilized, we utilized fluorescence resonance energy transfer (FRET) to compare the stability of nucleosome core particles from *S. cerevisiae* with those from *X. laevis*. Our lab previously utilized FRET successfully in order to study nucleosome stability by monitoring their salt-dependent dissociation (Park et al, publication in progress). Nucleosome core particles dissociate in high salt conditions, and nucleosomes with decreased stability will dissociate more readily in increasing salt concentrations as compared to those with higher stability. This process can be observed by monitoring the distance dependent fluorescence emission of chromophores within the nucleosome. For the experiments presented here, each end of a 146 bp α-satellite DNA fragment was labeled with a different chromophore (either the donor chromophore CPM or the acceptor chromophore FM). As salt was added, the decrease in donor quenching was monitored as donor emission increases when the distance between chromophores becomes too great for transfer to occur. The results show that yeast nucleosomes are indeed less stable than those from *X. laevis*, since yeast nucleosomes begin dissociating at a lower salt concentration (Fig. 3.3A). It has been found that the dissociation of *X. laevis* NCPs begins around 200mM NaCl. Because the yeast NCP begins to dissociate almost immediately in the presence of even 100 mM salt, a FRET experiment was performed where the initial salt concentration was 0 M NaCl. It was found that the salt concentration at which the yeast NCPs begin to dissociate was 100 mM NaCl (Fig. 3.3B) compared to the average 200 mM for *X. laevis* (Fig. 3.3B). Therefore, no baseline is

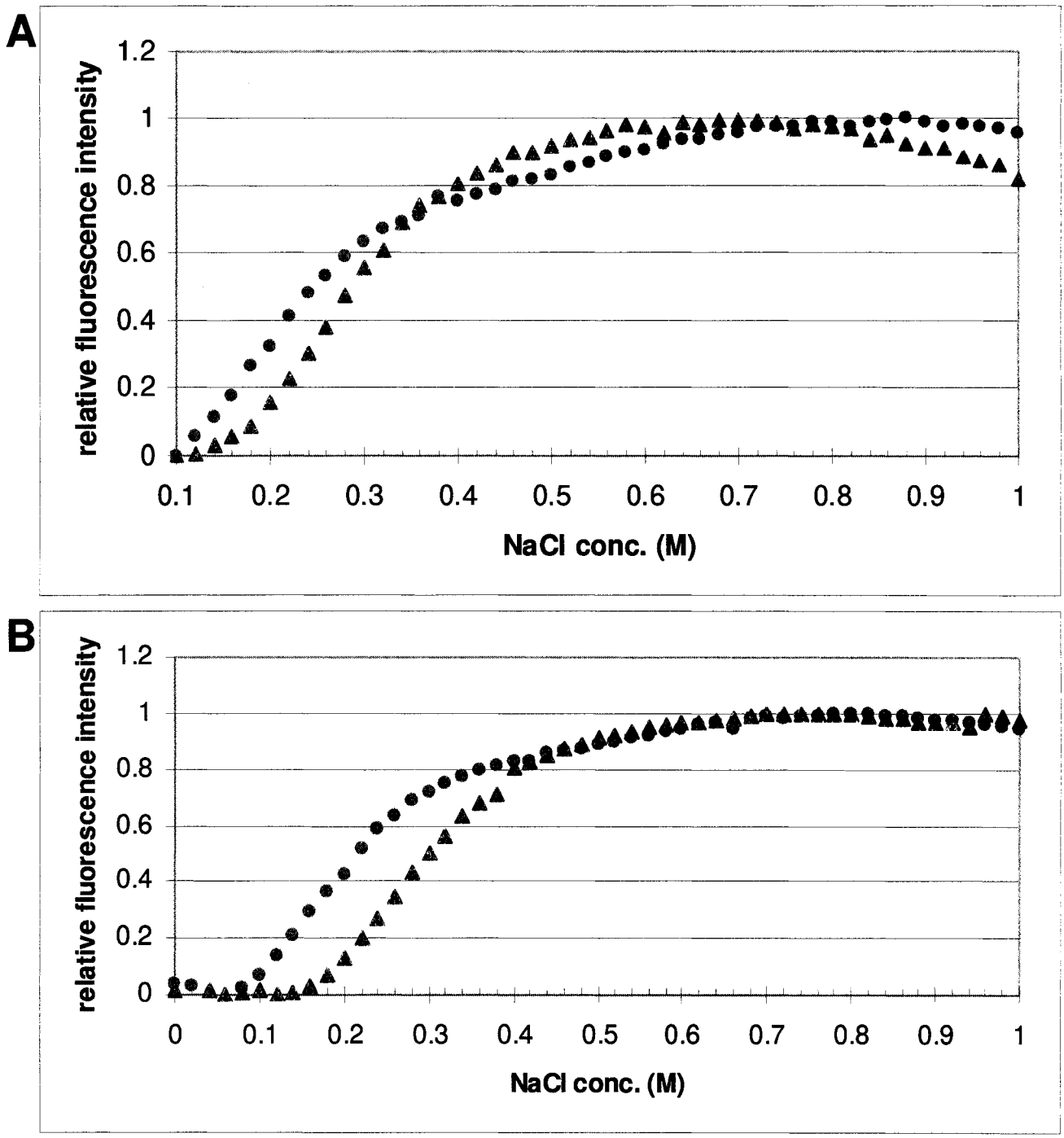

Figure 3.3 FRET studies reveal a decreased stability of the yeast nucleosome core particle

(A) The salt dependent dissociation of *S. cerevisiae* NCPs (purple circles) compared with *X. laevis* NCPs (blue triangles). NaCl was titrated from 0.1 M to 1.0 M in 0.02 M steps, and the donor emission was recorded at each step. The excitation wavelength was set at 385 nm and donor emission was monitored at 475 nm. Data was corrected for dilution and scaled to the same axis before plotting. **(B)** Dissociation data of *S. cerevisiae* NCPs (purple circles) compared to *X. laevis* NCPs (blue triangles) starting the salt titration from 0M NaCl, with donor emissions recorded at each 0.02 M step. Excitation and emission wavelengths are as in (A), and the data was corrected for dilution and scaled before graphing.

present for yeast NCPs in Figure 3.3A. Both data sets, however, show a decreased stability for *S. cerevisiae* NCPs (Fig. 3.3 A and B), with the approximate mid-point for the dissociation of the DNA ends at ~180 mM NaCl for *S. cerevisiae* NCP, whereas the midpoint is at ~280 mM NaCl for *X. laevis* NCP.

3.4c Yeast nucleosomes demonstrate increased sliding rates

In light of the fact that yeast nucleosomes demonstrate a decreased stability, we next wanted to determine if nucleosomes from yeast would show increased sliding rates as compared to those from higher eukaryotes. Sliding rates of nucleosome core particles on the 146 bp DNA fragment used in our experiments is based on the fact that upon salt-gradient reconstitution of nucleosomes at 4°C, multiple translational positions of the nucleosomes are obtained which are offset by 10 bp with respect to each other (refer to the schematic in Fig. 3.4). However, only the central position is the most thermodynamically stable since it utilizes the full range of protein-DNA interactions. The different translational positions adopted by the NCPs are readily resolved by native gel electrophoresis. Previous experiments in our lab have shown that the lowest free energy state can be obtained by heating the samples at 37°C for a length of time dependent on the inherent stability of the interactions between the protein and DNA (Luger et al., 1999), (Muthurajan et al., in press). As can be seen in Fig. 3.4, nucleosomes containing *S. cerevisiae* histones required less time for complete shifting than those containing *X. laevis* histones (10 minutes for *S. cerevisiae* compared to 30 minutes for *X. laevis*). The quantitation of the bands shown in Figure 3.4C shows this results clearly. The diffuse upper band observed when the gel is stained with ethidum bromide but not with the coomassie blue stain in the *S. cerevisiae* NCPs is probably a

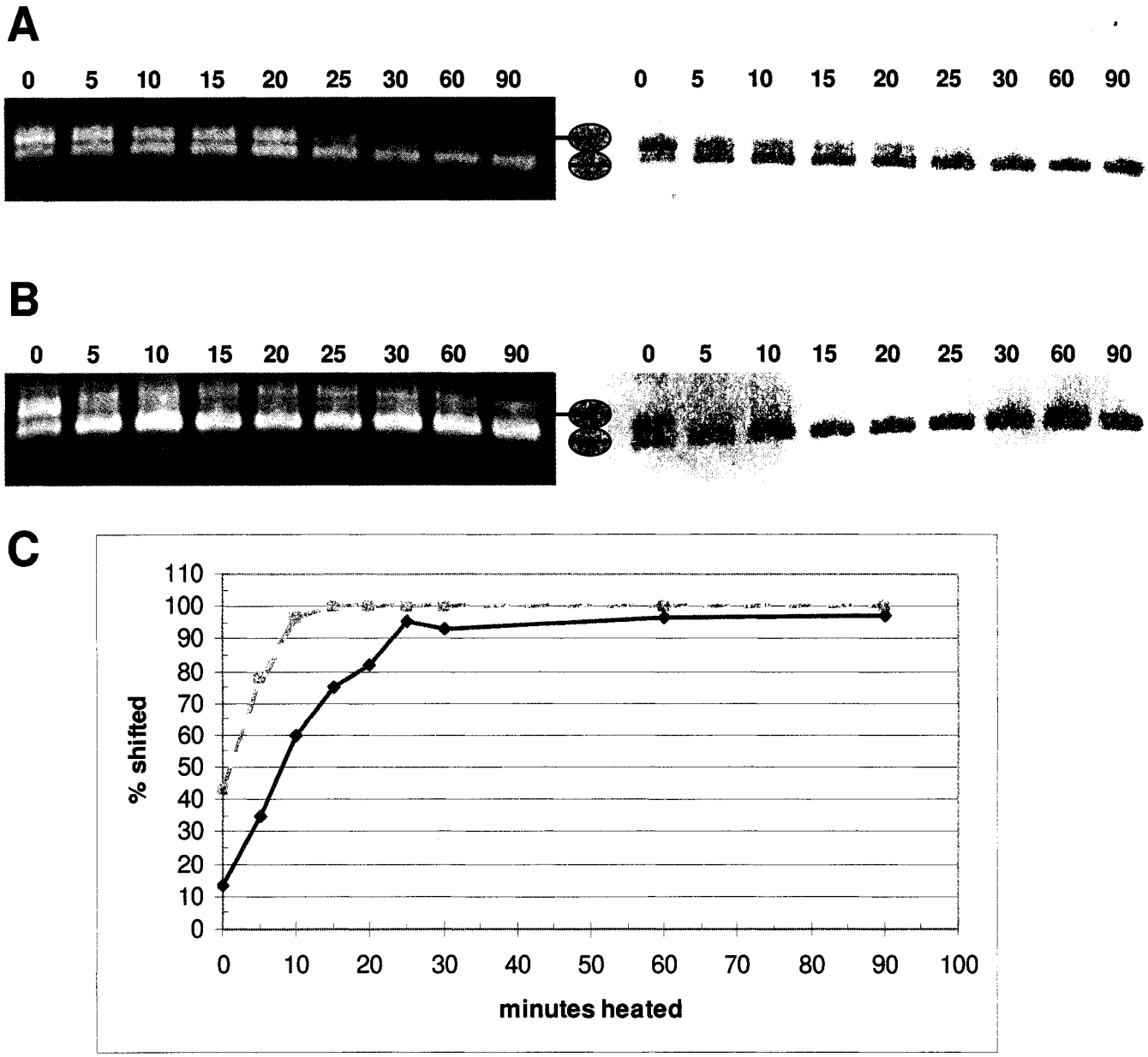

Figure 3.4 Temperature-dependent shifting studies of *S. cerevisiae* and *X. laevis* NCPs

(A) 5% Native-PAGE gel showing a nucleosomal shifting assay of *X. laevis* NCPs. The gel was stained in ethidum bromide (left panel) followed by Coomassie blue (right panel). Nucleosomes were heated at 37°C for the time points shown above each sample (time is given in minutes). The schematic on the far left gives the identify of the two bands. **(B)** 5% Native-PAGE of a shifting assay of *S. cerevisiae* NCPs. The panel on the left is the ethidum bromide stain, and the right panel is the coomassie blue stain. Nucleosomes were heated at 37°C for the minutes shown for each sample. **(C)** Plot of the commassie blue stain for each NCP type showing % NCP shifted for each time interval.

non-canonical nucleosome that we sometimes observe.

3.4d The L1 loops do contribute to the stability of a nucleosome core particle

The results outlined above show that nucleosomes from *S. cerevisiae* demonstrate a decreased stability as compared to higher eukaryotic organisms, such as *X. laevis*. The crystal structure of the nucleosome core particle from *S. cerevisiae* suggests that this decreased stability could be the result of two amino changes located within the H2A L1 loops, which result in a complete loss of interactions at this interface (Fig. 3.1C). In yeast, Glu41 is changed glutamine, and His79 is changed to alanine (H2A Glu42 and H2B Ala85 in yeast, Fig. 3.1A and C). To test whether these changes are directly related to the decreased stability observed for yeast NCPs, we mutated the *X. laevis* L1 loops to match the amino acid changes found in *S. cerevisiae*. Therefore, *X. laevis* H2A Glu41 was mutated to a glutamine, and H2B His79 was mutated to an alanine. These mutated histones were then expressed and purified, refolded into histone octamers, and reconstituted into nucleosome core particles by mixing the octamers with fluorescently-labeled 146 bp α-sat DNA. Thus, each core particle incorporates both mutations. We then analyzed these changes by monitoring their salt-dependent dissociation using FRET in order to see if these mutations makes the *X. laevis* nucleosomes less stable. As can been seen in Fig. 3.5, these mutations do not cause as much of a decreased stability of the *X. laevis* nucleosomes as the *S. cerevisiae* NCPs demonstrate. However, they do create a decrease in stability to some extent. Therefore, the L1 loops do, in part, contribute to the stability of the nucleosome core particle, but other nucleosomal interactions also play a role the overall stability.

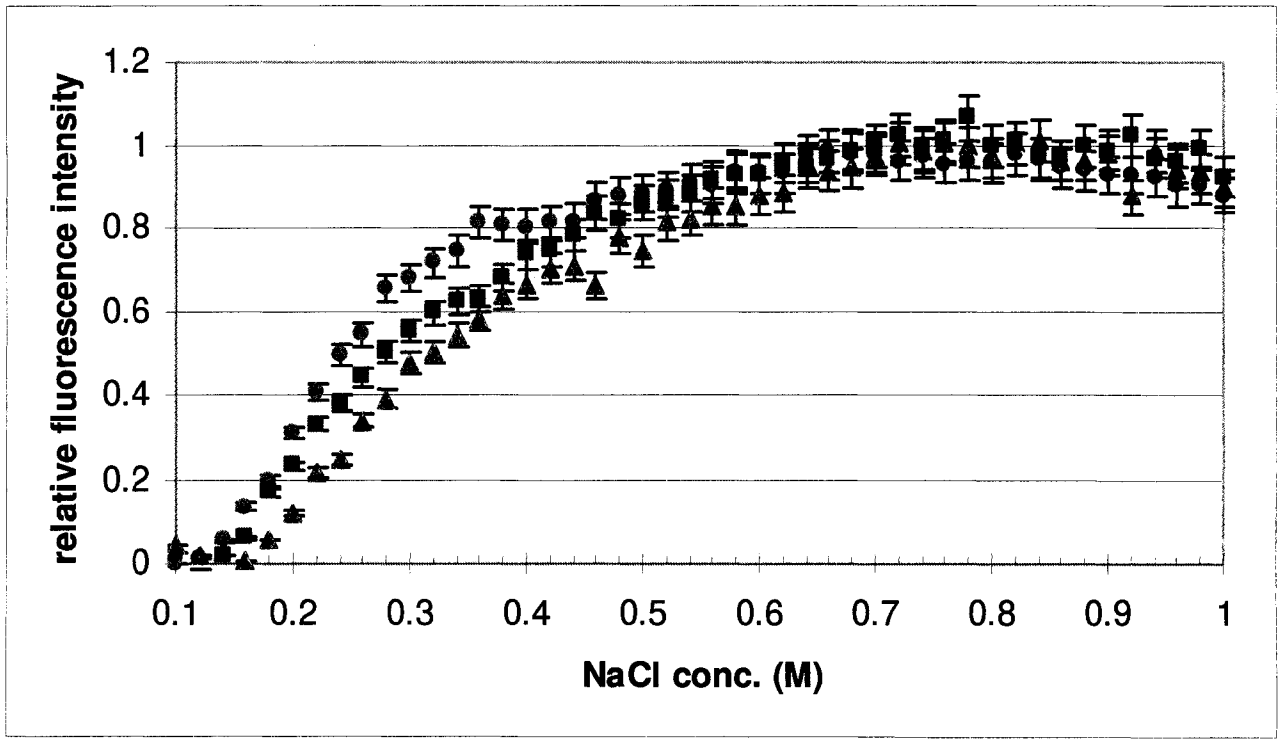

Figure 3.5 Changes in the L1 loop lead to a slight decrease in stability of *X. laevis* NCP

The salt dependent dissociation of *S. cerevisiae* NCPs (purple cirlces) compared with *X. laevis* NCPs (blue triangles) and *X. laevis* NCPs containing a mutated H2A L1 loop (green squares). NaCl was titrated from 0.1 M to 1.0 M in 0.02 M steps, and the donor emission was recorded at each step. The excitation wavelength was set at 385 nm and donor emission was monitored at 475 nm. Data was corrected for dilution and scaled to the same axis before plotting. Error bars for the averaged data sets are shown.

3.5 Discussion

Many things govern transcriptional activation on promoter regions. One key factor is the compaction of DNA into nucleosomes, since transcription factors must access their binding sites within a nucleosomal context. Therefore, the removal or rearrangement of nucleosomes on promoter regions is critical to the rapid expression of cellular genes. Much research has focused on this aspect of transcriptional activation. Some data has shown that a decrease in stability of the nucleosome core particle, perhaps by the incorporation of histone variants, for instance, could contribute to activated transcription (Li et al., 1993). Yeast are rather unique among most eukaryotic organisms because they do not exhibit the high level of cellular differentiation found in higher eukaryotes. In addition, they must be able to rapidly respond to changes in their external environment. Therefore, much of their genes remain in a transcriptionally active state. Some previous data has suggested that yeast nucleosomes are less stable than those from higher eukaryotes (Lee et al., 1982), (Morse et al., 1987), (Pineiro et al., 1991). It has thus been hypothesized that a decreased stability of yeast nucleosomes could be a factor in its rapid transcriptional activation, as well as keeping many areas of the yeast chromatin in a less compacted state.

The crystal structure of the nucleosome core particle from *S. cerevisiae* also suggests that yeast nucleosomes are destabilized due to changes in the L1 loop, a region through which the two H2A/H2B dimers interact (White et al., 2001). Therefore, we wanted to test the stability of the *S. cerevisiae* nucleosome core particle compared to that of the higher eukaryotic organism *X. laevis*. We first used the technique of Fluorescence Resonance Energy Transfer in order to access the inherent stability of these nucleosomes.

This method has proved very successful of measuring the stability of nucleosomes containing histone mutants by our lab (Park et al., manuscript in preparation). We confirmed that yeast nucleosomes are less stable than those from higher eukaryotes. Therefore, this could allow easier removal of yeast nucleosomes from promoter regions, as well as reflect the differerences in nucleosome organization *in vivo*.

We next investigated if the decrease in stability of the nucleosome core particle from *S. cerevisiae* would also allow the histone octamer to exhibit increased sliding rates along the DNA. This proved to be the case, with yeast NCPs showing a much reduced time to reach the DNA free energy minimum position as compared to *X. laevis* NCPs. The rate of nucleosome sliding is dependent on the interactions between the histone octamer and the DNA. However, except for a few exceptions, the protein-DNA contacts within the nucleosome are very conserved in yeast. Therefore, the increased sliding rate is somewhat of a surprise. However, a single change in protein-DNA contacts within the nucleosome have proved create a dramatic change in sliding rates (Muthurajan et al., publication in press). In yeast, there are four amino acid residues that directly interact with the DNA that are different from *X. laevis*. H2A K15 is changed to glutamine, H2B S33 is changed to a threonine, H2B S43 is changed to a glutamine, and H2B H79 is changed to an alanine. These are not among the major octamer-DNA contacts within the nucleosome structure from *X. laevis*. However, each of these residues makes a direct interaction with the DNA helix. The above changes in the S. cerevisiae structure does create a relative weakened contact. Therefore, because yeast NCPs exhibit increased sliding rates, this shows that even minor changes in protein-DNA contacts within the nucleosome can have major effects on nucleosomal mobility. This has profound

implications on transcriptional activation, since the incorporation of histone variants, for instance, could mimic these same changes in order to activate or repress transcription. Also, remodeling complexes need only to make rather small changes on nucleosomal structure in order to activate transcription.

Another assay that has proved successful in probing the stability of nucleosomes is a dilution assay. In low nucleosomal concentrations, the core particles tend to dissociate. Therefore, the less stable complexes fall apart at higher concentrations than those which demonstrate an increased stability. We thus performed this assay in order to confirm our results that yeast nucleosomes are less stable than those of higher eukaryotes. This experiment did confirm our results, with nucleosomes from *S. cerevisiae* dissociating at a higher concentration than those from *X. laevis* under the conditions used in our experiment. These results are very interesting in light of the fact that it has been shown that histone sequence changes in sea urchin sperm result in an increase in the stability of the nucleosomes (Simpson et al., 1980). These changes in stability directly correlate with a reduced transcripitonal activity in the sea urchin sperm chromatin (Simpson et al., 1980). Therefore, since yeast chromatin exhibit high levels of transcriptional activity, the reverse effect could be true.

The results outlined above led us to ask if the specific structural changes found in the yeast H2A L1 loops are directly responsible for this decreased stability. To this end, we mutated the *X. laevis* histones H2A and H2B to match the residues found in yeast. These changes proved to cause the NCPs to be slightly destabilized, but they did not show the degree of destabilization as yeast NCPs. This shows that the L1 loop changes are, to some degree, responsible for the reduced stability of yeast NCPs. However,

probably other changes within the S. cerevisiae structure creates a reduced stability as well. Since there are no other detectable structural differences that we could find in the yeast crystal structure at the resolution obtained (3 Å), other very minor changes must also result in the decreased stability. This again shows that even very small structural changes within the nucleosome can have large effects on NCP function.

However, we cannot rule out the possibility that, since we changed the *X. laevis* structure to match that of yeast, there could be other interactions within the structure which gives an added stability. If we were to change yeast to match the *X. laevis* structure, we might find that the yeast stability exactly matches that of *X. laevis*. Therefore, the *S. cerevisiae* L1 loop would need to be mutated to match that of *X. laevis* before any definite conclusions can be drawn. It still could be proved that in the *S. cerevisiae* NCP structure, the L1 loop is the major cause of the decreased stability. This result would not be surprising, since other data suggests that in many histone variant NCP structures solved in our lab, the H2A L1 loop is the main region in which structural differences are found (Suto et al., 2000), (Chakravarthy et al, unpublished data). Thus, the data suggests that this is a critical region within the nucleosome, the structure of which could have implications on activated or repressed transcription. Future experiments will surely answer these important questions.

In conclusion, we have shown that nucleosome core particles from the yeast *S. cerevisiae* display a decreased stability as compared to the higher eukaryote *X. laevis*. This decreased stability appears to partially be the direct result of structural changes within the H2A L1 loops. However, other very minor structural changes look to contribute to this destabilization as well. We have also shown that due to very minor

sequence changes which mediate protein-DNA contacts within the nucleosome, yeast nucleosomes demonstrate increased sliding rates on a 146 bp DNA fragment. Our data supports the hypothesis that only very minor structural changes within the nucleosome core particle can result in major changes in nucleosomal function, such as the activation or repression of transcription.

3.6 Acknowledgements

We thank Amelia Mellett and Shawn Daley for help with the mutagenesis, expression, and purification of mutant *X. laevis* proteins, as well as help with the FRET experiments and shifting assays. We also thank Joel Gottesfeld for help with the NCP dilution experiments. This work was supported by NIH grant GM61909.

Chapter 4

Effects of a Poly (dA·dT) Element on Nucleosome Stability and Transcription Factor Binding

The homopolymeric (dA·dT) element found in many eukaryotic promoter regions is essential for activated transcription. X-ray crystallographic studies and biophysical data have demonstrated that a poly (dA·dT) stretch is a very rigid DNA sequence. Therefore, poly (dA·dT) sequences have been thought to be incompatable with nucleosome core particle formation on promoter elements, or alternatively to cause an altered DNA conformation that facilitates transcription factor binding directly to nucleosomal DNA. Although it has been shown that transcription factors can bind to nucleosomal DNA, the structural implications of such binding on the histone octamer are unknown. We have set out to investigate these questions using various structural and biochemical experiments. This data has been submitted to *The EMBO Journal* as shown in the reference below.

White, C.L., and Luger, K. The effects of a Poly (dA·dT) element on nucleosome stability and transcription factor binding.

4.1 Abstract

Homopolymeric (dA·dT) sequence elements are present in many eukaryotic promoter regions where they contribute to transcription activation by unknown mechanisms. Here we present *in vitro* tests of the hypothesis that such sequence elements are disfavored in nucleosome formation, or if formed, result in structurally altered nucleosomes. We further study the effects of a poly (dA·dT) tract on the binding of the transcription factor Amt1 to its recognition site near the dyad of a highly positioned nucleosome. We find that a 147 bp DNA fragment containing an A_{16} sequence element forms more stable nucleosomes than a fragment with the same sequence without such an element, and observe no preference for either sequence during *in vitro* assembly. We also demonstrate that the DNA binding domain of Amt1 binds to poly (dA·dT) nucleosomes with only three-fold reduced affinity compared to free DNA, and that binding near the nucleosomal dyad is accompanied by the partial dissociation of the DNA ends from the surface of the histone octamer. We show conclusively that no dissociation of histones is required for binding. Together, our results demonstrate the surprising adaptability of nucleosomal DNA with respect to unusual DNA sequence elements, and in response to factor binding.

4.2 Introduction

Activation of a gene at any given time requires its identification within highly compacted chromatin. Local unpacking and remodeling of chromatin by remodeling factors then allows the binding of the transcription machinery. Chromatin is built from nucleosomes, the universally repeating protein-DNA complex in all eukaryotic cells. Several crystal structures of the nucleosome core particle (NCP) reveal an octameric

histone core around which 147 base pairs of DNA are wrapped in 1.65 superhelical turns (Luger et al., 1997) (Harp et al., 2000) (White et al., 2001). The histone octamer itself is composed of two copies each of the four histone proteins H2A, H2B, H3, and H4. Two heterodimers of histones H3 and H4 form a tetramer that binds the central ~ 70 base pairs of DNA, and two (H2A-H2B) dimers bind at either side of the $(H3\text{-}H4)_2$ tetramer – DNA complex to create two binding surfaces for the remaining 80 base pairs of DNA (40 bp on either side). Hundreds of thousands of nucleosomes (the NCP plus linker histone H1 and linker DNA) are further organized in multiple levels of higher order structures of largely unknown architecture (Van Holde, 1988) (Widom, 1998).

All activities that require access to the DNA template (such as the machinery involved in replication, transcription, or repair) must effectively deal with the repressive effect of chromatin. Nucleosomal DNA differs in several important aspects from free B-form DNA. First, major and minor groove parameters and other inter-and intra-base pair characteristics of nucleosomal DNA deviate strongly from canonical values as a consequence of superhelix formation. Second, nucleosomal DNA does not follow the path of a regular superhelix; rather, it is characterized by regions of strong curvature interspersed with almost straight stretches (see (Richmond, 2003) for a comprehensive analysis of the structure of nucleosomal DNA). Third, due to the tight interaction with the rigid framework of the histone octamer over its entire length, one face of the DNA is completely precluded from interactions with sequence-specific DNA binding factors. Although about 70% of nucleosomal DNA is solvent-accessible, a transcription factor can only access a maximum of 6-8 consecutive base pairs before being sterically blocked by the presence of the histones and by narrow DNA groove width.

The positioning of nucleosomes in promoter regions (which is likely to be governed by a combination of factors intrinsic to the DNA sequence (Widom, 2001)) regulates the access of transcription factors, and is thus implicated in the regulation of gene expression. A statistically significant enrichment of poly (dA·dT) tracts in the promoter regions of many yeast genes suggests that these sequences may be involved in gene regulation (Struhl, 1985). Structural analysis has shown that poly (dA·dT) tracts form rigid DNA structures that are stabilized by additional bifurcated hydrogen bonds due to high propeller twist (Coll et al., 1987; Dickerson et al., 1982). Because of these structural properties, it has been proposed that poly (dA·dT) tracts would not be able to conform well to the highly bent superhelix that is characteristic for the nucleosome. A study in which hundreds of nucleosomal DNA fragments were cloned and sequenced showed that longer adenosine tracts (containing five or more contiguous adenosines) were underrepresented in nucleosomal DNA *in vivo* (Satchwell et al., 1986). Many promoter regions which contain poly (dA·dT) elements have been shown to be nucleosome free *in vivo* (Filetici et al., 1998; Lascaris et al., 2000; Suter et al., 2000; Tanaka et al., 1996).

However, several examples to the contrary exist. The chromatin structure of the *S. cerevisiae* DNA topoisomerase I promoter has been shown to contain a 29 bp-long poly (dA·dT) element within a stably positioned nucleosome *in vivo* (Rubbi et al., 1997). Nucleosomes will form on a 20 bp poly (dA·dT) element inserted into plasmid DNA *in vivo*, but the tract shows a marked preference for the edges of the particle (Prunell, 1982). Other studies support the idea that poly (dA·dT) regions are excluded from the center of nucleosomes *in vivo* (Satchwell et al., 1986). In addition, a homopolymeric (dA·dT) element located adjacent to a metal response element (MRE) within the Amt1 gene

promoter of *Candida glabrata* has been shown to be incorporated into a positioned nucleosome *in vivo* (Zhu and Thiele, 1996) (Liu and Thiele, 1997), and this element is essential for rapid activation of the promoter in response to toxic copper levels. In this arrangement, the MRE is located very near the nucleosomal dyad, and the A_{16} element is 15 bp upstream. *In vivo* experiments have shown that the location and, to a lesser degree, the length of the A_{16} element with respect to the MRE is crucial for rapid response (Koch and thiele, 1999). The A_{16} element functions independently of the poly (dA·dT) binding protein Dat1p. A poly (dA·dT) DNA element also facilitates access to the mammalian glucocorticoid receptor if its recognition site faces outwards and is placed near the nucleosomal dyad, suggesting that homopolymeric (dA·dT) elements may facilitate transcription factor binding in a nucleosomal context.

Consistent with these examples, *in vitro* experiments have shown that extended poly (dA·dT) elements can be incorporated into nucleosomes (Rhodes, 1979) (Losa et al., 1990) (Puhl and Behe, 1995; Puhl et al., 1991) (Hayes et al., 1991). The T-tract structure that is characteristic of poly (dA·dT) is partially lost upon folding into nucleosomes, demonstrating that the structural constraints imparted by binding to the histone octamer dominate over those of poly A tracts (Schieferstein and Thoma, 1996). The fact that it is possible to form triple helices on a nucleosomal poly (dA·dT) element, whereas nucleosomes inhibit triplex formation with random sequence DNA, suggests that the DNA has locally moved away from the histone octamer (Brown and Fox, 1998), consistent with results shown in (Shimizu et al., 2000). Thus, poly (dA·dT) tracts alone are not sufficient to disrupt nucleosome formation, but might lead to local distortions in nucleosomal DNA, thereby permitting or enhancing the binding of transcription factors.

Because many chromatin modifying activities are recruited to the gene of interest, at least some transcription factors must access their binding site within the context of a folded nucleosome. Opening of compacted chromatin by early developmental transcription factors, such as HNF3 (FoxA) and GATA-4 (Cirillo et al., 2002), and the binding of the glucocorticoid receptor to a positioned nucleosome (Li and Wrange, 1995) are perhaps the best-studied examples. Sporadic accounts of factor binding to nucleosomes have appeared in the literature ((Wechsler et al., 1994) (Li et al., 1994) (Imbalzano et al., 1994) (Zhu and Thiele, 1996) (Steger and Workman, 1997) (Gao and Benyajati, 1998), and reviewed in (Beato and Eisfeld, 1997)). Transient exposure of transcription factor binding sites by partial dissociation of terminal regions of DNA from the histone octamer is an important mechanism to allow access of sequence-specific DNA binding proteins (Polach and Widom, 1995). However, this phenomenon has never been observed directly. It has also been suggested that partial dissociation of the histone octamer (for example, dissociation of a H2A/H2B dimer) would have to occur before a transcription factor would be able to bind to nucleosomal DNA. In light of the central importance of this question for transcription regulation in eukaryotes, it is surprising to note that no studies exist on the molecular and structural implications of transcription factor binding to DNA encompassed within a nucleosome.

The copper-responsive transcription factor Amt1 has been shown to bind to DNA encompassed within a nucleosome *in vivo* (Zhou et al., 1992), (Liu and Thiele, 1997). Amt1 binds to DNA as a monomer and consists of a basic N-terminal domain and an acidic C-terminal domain. The C-terminal domain is implicated in transcriptional activation, and the N-terminal domain, which encompasses the first 115 amino acids of a

total of 265 amino acids, is responsible for binding DNA and copper (Zhou and Thiele, 1993). This domain itself is bi-partite, consisting of a ~ 40 amino acid zinc-binding domain and an adjacent domain that forms a tetracopper-thiolate cluster (Graden et al., 1996). The three dimensional structure of the N-terminal Zinc-binding domain has been determined by NMR (Turner et al., 1998), whereas the structure of the copper-binding domain remains to be elucidated. The consensus recognition sequence for Amt1 binding is TNNNGCTG, and the protein makes critical interactions with this consensus sequence on one face of the DNA double helix at adjacent major and minor grooves (Koch and Thiele, 1996). These interactions can, in theory, easily be accommodated in the NCP, since Amt1 only contacts one face of the DNA, and since the entire site would be solvent-exposed on nucleosomal DNA according to *in vivo* mapping data (Zhu and Thiele, 1996).

The positioned nucleosome containing the Amt1 recognition sequence and a poly (dA·dT) sequence element presents the unique opportunity to study two important aspects of transcriptionally competent chromatin at the structural level. First of all, are nucleosomes which are reconstituted onto DNA containing a relatively long poly (dA·dT) tract structurally and functionally altered? Second, would nucleosomes preferably assemble on DNA fragments that do not contain such a sequence element? Third, can a transcription factor bind to its recognition site close to the nucleosomal dyad, and is this binding facilitated by the presence of a poly (dA·dT) sequence element? Upon transcription factor binding, what are the consequences for DNA structure and histone composition of the bound nucleosome? We address these questions by studying a highly-positioned mono-nucleosome that contains the sequence recognition element for Amt1,

either in the presence or absence of a 16 bp poly (dA·dT) DNA element (A_{16}). The relative position of all sequence elements with respect to the nucleosomal dyad is identical to that mapped *in vivo* (Zhu and Thiele, 1996). In this paper, we demonstrate that a 147 bp DNA fragment containing an A_{16} element is assembled into nucleosomes with the same affinity as a DNA fragment of the same sequence without the A_{16} element. We also show that A_{16}-containing nucleosomes are stabilized against salt-induced dissociation. Furthermore, the DNA binding domain of the transcription factor Amt1 can bind directly to its binding site near the nucleosomal dyad, without causing in any major structural changes within the nucleosome core. Finally, we show that the 16 bp poly (dA·dT) element adjacent to the MRE facilitates Amt1 binding to a nucleosome, but is not essential. Therefore, our results show that a transcription factor can access its binding site within the context of a nucleosome without disruption of the underlying histone octamer, and that this binding could be facilitated by specific DNA promoter elements.

4.3 Materials and Methods

4.3a Construction and amplification of the DNA fragment

Two pairs of oligonucleotides were synthesized as outlined in Fig. 1A, each containing one half of the 147 bp fragment. Design strategies are described in (Dyer et al., 2003). One half of the resulting 147 bp DNA fragment contained the Amt1 binding site and the 16 bp poly (dA·dT) element as found in the Amt1 gene in *Candida glabrata* (Zhu and Thiele, 1996), grafted onto the α-satellite DNA that has been used in previous studies (α-sat DNA) (Luger et al., 1997; White et al., 2001). The other half is identical to the α-satellite DNA sequence. The position of the Amt1 binding site and the A_{16} element was based on *in vivo* positioning of these elements on the nucleosome (Zhu and Thiele, 1996).

Each oligonucleotide also contained restriction enzyme sites which are required for plasmid insertion, fragment amplification, and DNA purification and ligation (Dyer et al., 2003). The oligonucleotides were annealed, and the duplex DNA was inserted into puc19 plasmids. The inserts were then amplified to obtain 16 copies of the DNA fragments, and 147mer DNA was prepared as described (Dyer et al., 2003). The sequence of the final 147bp DNA fragment (A_{16} DNA) is shown in Figure 1. α-sat DNA was prepared in a similar manner.

4.3b Expression, purification and reconstitution of NCPs

Histone proteins from *Xenopus laevis* were over-expressed in BL21 (DE3) plysS cells (Novagen) and purified using previously published protocols (Luger et al., 1999). The histone proteins were refolded to histone octamers, and reconstituted into nucleosome core particles using either the A_{16} DNA fragment or α-sat DNA (Luger et al., 1997). Milligram amounts of nucleosome core particles were subjected to heat shifting (37°C for α-sat NCPs, 55°C for A_{16} NCPs) in order to create the free energy minimum position of the DNA around the histone octamer. The nucleosomes were purified using preparative gel electrophoresis (Luger et al., 1999) (Dyer et al., 2003), and their quality was monitored by native gel electrophoresis over polyacrylamide gels (Luger et al., 1999).

4.3c Expression and purification of Amt1

Amt1-DBD protein expression plasmids (pET-9d) were a kind gift from Dr. Dennis Winge. Proteins were expressed in *E. coli* strain BL21 (DE3) plysS and grown to an OD_{600} nm of 0.5, at which time the cells were induced with 0.4 mM IPTG. Following a 30 minute incubation, $CuSO_4$ was added to a final concentration of 1.0 mM and the cells

were incubated for an additional 1.5 hours. Cells were harvested, washed in a 0.25 M sucrose solution, and frozen in 50 ml of lysis buffer (10mM K-phosphate pH 7.8, 0.1M KCl, 0.1% β-mercaptoethanol). To achieve cell lysis, cells were subjected to two freeze-thaw cycles, and then tissumized. The suspension was centrifuged at 30,100 x g for 35 minutes, and the supernatant was transferred to a clean bottle. The pellet was re-extracted by addition of 20 ml lysis buffer, tissumized, and centrifuged as above. 15 ml of a 5 mg/ml protamine sulfate solution was added to the combined supernatants while stirring over ice for 30 minutes. The suspension was clarified by centrifugation at 15,300 x g for 15 minutes. All of the above steps were carried out at 4°C. The supernatant was loaded onto a CM-sepharose column (2.6 x 5.1 cm) equilibrated in a potassium phosphate buffer (10mM K-phosphate pH 7.8, 0.1M KCl, 4.0 mM DTT), and a linear gradient of 0.1 M to 0.5 M KCl resulted in protein elution. The fractions were subsequently concentrated (Vivaspin 20 10,000 MWCO PES membrane) and dialyzed in Amt1 storage buffer (20mM Tris/Cl pH 7.8, 4.0 mM DTT). The protein was then loaded onto a pre-packed Mono S column (1 ml, Amersham Biosciences) equilibrated in storage buffer. The protein was eluted with a linear gradient of 0 M to 0.5 M KCl, and the pure fractions were concentrated and dialyzed back into Amt1 storage buffer. The protein was quantified using a Bradford assay (Biorad).

4.3d *In Vitro* Amt1-DBD binding assays

Oligonucleotides were designed and synthesized that spanned the Amt1 binding site of the Amt1 gene as reported in (Thorvaldsen et al., 1994). The oligonucleotides were Amt1t (5'-TCATGATAAGCTAA TTTGGCTGACT-3') and Amt1b (5'-AAGTCAGCCAAATTAGCTTATCATG-3'). The oligonucleotides were annealed, and

the oligos as well as the 147 bp A_{16} DNA, the 146 bp α-sat DNA, and a 88 bp non-specific DNA were end-labeled with ^{32}P using polynucleotide kinase (PNK). Gel shift reactions were performed by incubating Amt1-DBD with labeled DNA in a reaction mix of 65mM KCl, 5mM $MgCl_2$, 20mM Tris/Cl pH 7.8, 10% glycerol, and 0.1 mg/ml BSA. The reactions were incubated on ice for 30 minutes, and then loaded onto 5% polyacrylamide gels in 0.2X TBE and electrophoresed at 200 V for 2 hours at room temperature. For Amt1-DBD binding to nucleosomes, pre-assembled nucleosomes (described above) were end-labeled with ^{32}P using PNK. Gel shift reactions and electrophoresis were done as described above.

4.3e Fluorescence labeling of DNA and histone proteins

The purified 147 bp A_{16} DNA and the 146 bp α-sat DNA were labeled with the donor chromophore 7-diethylamino-3-(4'-maleimidylphenyl)- 4-methylcoumarin (CPM). In order to carry out the labeling reaction, the DNA fragments were first treated with polynucleotide kinase to attach the 5' phosphates, followed by phenol/CIA extraction and EtOH precipitation. The DNA was reacted with cystaminedihydrochloride/EDC (1-ethyl-3,3-dimethylaminopropylcarbo-diimide) in order to add a cystaminedihydrochloride onto the 5' ends of the DNA fragments. The DNA was then purified over an ion-exchange column in order to remove excess linker. The DNA was incubated with CPM dye overnight in the presence of TCEP. The excess dye was removed by chromatography over Sephadex G-25 resin.

In order to label histone proteins, site-directed mutagenesis was carried out to create *Xenopus laevis* H2B T112C and H4 T71C. The proteins were expressed and purified as described [Dyer, 2003 #1638]. The proteins were dissolved in a 6M guanidinium HCl

unfolding buffer containing 0.4mM TCEP. The fluorescent dye [either 7-diethylamino-3-(4'-maleimidylphenyl)- 4-methylcoumarin (CPM) or fluorescein-5-maleimide (FM)] was added at a 30:1 (dye:protein) molar ratio and incubated overnight. Excess dye was removed by size-exclusion chromatography over Sephadex G-25 resin, and the histones were subsequently concentrated using a Vivaspin 20 10,000 MWCO PES membrane. Octamers were refolded with the appropriate combinations of labeled and unlabeled *Xenopus laevis* histones, and nucleosomes were reconstituted as described above.

4.3f Fluorescence Resonance Energy Transfer (FRET) Experiments

FRET experiments were carried out as described in detail in Park et al. (manuscript in preparation). Briefly, nucleosomes containing either donor (CPM) labeled DNA with acceptor (FM)-labeled H2B (for protein-DNA FRET), or donor (CPM) labeled H2B with acceptor (FM) labeled H4 (for dimer-tetramer FRET), were mixed with 0.1 M NaCl to a final concentration of 20 μg/ml and incubated for 30 minutes in a buffer containing 10mM Tris/Cl (pH 8.0) and 0.1mM EDTA. For stability measurements, donor emission quenching as a result of energy transfer to the nearby acceptor was monitored at 475 nm (excitation at 385 nm) in response to increased ionic strength up to 1.5 M. To monitor structural transitions upon Amt1-DBD binding to nucleosomes, FRET between the DNA ends and histones H2B were monitored at a constant salt concentration of 100mM as increasing amounts of Amt1-DBD protein was added. Samples were allowed to equilibrate for 15 minutes at 20°C before taking the reading. Donor emission was monitored at 475nm upon excitation at 385nm. All experiments were carried out at 20°C, and the data was corrected for dilution before analysis.

4.3g DNase I footprinting reactions

Nucleosomes used in footprinting experiments were reconstituted by mixing ^{32}P end-labeled DNA with *Xenopus laevis* histone octamers at different ratios in 2M NaCl. Nucleosome reconstitution was performed by a stepwise dilution protocol as described in (Gottesfeld et al., 2001), using steps of 1M, 0.8 M, 0.67 M, and 0.2 M NaCl. Incubations were carried out at room temperature, and the final NCPs were heat shifted at the given temperatures described above. DNase I digestions were carried out in a 200ul reaction volume containing 2 - 5 nM labeled nucleosomes in 65mM KCl, 5mM $MgCl_2$, and 20mM Tris/Cl pH 7.8. DNase I digestion was allowed to proceed for 5 minutes in the presence of 2.5 mM $CaCl_2$ with 0.02 units of DNase I (Roche Molecular Biochemicals). Samples were analyzed by running on an 8% denaturing sequencing gel at 1500 V for two hours. For studies involving Amt1-DBD binding to nucleosomal DNA, Amt1-DBD was allowed to incubate with labeled nucleosomes for 15 minutes before digestion with DNase I.

4.4 Results

4.4a A poly (dA·dT) DNA element does not preclude nucleosome formation *in vitro*

We constructed a 147 bp DNA fragment with a 16 bp poly (dA·dT) repeat (A_{16}) and the binding site for the *Candida glabrata* transcription factor Amt1 (metal response element, or MRE), grafted onto the previously used palindromic 146 bp DNA fragment derived from human α-satellite DNA (α-sat DNA) (Luger et al., 1997). The rationale for this design lies in the unique positioning qualities of α-sat 146mer, which we hoped would facilitate analysis of *in vitro* results, and which would permit structural studies. For ease of interpretation, only one half of the DNA was modified. This constructed 147

bp DNA fragment is referred to as A_{16} DNA. Figure 4.1A shows a sequence alignment of the two DNA fragments used in this study. Coincidentally, the palindromic 'parent' α-sat DNA fragment also contains two Amt1 binding sites adjacent to each side of the nucleosomal dyad, only one base pair closer to the dyad than the designed A_{16} 147mer fragment (Figure 4.1A). In designing the A_{16} 147mer, the second Amt1 binding site was destroyed by changing one base pair in the recognition sequence (Fig. 4.1A).

The location of the two newly introduced DNA elements with respect to the nucleosomal dyad corresponds to their position within the *in vivo* mapped nucleosome ((Zhu and Thiele, 1996)). This places the A_{16} element 36 - 52 bp from the 5' DNA end, with the Amt1 binding site positioned just 3' of the central base pair (the nucleosomal dyad; Figure 4.1B). In this structural context, the bases of the entire MRE are solvent-exposed and are, in principle, available for site-specific recognition. The A_{16} element is located in a relatively straight stretch of nucleosomal DNA (Fig. 4.1B) which might be better suited to accommodate the T-tract structure than more bent areas. We are thus confident that this arrangement accurately reflects the most populated *in vivo* nucleosome position.

In order to test if the presence of a poly (dA·dT) element would affect nucleosome formation *in vitro*, nucleosomes were reconstituted with either α-sat or with A_{16} DNA using salt-gradient dialysis, resulting in α-sat NCP and A_{16} NCP, respectively. As shown in Fig. 4.2A and B, both DNA fragments reconstituted into nucleosomes with identical electrophoretic mobility. This electrophoretic mobility assay is a very sensitive measure of nucleosome structure (Luger et al., 1999), and we are thus confident that A_{16} NCPs are structurally intact.

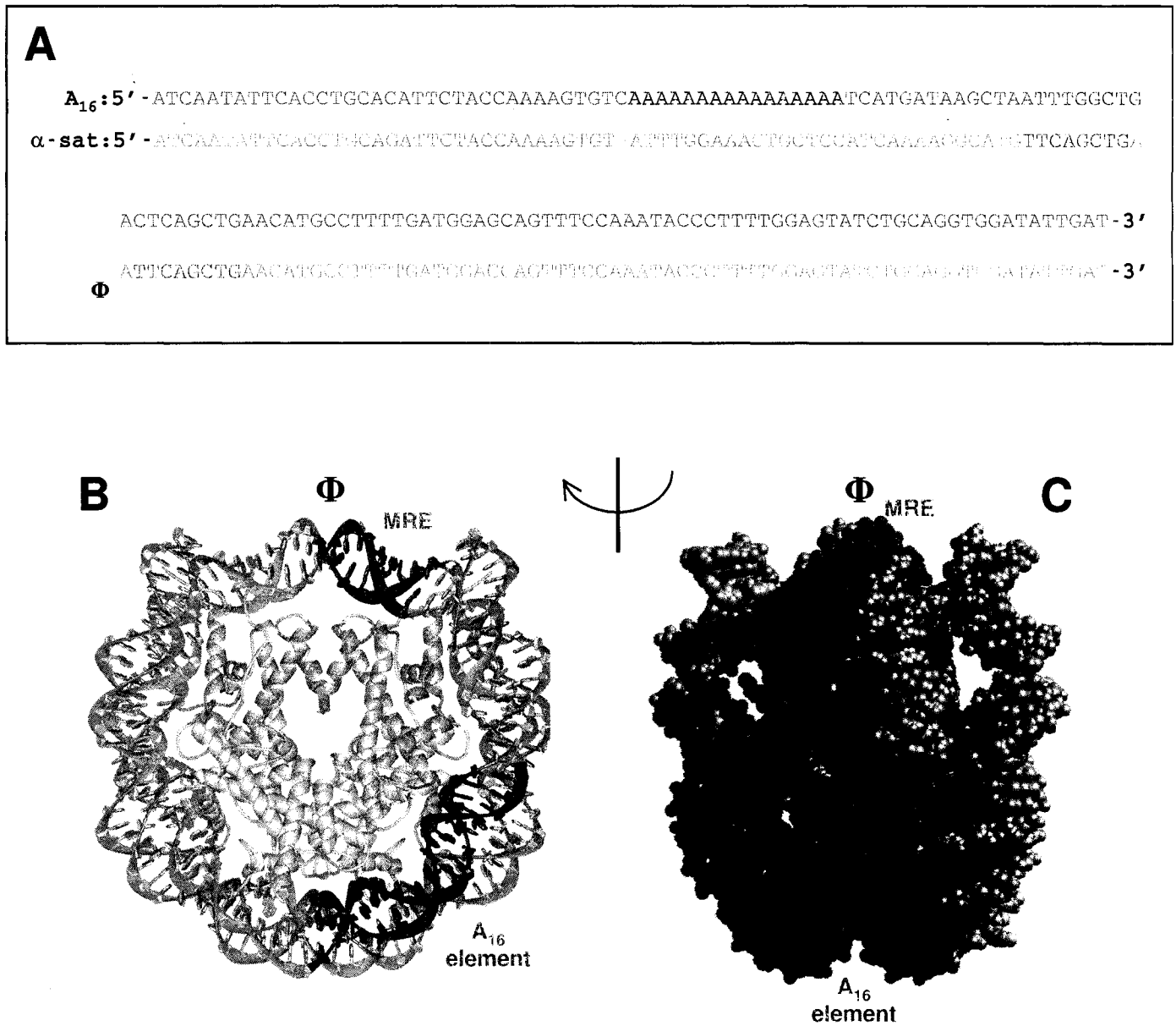

Figure 4.1 Design of a 147 bp DNA fragment containing the mapped poly (dA·dT) element and MRE of the Amt1 gene promoter.

(A) Sequence alignment of the designed A_{16} DNA (gray) and α-satellite DNA (brown). The A_{16} DNA is a 147 bp DNA fragment that contains the poly (dA·dT) element (shown in blue) and the MRE for the Amt1 transcription factor (shown in red). The rest of the DNA sequence is the same as that from human α-satellite DNA, which also contains two Amt1 binding sites (shown in red). The position of the molecular dyad axis is labeled (Φ). **(B)** The crystal structure of the yeast nucleosome core particle, viewed down the superhelical axis. Histone chains are colored light yellow for H2A, light red for H2B, light blue for H3, and light green for H4. The DNA is shown in gray. The position of the Amt1 MRE (red) and the poly (dA·dT) element (blue) are shown as they are positioned within the nucleosomal DNA. The molecular dyad axis is indicated (Φ). **(C)** Space-filling model of a partial side view of the crystal structure of the yeast nucleosome core particle obtained by rotation of 50° around the axis of non-crystallographic symmetry. The coloring scheme is as stated above.

In each assembly reaction described above, the only DNA available to the histone octamer is either α-sat or A_{16} DNA. Given the findings that poly (dA·dT) DNA elements often preclude nucleosome formation *in vivo*, we investigated whether A_{16} 147mer would be discriminated against during *in vitro* nucleosome reconstitution in a competition with α-sat 146mer. To distinguish the two nucleosomes (which have identical electrophoretic mobilities, see Fig. 1C), the two DNA fragments were individually labeled with fluorophores prior to nucleosome assembly. NCPs were reconstituted by mixing one mole of α-sat 146mer and one mole of A_{16} 147mer with one mole of histone octamer. In two separate experiments, either α-sat 146mer or A_{16} 147mer carried a fluorescence label. If nucleosomes preferably were to reconstitute onto α-sat DNA, the fluorescence signal would be unequally distributed between the nucleosomal band and the free DNA band. However, as seen in Fig. 4.2C, the distribution of fluorescence between free DNA and nucleosomal DNA for each nucleosome is the same (compare lanes 2 and 3). Thus, A_{16} and α-sat DNA are assembled into nucleosomes with equal preference. To demonstrate that the presence of the chromophore on the DNA does not impair its ability to be assembled into nucleosomes, we repeated the experiment by mixing labeled and non-labeled α-sat DNA at equimolar ratios. Again, the distribution of fluorescence label between the two bands was approximately 50 % (Figure 4.2C, lane 4). These results are in accord with earlier results which suggested that poly (dA·dT) sequence are reconstituted into nucleosomes with equal affinity (Puhl, 1991).

4.4b The A_{16} element does not destabilize the nucleosome core particle

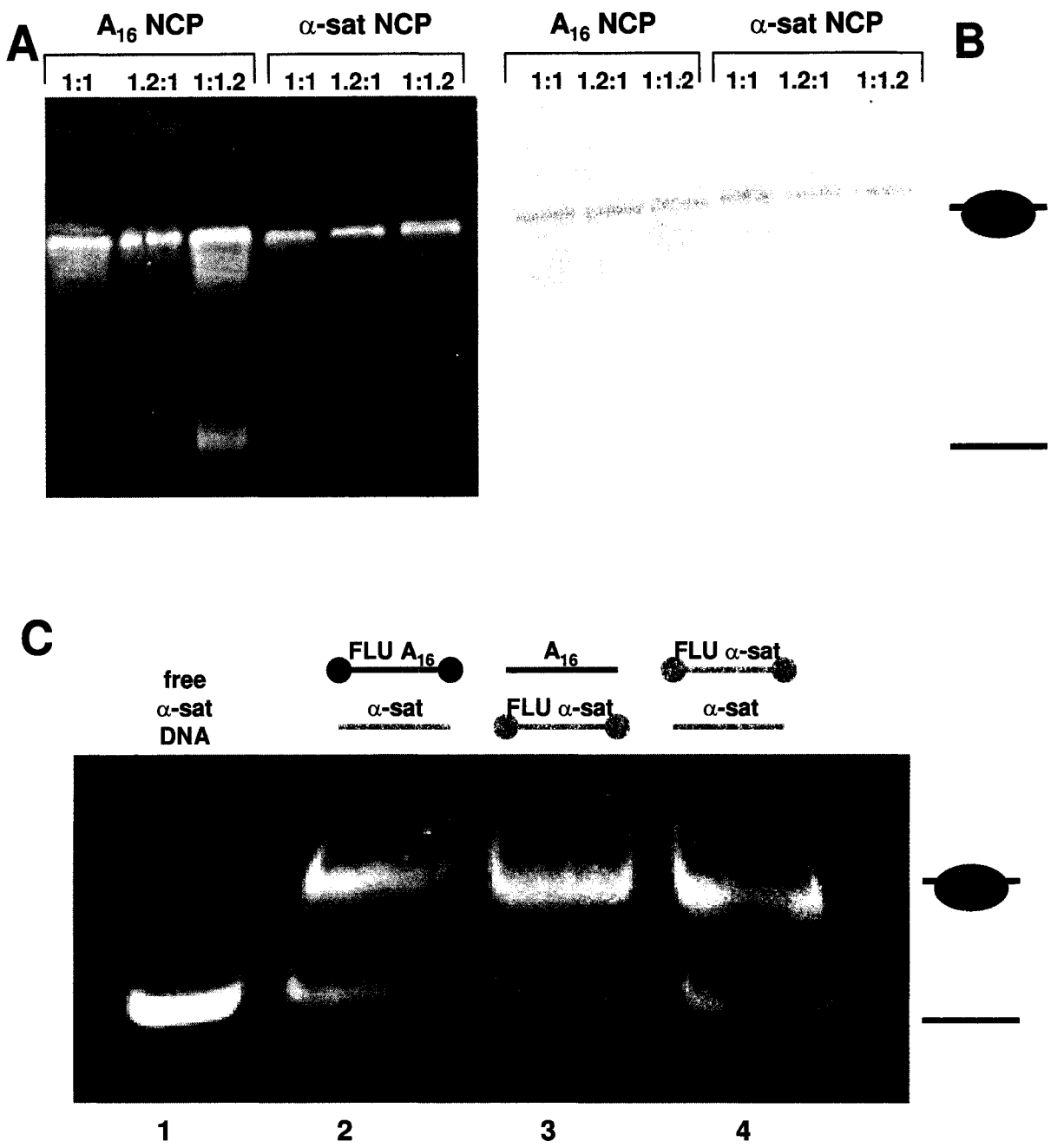

Figure 4.2 The formation of nucleosome core particles from DNA containing a poly (dA·dT) element.

(A and B) 5% Native-PAGE gel showing reconstituted nucleosome core particles from *X. laevis* histone octamer and either A_{16} or α-sat DNA. The octamer:DNA ratios used in each reconstitution are shown. The gel was stained with ethidum bromide (A), followed by commassie blue (B). **(C)** 5% Native-PAGE gel showing reconstituted nucleosomes from *X. laevis* octamer and A_{16} and α-sat DNA. The ratios used for octamer : A_{16} DNA : α-sat DNA were 1:1:1. For each reaction, either the A_{16} or α-sat DNA was labeled with the chromophore CPM (as shown). The gel was viewed using UV light at 365 nm.

It has been speculated that the rigid nature of poly (dA·dT) tracts causes the destabilization of nucleosomes, if they were able to form on such sequences at all (Suter et al., 2000), (Lascaris et al., 2000). On the other hand, it appears that highly stable nucleosomes are formed on a 146 bp poly (dA·dT) tract at elevated temperatures (Puhl and Behe, 1995). To resolve this issue, we utilized fluorescence resonance energy transfer (FRET) to compare the stability of NCPs reconstituted with either α-sat or A_{16} DNA. We have previously shown that FRET can be used to study the salt-dependent dissociation of NCPs by monitoring the distance-dependent fluorescence emission of chromophores within the nucleosome ((Muthurajan et al., 2003), and Y-J. Park and K.L., manuscript in preparation).

In order to determine if poly (dA·dT) DNA tracts destabilize NCPs, FRET experiments were performed in which the ends of each DNA fragment were labeled with CPM (donor), and histone H2B was labeled with FM (acceptor) prior to nucleosome assembly. Quenching of donor fluorescence emission is observed as a result of FRET, and this quenching effect disappears upon dissociation of the nucleosome into its components at elevated salt concentrations (Muthurajan et al., 2003), and Fig. 4.3A. In contrast, when salt is added to nucleosomes containing only donor chromophore, no loss of signal is detected (data not shown). Our lab has repeatedly observed two distinct transitions of NCP dissociation when monitoring FRET between the DNA ends and the $(H3\text{-}H4)_2$ tetramer. This is confirmed for FRET between the ends of the DNA and the(H2A-H2B) dimer for α-sat NCPs, and is also apparent for A_{16} NCPs (Fig. 4.3B). The first, fully reversible transition corresponds to the dissociation of the peripheral DNA

Figure 4.3

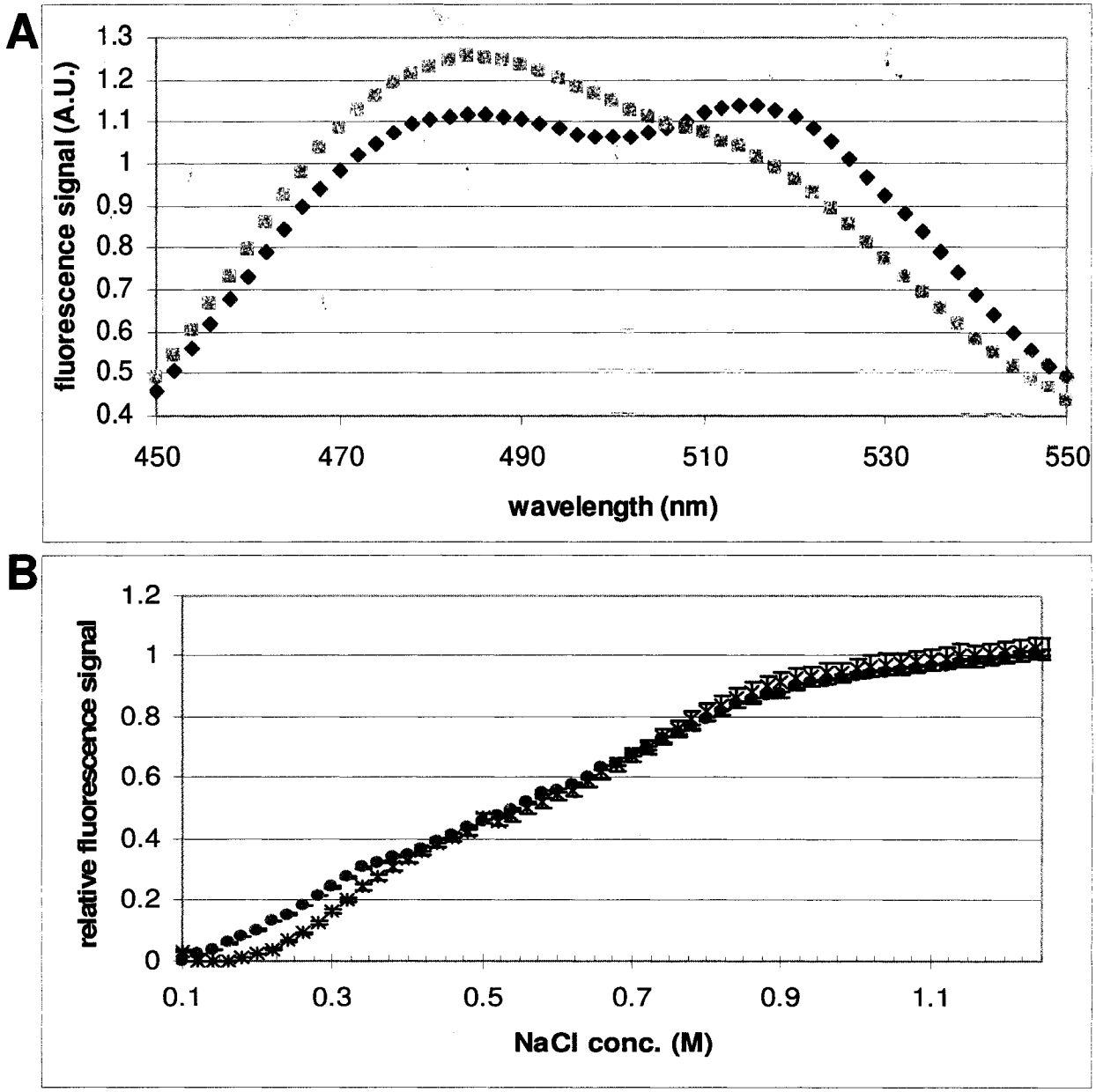

Figure 4.3. Poly (dA·dT) DNA does not cause nucleosome core particle destabilization.

(A) Emission spectra of A_{16}-NCP, incubated for 30 min in either 0.1 M NaCl (blue diamonds) or 1.5 M NaCl (purple boxes). The ends of each DNA were labeled with the chromophore CPM (donor) and histone H2B T112C was labeled with chromophore FM (acceptor). The excitation wavelength was set at 385 nm and the emission was monitored at the wavelengths shown. **(B)** The salt dependent dissociation of A_{16}-NCPs (green asterisks) compared with α-sat NCPs (blue circles). NaCl was titrated from 0.1 M to 1.5 M in 0.02 M steps, and the donor emission was recorded at each step. The excitation wavelength was set at 385 nm and donor emission was monitored at 475 nm. Data was corrected for dilution and scaled to the same axis before plotting. Error bars are shown for the three data sets averaged for each type. **(C)** Reconstituted, purified nucleosome core particles ran on a 5% Native-PAGE gel stained in ethidum bromide and viewed by UV light. NCPs reconstituted from α-sat DNA was heat-shifted at 37°C for 1.5 hrs. Nucleosomes of A_{16}-DNA were heat-shifted at 1.5 hrs. at the temperatures shown. DNA size markers are given. Shifting representation is given for band identification.

ends (Y-J. Park, and KL, manuscript in preparation). The second transition is caused by the dissociation of the histone dimer. When comparing α-sat NCPs with A_{16} NCPs, the dissociation of the DNA ends from the histone octamer initiates at significantly higher salt concentration for the NCPs containing the poly (dA·dT) element (Figure 4.3B). The approximate mid-point for this first transition is at ~245 mM NaCl for α-sat NCP, whereas the midpoint is at ~320 mM NaCl for A_{16} NCP. Similarly, the (H2A-H2B) dimer dissociates from the DNA with a midpoint of 630 mM NaCl for α-sat NCP, compared to a midpoint of 735 mM for A_{16} NCP, consistent with delayed dissociation of the DNA termini in A_{16} NCP. Thus, A_{16} NCPs are slightly stabilized with respect to α-sat NCP.

This result supports the conclusion that the A_{16} element in this particular structural context is accommodated within the NCP without energetic penalty, and is consistent with our observation that A_{16} NCP requires higher temperatures for the DNA to attain the thermodynamically stable central position around the histone octamer (Fig. 4.3C). When DNA fragments reconstitute onto the histone octamer by salt-gradient deposition, the DNA adopts several translational positions with respect to the histone octamer. Heating allows nucleosomes to attain the thermodynamically free energy minimum. We have shown previously that α-sat NCPs completely shifts by heating at 37° C after 30 minutes (Muthurajan et al, manuscript submitted). However, A_{16} NCPs do not exhibit complete shifting under these conditions, but require heating at 55° C in order to obtain a species that co-migrates with α-sat NCPs (Figure 4.3C).

4.4c The A_{16} element creates areas of altered DNA accessibility

To determine if the A_{16} element in this particular position confers localized distortion of nucleosomal DNA *in vitro* (as suggested in (Zhu and Thiele, 1996)), DNase I digestion was performed on core particles reconstituted with either A_{16} 147mer or with α-sat 146mer. Increasing amounts of DNase I was added to constant amounts of nucleosomes, and the deproteinized reactions were analyzed on a sequencing gel. Fig. 4.4A shows that there are differences in the digestion patterns of A_{16} NCPs compared to α-sat NCPs throughout the entire sequence. Not surprisingly, the most marked differences occur at the A_{16} and MRE sequence elements. Note that because both 5' ends of the DNA were labeled and because the A_{16} 147mer is not a perfect palindrome, the G-A tract and the footprinting pattern is actually a convolution of the two halves of nucleosomal DNA for A_{16} NCPs. Therefore, the Amt1 binding site and A_{16} element are shown on both sides of the dyad in A_{16} NCPs.

Quantitative phosphorimaging shows that hypersensitive sites are created by the A_{16} element, whereas other areas are less sensitive to DNase I digestion compared to α-sat NCPs (Figure 4.4B). One area of pronounced DNA hypersensitivity is located directly upstream of the poly (dA·dT) element (Figure 4.4A). Other changes in banding patterns are located in the area of the Amt1 binding site (Figure 4.4A). The footprint also shows that differences are not only located directly upstream and downstream of the poly (dA·dT) element, but that they are propagated throughout other regions of the nucleosomal DNA (indicated by stars). A complete investigation of the structural changes imparted on the structure of nucleosomal DNA by the presence of the poly (dA·dT) sequence element will have to await structural analysis of A_{16} NCPs. Preliminary analysis of crystallographic data of A_{16} NCPs confirms that the DNA

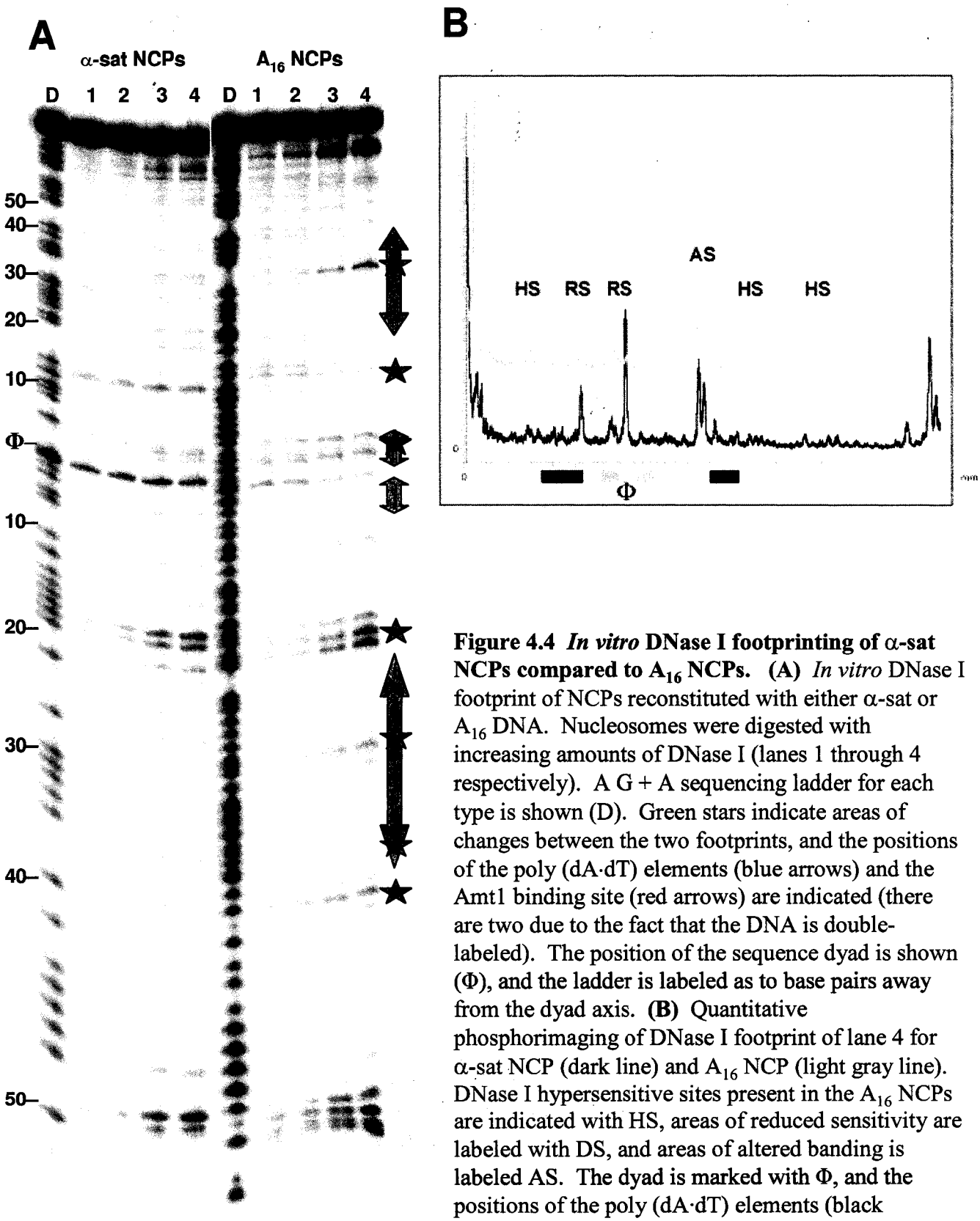

Figure 4.4 *In vitro* DNase I footprinting of α-sat NCPs compared to A_{16} NCPs. **(A)** *In vitro* DNase I footprint of NCPs reconstituted with either α-sat or A_{16} DNA. Nucleosomes were digested with increasing amounts of DNase I (lanes 1 through 4 respectively). A G + A sequencing ladder for each type is shown (D). Green stars indicate areas of changes between the two footprints, and the positions of the poly (dA·dT) elements (blue arrows) and the Amt1 binding site (red arrows) are indicated (there are two due to the fact that the DNA is double-labeled). The position of the sequence dyad is shown (Φ), and the ladder is labeled as to base pairs away from the dyad axis. **(B)** Quantitative phosphorimaging of DNase I footprint of lane 4 for α-sat NCP (dark line) and A_{16} NCP (light gray line). DNase I hypersensitive sites present in the A_{16} NCPs are indicated with HS, areas of reduced sensitivity are labeled with DS, and areas of altered banding is labeled AS. The dyad is marked with Φ, and the positions of the poly (dA·dT) elements (black rectangles) and the Amt1 binding sites (gray rectangles) are inidcated.

position is maintained on the histone octamer (C.W and Y. Bao, unpublished results). Thus, the changes in the footprint of NCPs containing the poly (dA·dT) element are not the result of a different rotational or translational position of the DNA with respect to the histone octamer.

4.4d The DNA binding domain of the transcription factor Amt1 binds near the nucleosomal dyad

Expanding on the above results, we wanted to study the structural implications of transcription factor binding to nucleosomal DNA *in vitro*. The DNA binding domain of the transcription factor Amt1 (Amt1-DBD) was expressed in *E. coli* and purified to >90% homogeneity using ion-exchange chromatography (supplemental figure 4.1A). Using size exclusion chromatography, we demonstrated that Amt1-DBD exists as a monomer under assay conditions (data not shown).

In order to ascertain the activity and binding specificity of Amt1-DBD, and to determine whether Amt1-DBD recognizes its binding site not only in the context of a short DNA fragment, but also when encompassed within a 147 bp DNA fragment, gel shift assays were performed using four different types of radio-labeled free DNA: A_{16} 147mer, α-sat 146mer, a 25 bp DNA fragment harboring an MRE (previously used to determine binding affinities (Thorvaldsen et al., 1994)), and an 88 bp DNA fragment that does not contain an Amt1 MRE. Purified Amt1-DBD shifted all three labeled DNA fragments, but failed to bind to the non-specific DNA control fragment (supplemental Figure 4.9B). The K_D for Amt1-DBD binding to the 25 bp MRE oligo DNA is 5.8 nM, which is in accordance with the previously reported value of 6.0 nM using the same DNA fragment (Thorvaldsen et al., 1994). The two longer DNA fragments are also shifted by

Amt1, with almost identical K_Ds (supplemental Figure 4.9B, lanes 6-10 and 16-20). It is noteworthy that the shift induced by Amt1-DBD binding is identical for both long DNA fragments (A_{16} 147mer and α-sat 146mer; supplemental Figure 4.9B). This strongly suggests that only one protein binds to α-sat 146mer, despite the presence of two closely juxtaposed MREs on this DNA fragment (Fig. 4.1A). This is due to the fact that since the binding sites lie so close together, the binding of two factors simultaneously is prevented. From these experiments we conclude that recombinant purified Amt1-DBD is highly active and binds specifically to its MRE, irrespective of the length and sequence of the flanking regions.

To determine if Amt1 can bind to its MRE within a nucleosome, purified Amt1-DBD was added in increasing concentrations to ^{32}P-labeled A_{16} NCPs. Fig. 4.5A demonstrates the appearance of a shifted nucleosome band upon addition of increasing amounts of Amt1-DBD. Not surprisingly, the affinity of Amt1-DBD for free DNA is higher than for the same DNA in the context of a nucleosome, as seen by a shift in mobility of residual free DNA at low Amt1-DBD concentrations (Fig. 4.5A, compare lanes 2 and 6). Complete super-shifting of the nucleosome band was observed when Amt1-DBD was added in a 15-fold molar excess over A_{16} NCPs. The concentration of Amt1-DBD required for shifting 50% of the labeled NCPs was approximately 18 nM (Fig. 4.5A). Thus, the affinity of Amt1-DBD to its binding site near the nucleosomal dyad is only about three-fold reduced compared to the same in non-nucleosomal DNA. The binding of Amt1-DBD to α-sat NCPs was also studied (supplemental Fig. 4.10A). When higher concentrations of Amt1-DBD were added, further supershifts were observed, which indicates the nonspecific binding of additional Amt1-DBD molecules

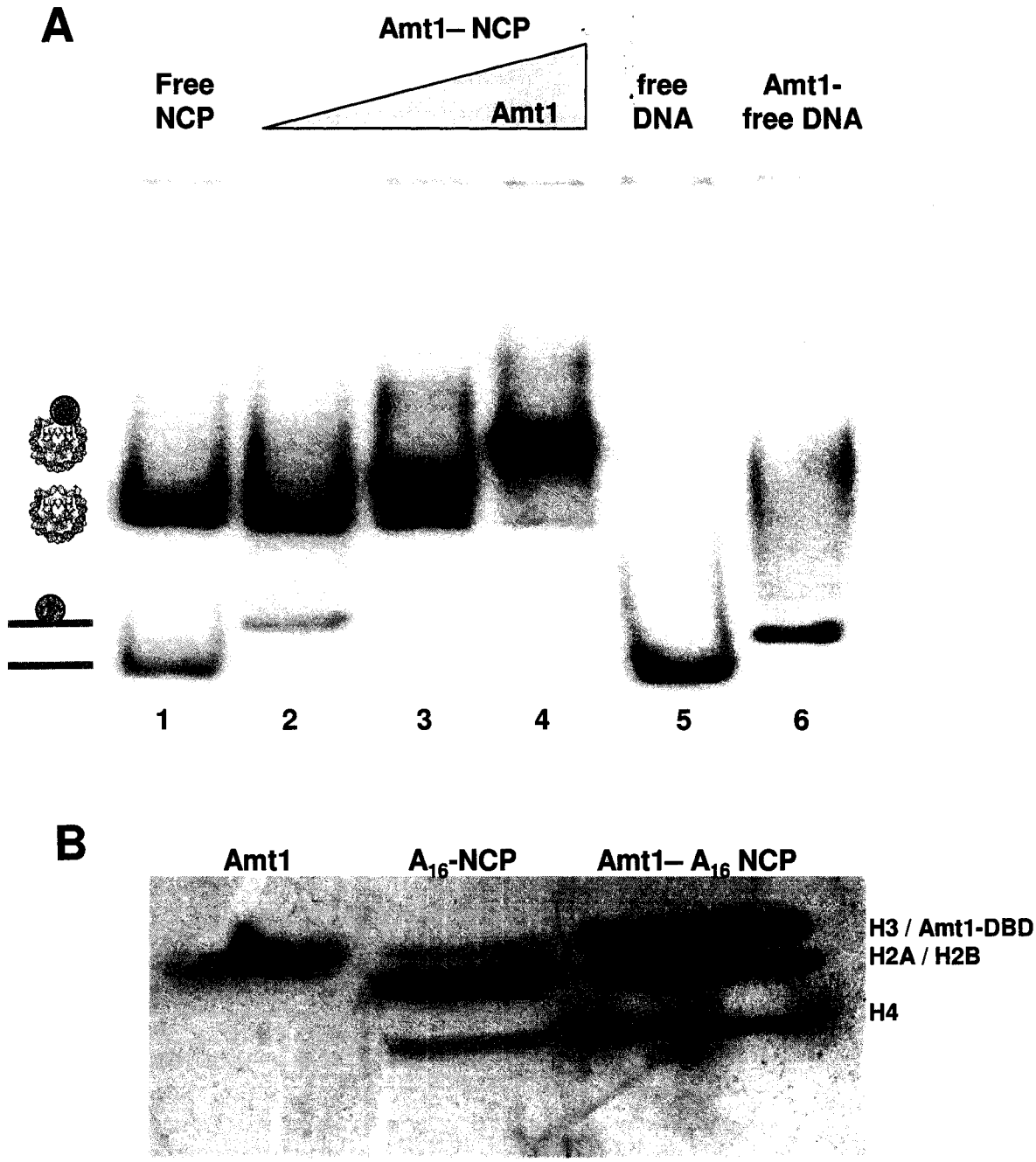

Figure 4.5 Amt1-DBD transcription factor binding to poly (dA·dT) NCPs.

(A) 5% native-PAGE gel showing a gel shift assay of Amt1-DBD binding to A_{16} NCPs. NCPs were labeled with ^{32}P and incubated with increasing amounts of Amt1-DBD. Free A_{16} DNA and DNA incubated with Amt1-DBD are also shown for comparison. Bands are identified by schematics shown. The gel was analyzed by phosphorimage analysis. **(B)** SDS-PAGE gel analysis of Amt1-DBD binding to A_{16} NCP. Free Amt1-DBD, free NCP, and Amt1-DBD-NCP complex was run on a 5% native-PAGE gel, and the resulting bands were cut out and loaded onto the 18% SDS-PAGE gel shown. The gel was stained by silver stain. The bands are labeled as shown. Complex lane reveals that the shifted complex contains all four histone proteins as well as Amt1-DBD.

(supplemental Figure 4.10A). This complicates quantitative analysis of the gel shift data, and thus the binding constant reported here for Amt1-DBD binding to the NCP is only an approximation.

4.4e Amt1 binding to nucleosomal DNA causes dissociation of DNA ends, but does not disrupt the histone octamer

We were next interested in the structural reorganizations that the nucleosome might have to undergo to accommodate transcription factor binding near the nucleosomal dyad. We first tested whether binding resulted in the loss of histone subcomplexes, for example a (H2A-H2B) dimer. In order to determine this, the NCP – Amt1-DBD complex was excised from a polyacrylamide gel run under native conditions (e.g. as shown in Fig. 4.5A, but with unlabelled DNA), and was loaded onto an 18% SDS-PAGE gel. As controls, bands of Amt1-DBD and NCP were also excised and loaded onto the SDS-PAGE gel, and the gel was silver-stained (Figure 4.5B). Amt1-DBD and histone H3 co-migrate on a SDS gel. The excised NCP – Amt1-DBD complex displays a much darker band in this location than is observed for the same concentration of free NCP. The intensity of the bands corresponding to H2A/H2B and H4 are identical. These results confirm that Amt1 is indeed bound to the nucleosome, and indicate that the histone octamer remains intact upon Amt1 binding.

To confirm this finding with a more direct approach, we monitored FRET between the (H2A-H2B) dimer and $(H3\text{-}H4)_2$ tetramer within a folded nucleosome in the presence of increasing amounts of Amt1-DBD. If one or both (H2A-H2B) dimers were to dissociate upon Amt1-DBD binding to the nucleosome, this would result in a loss of FRET between donor and acceptor chromophores attached to H2B and H4, respectively.

Histones were labeled and refolded to octamers as described in materials and methods, and nucleosomes were reconstituted using non-labeled A_{16} 147mer. FRET between the dimer and tetramer was monitored by measuring donor emission quenching as increasing amounts of Amt1 was added. No loss of FRET was observed over the range of Amt1-DBD added (Figure 4.6A), which was comparable to molar concentrations used in binding studies discussed above (15 fold molar excess) (Figure 4.5A, see also 4.6B). In order to make sure that loss of FRET would indeed be observed upon dimer dissociation in this system (and in the presence of Amt1-DBD), 1.5 M salt was added to the Amt1-NCP complex (Fig. 4.6A). Under these conditions, the nucleosome is completely dissociated into its individual components. As expected, this resulted in a dramatic increase in fluorescence donor emission as a consequence of loss of FRET between the (H2A-H2B) dimer and the $(H3\text{-}H4)_2$ tetramer. We conclude that the histone octamer remains intact upon Amt1-DBD binding to the nucleosome.

We next investigated whether distortion of nucleosomal DNA would be observed upon Amt1-DBD binding. Since the Amt1 binding site is positioned adjacent to the dyad, which is in close proximity to the last turn of DNA that is bound by the histone octamer, it seemed possible and even likely that Amt1 binding to the nucleosomal dyad would result in the partial dissociation of the ends of the DNA from the histone octamer (Figure 4.1C). To test this hypothesis, we measured FRET between the ends of the DNA and the (H2A-H2B) dimer in response to the addition of increasing amounts of Amt1-DBD to folded NCPs. The results are shown in Fig. 4.6B. Indeed, loss of donor quenching was first observed at a 15x molar excess of Amt1-DBD over the nucleosome, which is the molar ratio necessary for complete nucleosome shifting as determined by gel

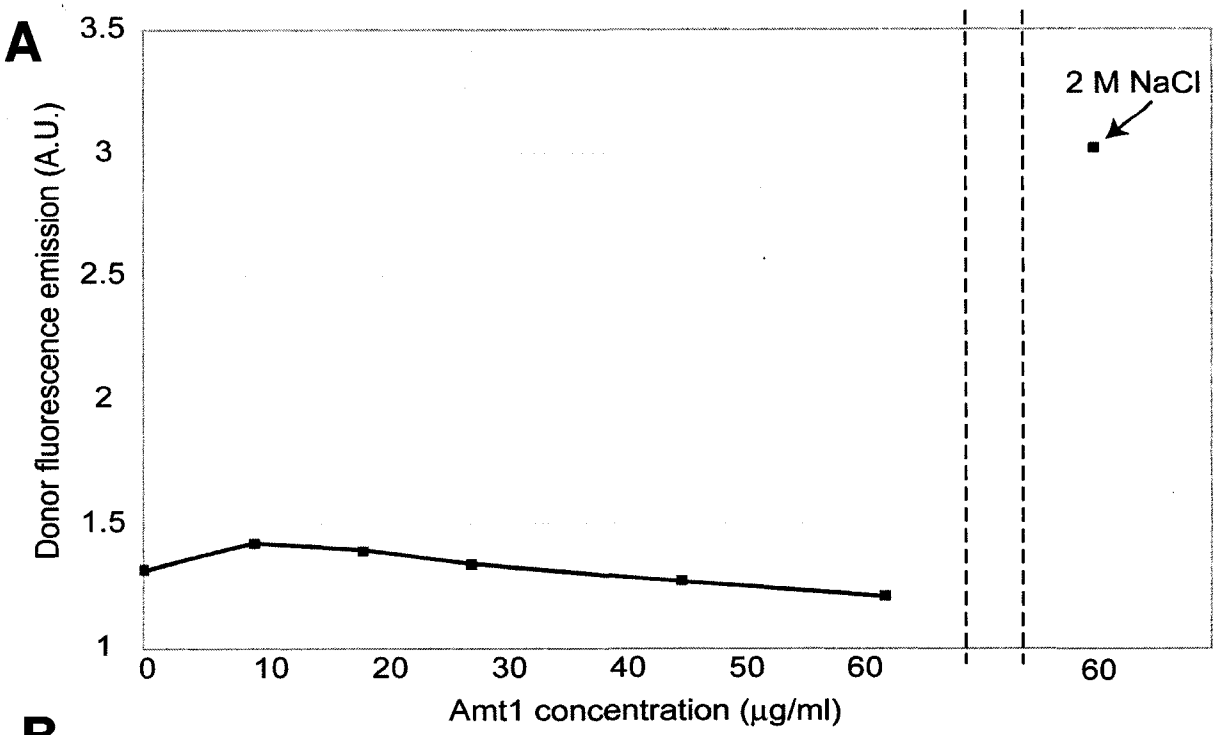

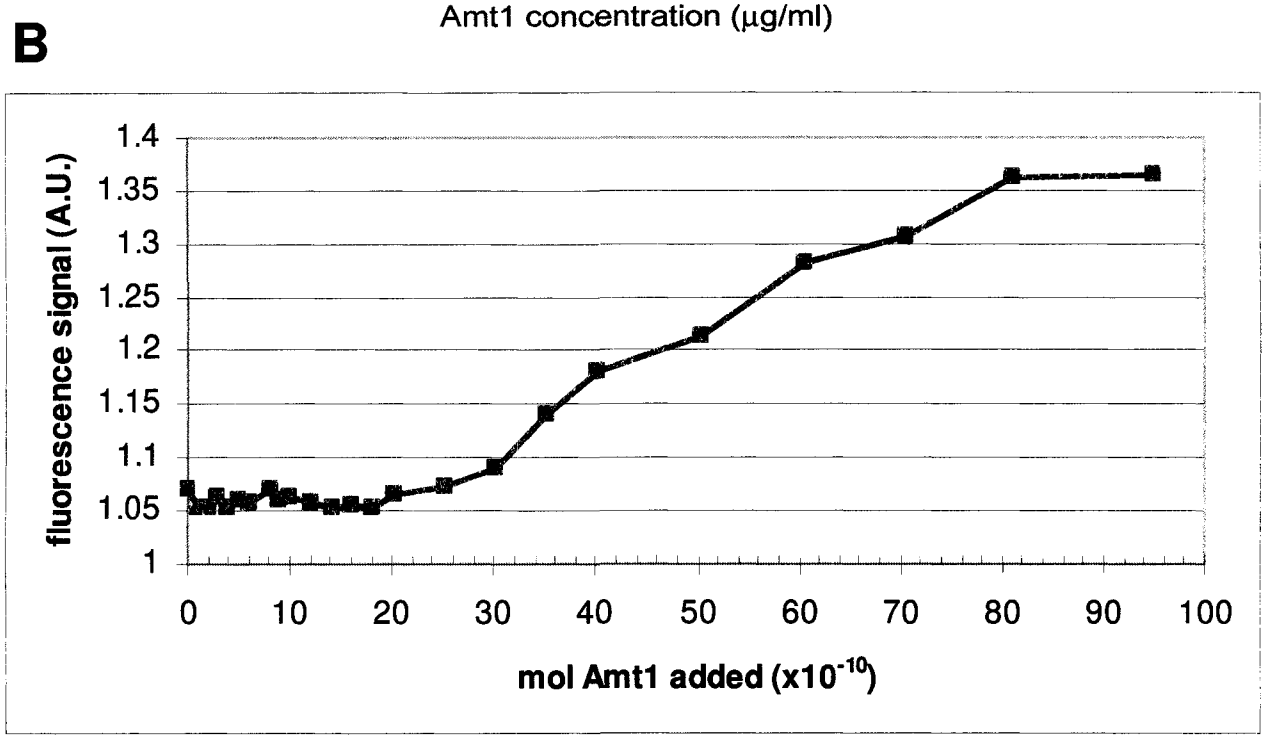

Figure 4.6 FRET studies of Amt1-DBD binding to nucleosomal DNA.

(A) Amt1-DBD addition to A_{16} NCP while monitoring dimer-tetramer FRET. Interactions between the dimer and tetramer within the histone octamer was monitored as increasing amounts of Amt1 was added (as shown). The histone H2B T112C was labeled with the donor chromophore CPM and H4 T71C was labeled with the acceptor chromophore FM. The excitation wavelength was set at 385 nm and the donor emission was recorded at 475 nm. The last point shows donor emission after 2 M NaCl was added. **(B)** Amt1-DBD binding to A_{16} NCPs. Dissociation of the DNA ends were monitored as increasing amounts of Amt1-DBD protein was added (as shown). DNA ends were labeled with the donor chromophore and histone T112C was labeled with the acceptor.

shift assays. The increase in fluorescence signal is the same as compared to complete dissociation of the DNA ends from salt addition (data not shown). In comparison, addition of the same amounts of buffer to labeled nucleosomes resulted in no change in FRET (data not shown). Since FRET is inversely proportional to the sixth power of the distance between donor and acceptor, this result clearly demonstrates that the distance between the ends of the DNA and the (H2A-H2B) dimer has increased from ~60 Å to > ~100 Å. Taken together, these experiments unequivocally demonstrate that the ends of the DNA partially dissociate from the surface of the histone octamer to make room for the binding of the transcription factor near the dyad, but that this is not accompanied by the dissociation of one or two (H2A-H2B) dimers.

4.4f Amt1 binding to nucleosomes causes increased DNA accessibility directly downstream of the binding site

To further characterize the structural changes imparted on nucleosomal DNA upon transcription factor binding, we employed *in vitro* DNase I footprinting methods. Nucleosomes were assembled from ^{32}P-labeled A_{16} 147mer and histone octamers (Gottesfeld et al., 2001). Amt1-DBD was then added to the nucleosomes in increasing concentrations. The Amt1-DBD : NCP ratios were comparable to those used in the gel shift assays shown in Figure 4.4A (15 fold molar excess of Amt1-DBD). The complex was digested with DNase I, and the samples were deproteinated and analyzed on a sequencing gel. As seen in Figure 4.7A, the binding of Amt1 directly upstream of the dyad can be detected. Since the DNA is labeled on both 5' ends, the footprint to the other side of the dyad axis can be detected as well. The most noticeable change resulting from Amt1-DBD binding is a dramatic increase in DNase I hypersensitivity at the nucleosomal

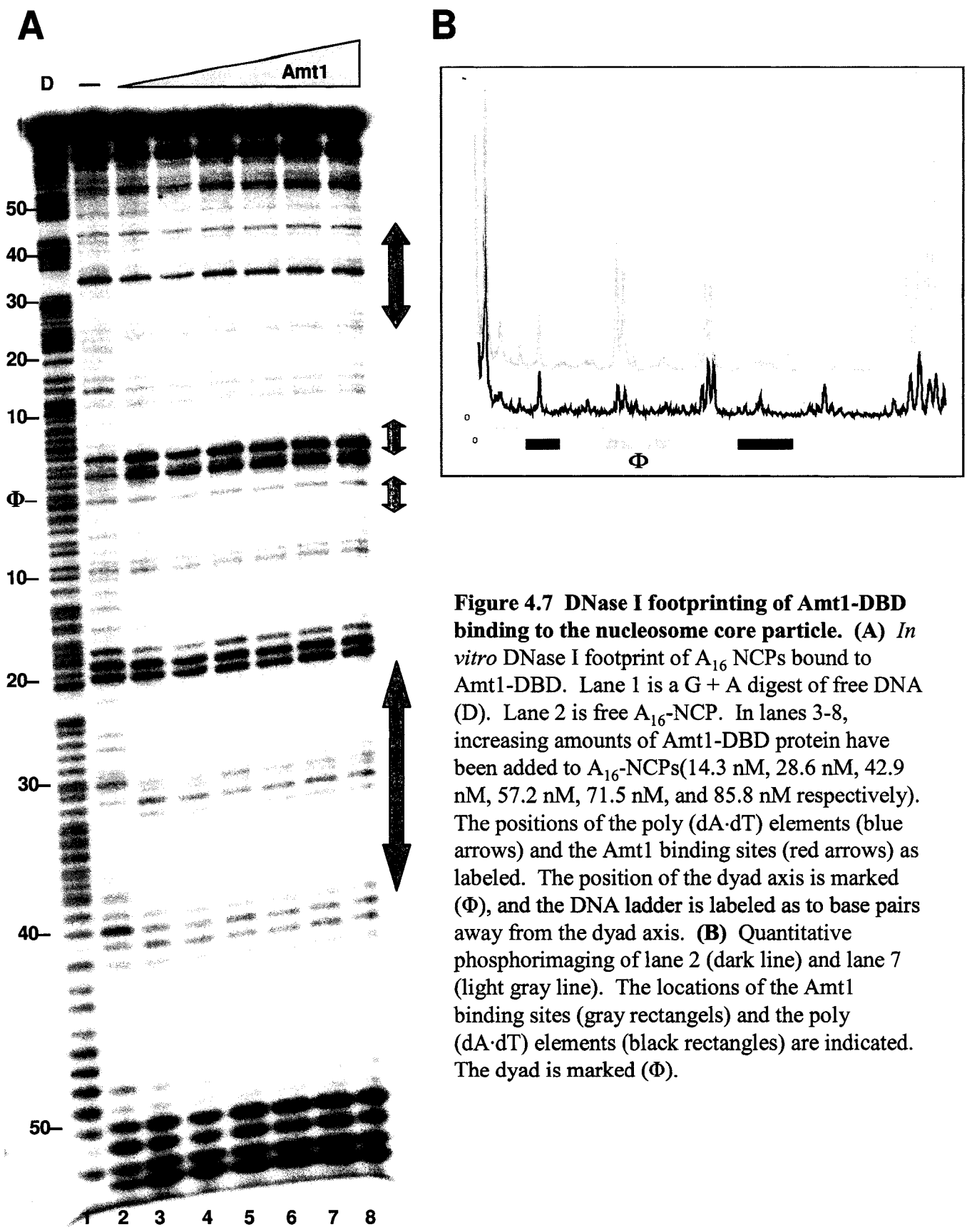

Figure 4.7 DNase I footprinting of Amt1-DBD binding to the nucleosome core particle. (A) *In vitro* DNase I footprint of A_{16} NCPs bound to Amt1-DBD. Lane 1 is a G + A digest of free DNA (D). Lane 2 is free A_{16}-NCP. In lanes 3-8, increasing amounts of Amt1-DBD protein have been added to A_{16}-NCPs(14.3 nM, 28.6 nM, 42.9 nM, 57.2 nM, 71.5 nM, and 85.8 nM respectively). The positions of the poly (dA·dT) elements (blue arrows) and the Amt1 binding sites (red arrows) as labeled. The position of the dyad axis is marked (Φ), and the DNA ladder is labeled as to base pairs away from the dyad axis. **(B)** Quantitative phosphorimaging of lane 2 (dark line) and lane 7 (light gray line). The locations of the Amt1 binding sites (gray rectangels) and the poly (dA·dT) elements (black rectangles) are indicated. The dyad is marked (Φ).

dyad (Fig. 4.7B). This could be due to two factors. First, as Amt1 binds to its MRE, it could cause the DNA to pull away from the histone octamer around the region of transcription factor binding. Thus, the DNA becomes hypersensitive to DNase I digestion. Second, we have shown above that Amt1-DBD binding to the nucleosomes causes dissociation of the DNA ends from the surface of the nucleosome. As a result, the region around the dyad may be rendered more accessible to DNase I.

4.4g The A_{16} element facilitates Amt1-DBD binding to the nucleosome

We next wanted to determine if the binding of the Amt1 transcription factor requires the presence of the A_{16} sequence element *in vitro*. To this end, we compared the binding of Amt1-DBD to A_{16} NCPs and α-sat NCPs, using loss of FRET between the (H2A-H2B) dimer and DNA ends as a signal for Amt1 binding to nucleosomes. α-sat DNA differs from A_{16} DNA only by the absence of the A_{16} element, and by the shift of one of the two MRE's present on this DNA fragment by one base pair towards the dyad. We confirmed by gel shift assay that Amt1-DBD binds to both types of nucleosomes, and K_Ds of 6.0 nM were obtained for Amt1 binding to both DNA free fragments (Figure 4.5A, and supplemental figure 4.10B). Therefore, Amt1 binds to both DNA fragments with equal affinity. The NCPs were labeled as described above, and donor emission was monitored as increasing amounts of Amt1 were added (Figure 4.8). A lower concentration of Amt1-DBD is necessary to initiate dissociation of the DNA ends from A_{16} NCPs as compared to α-sat NCPs (Figure 4.8), indicating that Amt1 has a higher affinity for A_{16} NCP than for α-sat NCP. The Amt1-DBD and nucleosomal concentrations used in both the A_{16} NCP and α-sat NCP binding reactions were identical. Although two MREs are present on each α-sat NCP (Fig. 4.1A), we have shown by native gel electrophoresis that only one

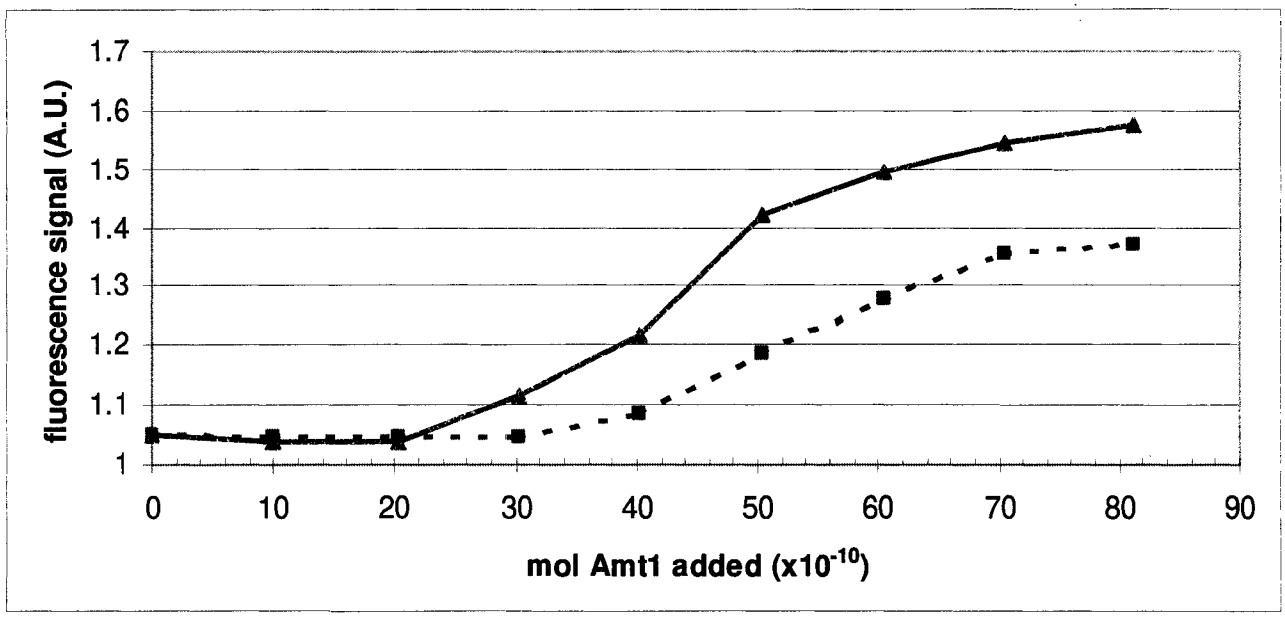

Figure 4.8 The binding of Amt1-DBD is facilitated by the A_{16} element.

Amt1-DBD titration of A_{16}-NCP (blue triangles) compared to α-sat-NCP which contains the Amt1 MRE without the poly (dA·dT) element (green squares). Histone H2B T112C was labeled with the acceptor FM and the DNA ends were labeled with the donor CPM. Amounts of Amt1-DBD added is shown. Donor emission was monitored at 475 nm after excitation at 385 nm.

of them is likely to be occupied by Amt1-DBD at a given time (supplemental Figure 4.9B). The conserved Amt1 binding site is TNNNGCTG. Although two of the variable bases in the binding site vary between the two sequences, it has been shown that Amt1 exhibits no discrimination (Zhou et al., 1992). We therefore conclude that the difference in Amt1-DBD binding between the two different nucleosomes is due the presence of the A_{16} sequence element.

4.5 Discussion

The mechanisms by which chromatinized DNA is converted into transcriptionally active states are under intense investigation. Posttranslational modification of histone tails, ATP-dependent chromatin remodeling, nucleosome positioning, and the ability of certain transcription factors to recognize their binding site in the context of a nucleosome all contribute to a varying extent, depending on the system (for recent reviews, see (Vaquero, 2003), (Jenuwein and Allis, 2001)). None of these processes is well understood at the mechanistic level. Here we investigate the hypothesis that poly (dA·dT) tracts either exclude nucleosomes, or form 'remodeled' nucleosomes, thereby facilitating activation of specific genes. We further investigate whether such regions facilitate the binding of the transcription factor Amt1 to nucleosomal DNA, and characterize the structural transitions that result from Amt1 binding to nucleosomes.

Using *in vitro* approaches, we confirm that a 147 bp DNA fragment containing a poly (dA·dT) tract of 16 bp in length can form stably folded nucleosomes, and show that our reconstitution system does not discriminate against such an unorthodox DNA sequence. In fact, NCPs reconstituted with a DNA fragment containing a poly (dA·dT) tract are stabilized against salt-induced dissociation. We also reconstructed the

positioned nucleosome encompassing the recognition sequence for the metallo-regulatory transcription factor Amt1 and a poly (dA·dT) tract that has been mapped *in vivo* in *Candida glabrata,* and find that the Amt1 binding site near the nucleosomal dyad is made accessible by partial dissociation of the ends of the DNA. This is not accompanied by the dissociation of histone sub-complexes.

Poly (dA·dT) elements located within many yeast promoters are required for activated transcription of many genes (Filetici et al., 1998), (Tanaka et al., 1996), (Lascaris et al., 2000). These elements are also found in higher eukaryotes, but their role has been less studied. These elements are a frequent feature of yeast promoter regions, with poly (dA·dT) tracts >10 bp occurring at much higher frequencies than expected in the genome (Dechering et al., 1998). Although many of these regions have been shown to be nucleosome-free *in vivo,* the poly (dA·dT) element alone is not sufficient for nucleosome exclusion (Losa et al., 1990; Moreira et al., 2002; Suter et al., 2000). It has been suggested that the yeast histone acetyltransferase GCN5 is responsible for creating nucleosome free regions around poly (dA·dT) elements in the yeast HIS3 promoter (Filetici et al., 1998). Other studies, however, arrive at different conclusions (Suter et al., 2000). Our observation that no energetic penalty exists for the salt-dependent deposition of histones on such a DNA fragment, and that nucleosomes reconstituted with poly (dA·dT)-tract containing DNA fragments are in fact slightly stabilized against salt-induced dissociation, is consistent with these results.

The system under investigation here has been chosen explicitly because a positioned nucleosome encompassing the poly (dA·dT) element and the binding site for the transcription factor Amt1 has been mapped to high resolution *in vivo* (Zhu and Thiele,

1996). This places the A_{16} stretch in a relatively straight segment of nucleosomal DNA, and the metal response element to which Amt1 binds adjacent to the nucleosomal dyad 15 bp upstream. Although mono-nucleosomes reconstituted with this DNA sequence are virtually indistinguishable on high-resolution native gels from nucleosomes reconstituted with 'canonical' positioning sequences, analysis of DNase I footprints suggests that the conformation of the DNA has adapted to accommodate the unusual DNA tract. We show that the poly (dA·dT) element creates hypersensitive sites directly upstream of its nucleosomal position, as well as in other areas throughout the nucleosomal DNA. These structural changes may facilitate binding of the transcription factor Amt1 to its binding site. We cannot, however, rule out the possibility that poly (dA·dT) tracts placed in other areas of the nucleosome could lead to nucleosomal destabilization or exclusion.

Using gel-shifts, DNase I footprinting, and fluorescence techniques, we have shown conclusively that the transcription factor Amt1 binds directly and specifically to nucleosomal DNA near the dyad *in vitro*. The affinity of Amt1 for a nucleosome is only three-fold reduced compared to histone-free DNA. The $(H3\text{-}H4)_2$ tetramer and both (H2A-H2B) dimers remain associated with the DNA upon Amt1 binding. However, we do observe that the ends of the DNA dissociate from the surface of the histone octamer to avoid steric clashes with Amt1 binding near the nucleosomal dyad. The presence of the A_{16} tract facilitates binding, although it is not essential. Since we have shown that the A_{16} tract actually decreases the propensity of the ends of the DNA to reversibly dissociate in a salt-dependent manner, this effect must be due to the minor changes in DNA structure that are observed by comparing the DNase footprints between NCPs either with or without this sequence element.

Previous analysis of transcription factor – NCP complexes have postulated that some undefined structural rearrangements in nucleosome structure may be required for high-affinity binding. Given the architecture of the nucleosome, this must be especially true for DNA binding factors that embrace the DNA from both sides (reviewed in (Beato and Eisfeld, 1997)), but may also apply to the many transcription factors that only recognize one face of the DNA double helix (reviewed in (Garvie and Wolberger, 2001)). In the latter case, transcription factor binding is sterically hindered by the histones, but may be partially occluded by the adjacent gyre of the DNA supercoil. A compelling model for regulating access to nucleosomal DNA has been proposed and tested experimentally by Widom and colleagues ((Anderson and Widom, 2000) and references therein). This 'site exposure model' postulates that the ends of the DNA are in rapid equilibrium between histone-bound and unbound state, and that the unbound state may be captured and stabilized by the binding of a site-specific transcription factor.

This model is compatible with structural data, which show that protein – DNA interactions are at their weakest towards the ends of histone-bound DNA, but direct biophysical evidence of site exposure has never been shown. Fluorescence resonance energy transfer (FRET) is used as an absolute and relative molecular ruler, since the efficiency of transfer between two sites within a single molecule is inversely proportional to the sixth power of the distance. Our finding that Amt1 binding to nucleosomes results in the loss of FRET between the two ends of nucleosomal DNA provides the first biophysical evidence for this biologically relevant phenomenon. These results also demonstrate that site exposure facilitates access not only to DNA regions that are actually dissociated from the surface of the histone octamer, but also to regions near the

nucleosomal dyad which are still firmly bound by the histone octamer upon transcription factor binding.

This has implications for our understanding of transcriptional activation in a chromatin context. We show that nucleosomal DNA is accessible for site-specific recognition without requiring the dissociation of histones, confirming earlier results (Gottesfeld et al., 2001) (Suto et al., 2003), and provide a direct measurement for site exposure. Our results show that the binding of a transcription factor near the nucleosomal dyad results only in a very moderate loss of affinity compared to histone-free DNA, and does not require chromatin remodeling. However, we do not exclude that a further enhancement of binding might be observed in the presence of chromatin remodeling factors, as has previously been observed for the binding of TBP near the nucleosomal dyad (Imbalzano et al., 1994).

Accessibility of any given site is strongly dependent on nucleosome positioning (Gottesfeld et al., 2001) (Suto et al., 2003), the signals for which are poorly understood to date. Positioned (or 'preset') nucleosomes may provide an architecture for synergistic transcription factor binding, thus facilitating recruitment of the transcription machinery. In one particular case transcription factor binding actually leads to the positioning of nucleosomes, by stabilizing an inherently dynamic chromatin structure in a particular conformation (Shim et al., 1998).

It has become obvious that no single mechanism exists for activating gene expression in a chromatin context. The necessary molecular events depend strongly on local chromatin and nucleosome structure, and on the structure and mode of binding of the specific transcriptional activators that are required for activation. We have shown

here that at least one facet of the dizzying number of possibilities is the direct binding of a transcription factor to a positioned nucleosome, and that local distortions as a result of the incorporation of unusual DNA sequences contribute to binding. This may be of particular importance for rapid transcriptional response, as is required for copper detoxification in this specific system. However, this surely applies to other eukaryotic promoters as well.

4.6 Acknowledgments

We thank Dr. Dennis Winge for Amt1-DBD expression plasmids, and Dr. Joel Gottesfeld for help with footprinting experiments. This work was supported by NIH grant GM61909.

Supplemental Figures for Chapter 4

The following figures were cited as supplemental figures or data not shown in the text.

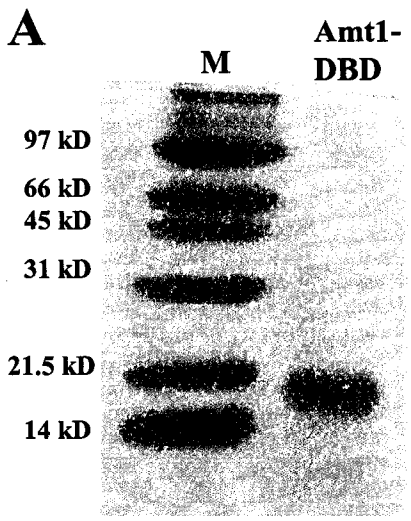

Figure 4.9. Amt1-DBD purification and activity assay (supplemental Figure 4.9 in the text).

(A) 18% SDS-PAGE gel showing purified Amt1-DBD expressed in E-coli and purified using ion-exchange chromatography. Gel was stained in commassie blue. Molecular weight markers are labeled. **(B)** 5% native-PAGE gel showing a Amt1-DBD binding assay to ^{32}P-labeled DNA. 25 bp designed oligo sequence contains Amt1 binding site. Non-specific DNA is 88 bp without an Amt1 binding site. 147 bp A_{16} DNA is as described in the text. 146 bp α-sat DNA contains Amt1 binding site without A_{16} element.

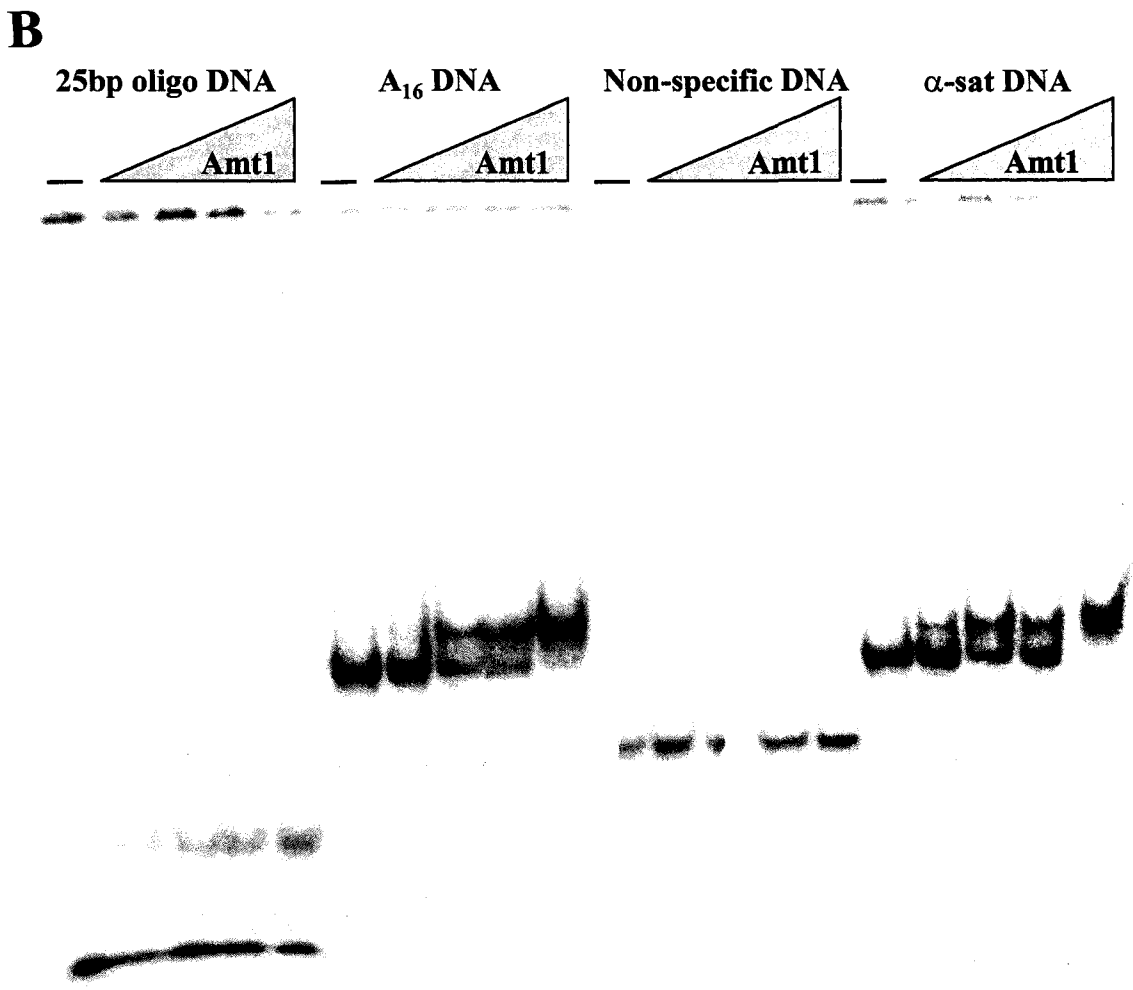

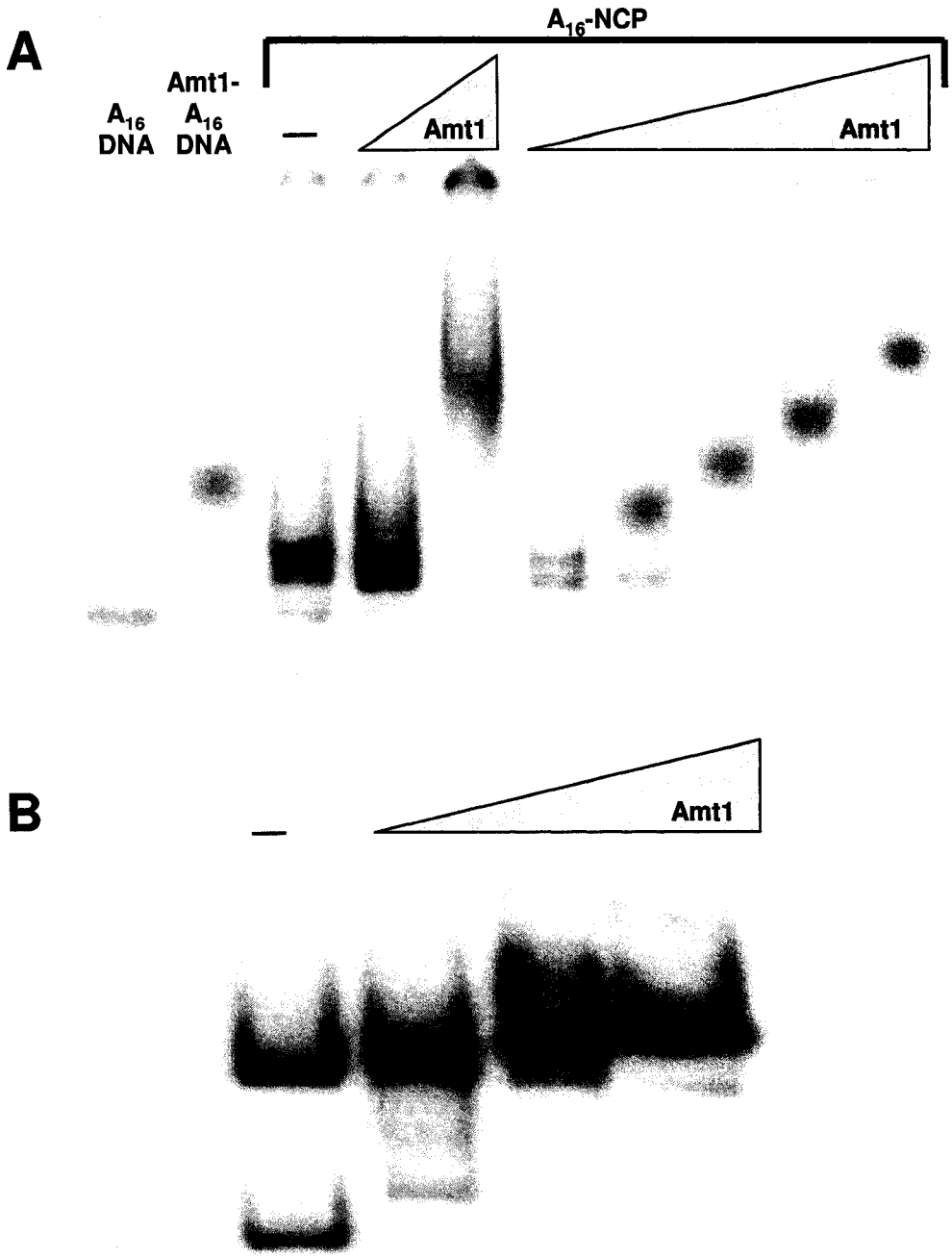

Figure 4.10 Amt1-DBD binding to A_{16} and α-sat NCPs (supplemental Figure 4.10 in the text).

(A) Gel shift assay of Amt1-DBD binding to A_{16} NCPs. NCPs were labeled with ^{32}P and incubated with increasing amounts of Amt1-BDB. Higher concentrations of Amt1-DBD results in supershifting of the complex band. **(B)** Gel shift assay of Amt1-DBD binding to α-sat-NCPs. NCPs were labeled with ^{32}P and incubated with increasing amounts of Amt1-DBD. Gel shows that Amt1-DBD binds to nucleosomes even in the absence of the poly (dA·dT) element.

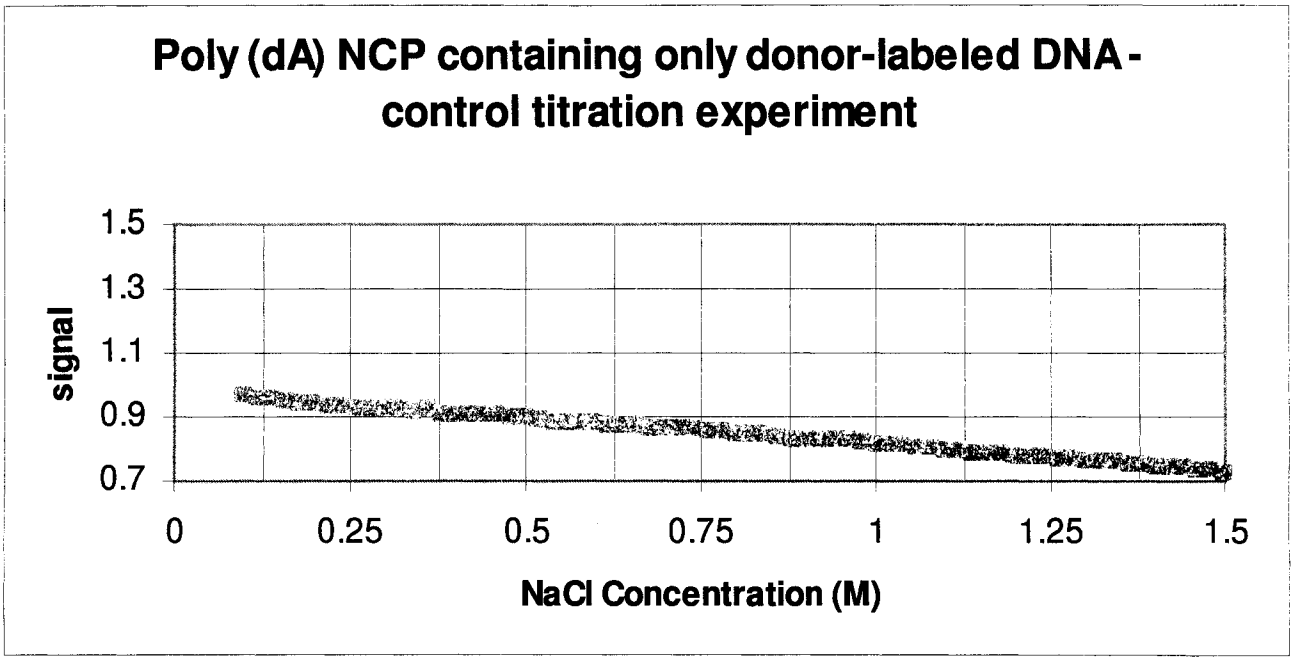

Figure 4.11. Donor-labeled only A_{16} NCP shows no loss of FRET.

Fluorescence emission of donor-only labeled A_{16} NCP. A_{16} DNA was labeled with the donor chromophore CPM and reconstituted into nucleosome core particles with non-labeled *X. laevis* octamer. The donor emission was detected as NaCl was titrated in from 0.1 M to 1.5 M in 0.02 M steps. The excitation wavelength was set at 385 nm and donor emission was monitored at 475 nm. Data was corrected for dilution before plotting.

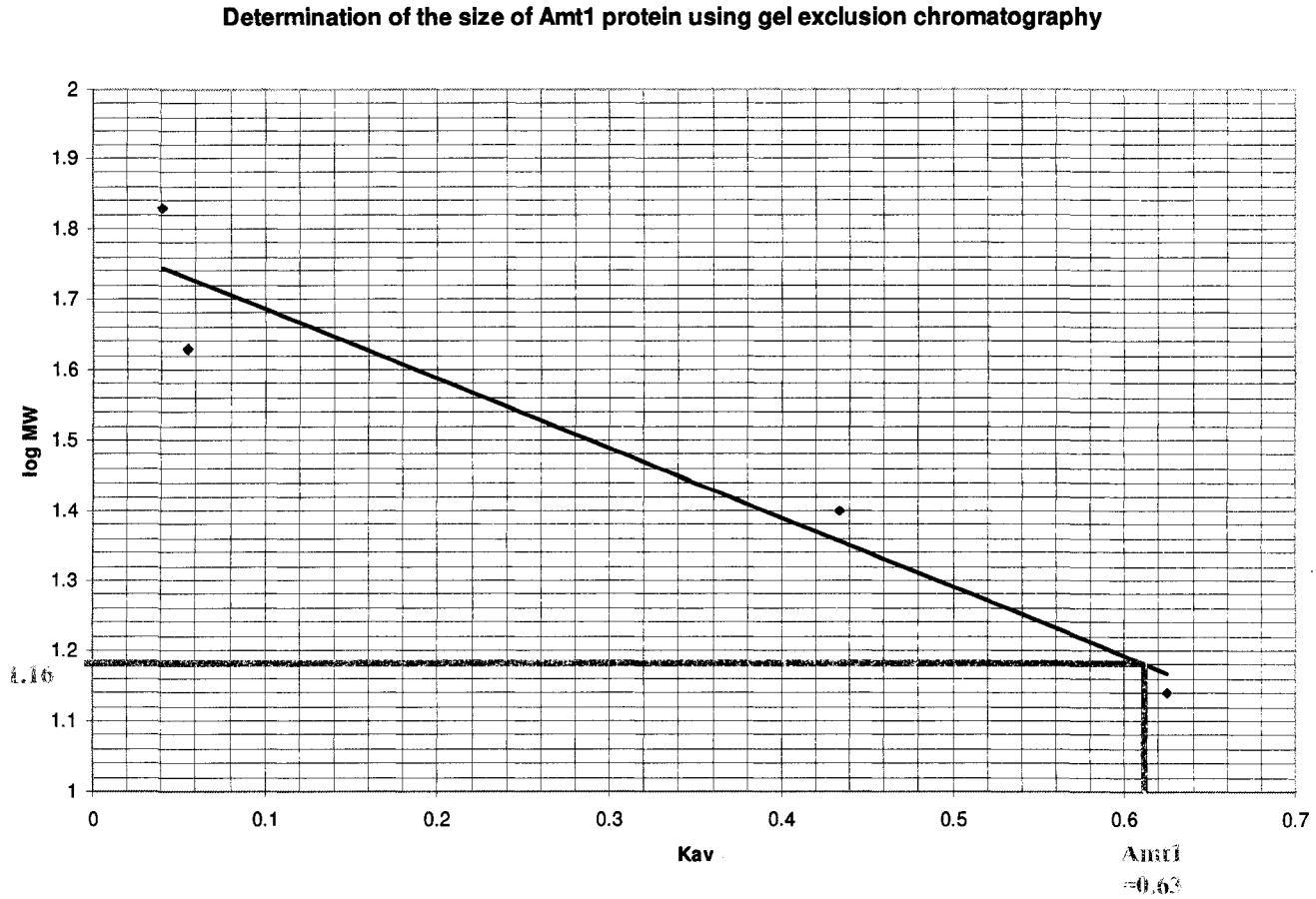

Figure 4.12. Molecular weight determination of Amt1-DBD.

The purified Amt1 DNA binding domain (MW = 13.9 kDa) was loaded onto a Superdex 75 gel filtration column. The elution volume was recorded and a Kav was calculated. This value was compared to known molecular weight proteins. Calculations of Amt1-DBD elution shows that the protein exits as a monomer (as shown).

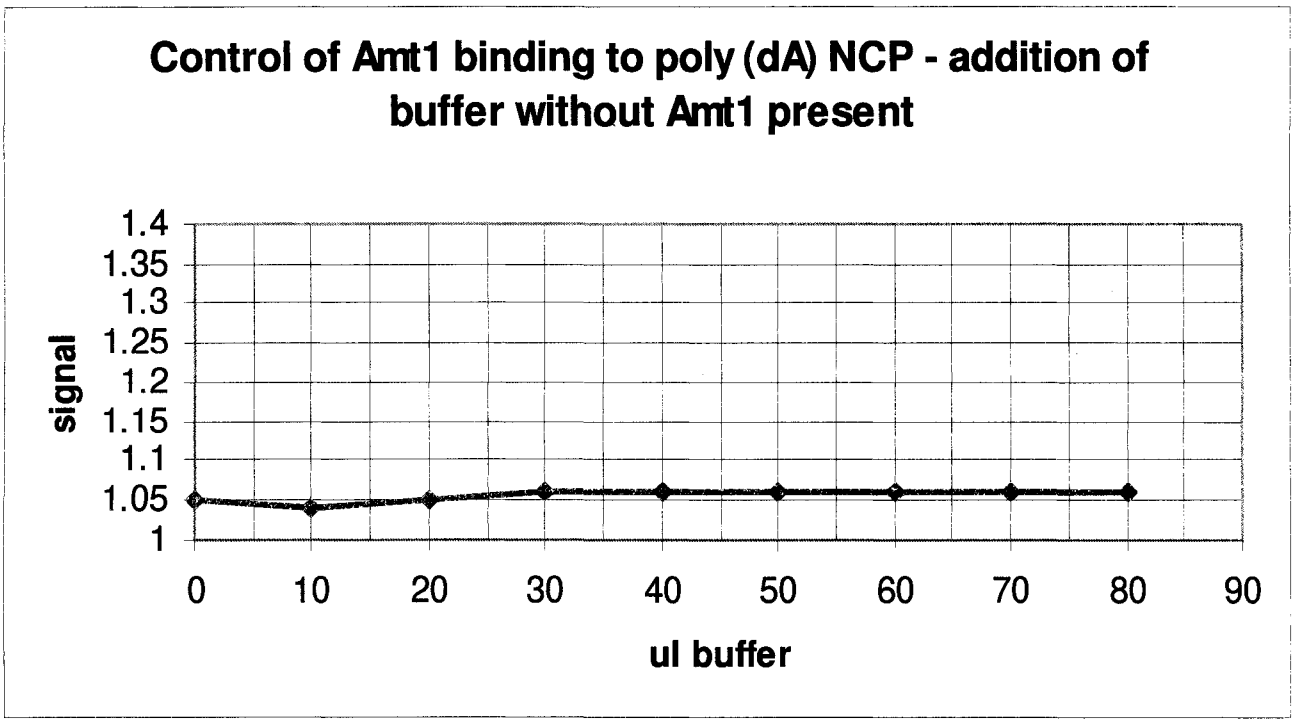

Figure 4.13. Addition of buffer without the Amt1-DBD protein shows no change in FRET.

A_{16} DNA ends were labeled with the donor chromophore CPM and histone H2B T112C was labeled with the acceptor chromophore FLU. Amt1 0M salt storage buffer (without Amt1-DBD) was added in increasing volumes as shown. Donor emission was monitored at 475 nm after excitation at 385 nm. Results show no change in fluorescence signal. Thus, the change in signal seen with the addition of Amt1-DBD is not due to buffer addition, but rather to Amt1-DBD binding to the nucleosome.

Chapter 5

X-ray Crystallographic Studies on the Effect of poly (dA·dT) Elements on the DNA Structure of the Nucleosome Core Particle

It has been hypothesized that the poly (dA·dT) elements common to many yeast promoter regions confer localized DNA distortion within nucleosome core particles in order to allow more rapid transcriptional activation. In order to study the role of poly (dA·dT) elements on nucleosomal DNA structure, we set out to determine the crystal structure of a nucleosome core particle containing a sixteen base pair poly (dA·dT) tract. The construction of the poly (dA·dT) DNA fragment, the refolding and characterization of nucleosome core particles, all crystallization trials and setups, and all of the initial data collection and analysis were completed solely by me. Yunhe Bao helped in the data collection and analysis of the last data set collected on the best diffracting crystal to date.

5.1 Abstract

Previous studies have shown that the homopolymeric (dA·dT) element found in many eukaryotic promoter regions is essential for activated transcription. The poly (dA·dT) stretch is a very rigid DNA sequence. In some instances, it is necessary for the poly (dA·dT) element in a promoter to be incorporated within a nucleosome in order to obtain transcriptional activation (Zhu and Thiele, 1996). Thus, it is thought that the poly (dA·dT) element locally disrupts the normal circular path of nucleosomal DNA, thus making promoter regions more accessible for transcription factor binding. However, we have shown that this sequence forms very stable nucleosome core particles (chapter 4). In order to determine the exact structural alterations created by the insertion of a poly (dA·dT) sequence into a nucleosome, I attempted to solve the crystal structure of a nucleosome core particle containing a 16 bp poly (dA·dT) tract. Electron density maps of the structure show that this sequence does indeed create areas of altered DNA structure. This is the first nucleosomal crystal structure solved to date with an altered DNA sequence. Therefore, this structure gives us insight in the differences in nucleosomal structure created by varying DNA sequences, as well as the role of nucleosome distruption in transcriptional activation.

5.2 Introduction

The packaging of DNA into chromatin generally limits access of transcriptional machinery to their respective genes, resulting in general repression. However, cells have various mechanisms by which they overcome the transcriptional repression resulting from chromatin compaction. It is proposed that one mechanism that cells employ is the incorporation of unusual DNA sequences, such as poly (dA·dT) tracks, into gene

promoter regions. These rigid DNA tracks are thought to disrupt nucleosome formation in some way so as to allow easier access of the promoter regions to the transcriptional machinery. Poly (dA·dT) tracks occur quite frequently in gene promoters. When studying these regions in the yeast *Saccharomyces cerevisiae*, poly (dA·dT) tracks greater than ten base pairs occur 2495 times, with 1760 of these elements located within 500 base pairs of the untranslated region of an open reading frame (ORF) (Shimizu et al., 2000). Moreover, when these elements are deleted in one case studied, transcriptional activation is greatly reduced (Struhl, 1985). This data supports the conclusion that poly (dA·dT) elements could modulate chromatin structure in order to make transcription factors accessible to the promoters of constitutively expressed genes.

In times past, it was thought that poly (dA·dT) DNA sequences could not accommodate the bending required to form nucleosome core particles, thus completely eliminating nucleosomes from forming in these promoter regions. This thinking was due to the fact that poly (dA·dT) DNA adopts a straight, rigid DNA structure (X-form DNA). They also have a compressed minor groove, contain a short helical repeat of 10bp per turn, and have a base pair propeller twist that is higher than B-form DNA (reviewed in (Breslauer, 1991)). However, it has more recently been shown that poly (dA·dT) sequences can indeed be incorporated into nucleosomes in a length-dependent manner. Shimizu et al. showed that poly (dA·dT) sequences of 34 bas pairs in length completely disrupted nucleosome formation on promoter regions, whereas tracks of 18 base pairs only lead to partial nucleosome disruption, and tracks of 12 base pairs showed no disruption (Shimizu et al., 2000). It has also been demonstrated that poly (dA·dT) tracks of 20 base pairs can form nucleosomes but are excluded from the center (Suter et al.,

2000). These studies suggest that, when size is moderate, the unusual DNA conformation adopted by poly (dA·dT) may distort local nucleosomal structure, which may facilitate the access of transcriptional machinery.

To date, all data looking at the effects of poly (dA·dT) elements upon nucleosomal structure involves *in vivo* or *in vitro* DNase digestion assays. While these assays are good at determining general nucleosomal accessibility, they do not give exact structural data. Solving the crystal structure of a nucleosome core particle containing a poly (dA·dT) element would allow us to see the exact structural changes that would occur if these sequences were incorporated into nucleosomes in promoter regions. With data from a crystal structure, we would be able to directly see if DNA distortions occur as to allow the DNA to be more accessible to transcription factor binding. Therefore, we have set out to determine the X-ray crystal structure of a nucleosome core particle containing a poly (dA·dT) element. As stated in chapter 4, one gene which contains a poly (dA·dT) element of 16 base pairs in length is the Amt1 gene promoter in the yeast *Candida glabrata*. Within the Amt1 promoter region, a poly (dA·dT) track lies upstream of the metal responsive element (MRE) (the Amt1 binding site), and it has been shown that this element is essential for rapid Amt1 binding and autoregulation (Zhu and Thiele, 1996). Using micrococcal nuclease sensitivity, it was shown that the poly (dA·dT) element and MRE are embedded within a stably positioned nucleosome, and that this element confers localized DNA distortion which renders the MRE hypersensitive to DNase I cleavage.

In the previous chapter, I described studies I completed aimed at looking at the effect that this rigid element has on nucleosome core particle formation and stability. My results suggested that this element causes localized distortion within nucleosomal DNA,

which may facilitate transcription factor binding. Expanding on these results, I have attempted to determine the crystal structure of a nucleosome core particle containing the Amt1 gene promoter poly (dA·dT) element and MRE. The structural data obtained thus far suggests that this DNA sequence does create some extent of disorder within the DNA molecule.

5.3 Materials and Methods

5.3a Construction of a 147 bp DNA fragment containing the Amt1 poly (dA·dT) element and MRE.

Two DNA oligo sequences were designed which placed both elements within the mapped positions of the nucleosome core particle. These elements were placed in the canonical 146 bp α-satellite DNA used previously in order to solve the crystal structure of the yeast nucleosome core particle (White et al., 2001), as well as other nucleosomal structures solved by our lab (Luger et al., 1997), (Suto et al., 2000), (Suto et al., 2003). This was done so as to deviate from the known structure as little as possible, except for the elements being studied. Four oligo DNA fragments were synthesized, in which one pair incorporated the poly (dA·dT) element, and the other contained the canonical α-satellite DNA sequence used in previous nucleosome structures. Each constructed oligo also contained sites that would allow the sequence to be cut out and amplified. The annealed oligos were ligated into two seqarate puc19 plasmid DNAs. The sequences were then amplified to contain sixteen repeats using an optimized protocol for the construction of plasmids containing multiple direct repeats. The plasmid containing the proper insert was cut with restriction enzymes KpnI and BglII, and the vector DNA was subsequently

purified. More plasmid DNA containing the inserts was cut with a second digest of KpnI and BamHI. The insert DNA was purified away from the plasmid vector. The insert (created by digest 2) was ligated with the vector DNA (created by digest 1). The above steps were repeated to obtain the desired number of repeats. For each cloning round, digestion of each plasmid with EcoRV was performed to make sure the sites for insert removal were being maintained, as well as running uncut and cut DNA on an agarose gel to make sure that no larger DNA fragments were being ligated into the plasmids. In order to obtain mass quantities of the DNA fragment, large amounts of both plasmids were purified following previously published protocols (Dyer et. al., 2003). The fragments were cut out and ligated together using designed HinfI sites (GANTC). The reason a HinfI site was used is that cutting DNA with HinfI creates an overhang that prevents self-ligation of the same fragments, since you can place two different base pairs for the N position (we used G in one sequence, C in another). In order to make sure that the correct 147 bp sequence was obtained, kinased 147 bp fragments were ligated into puc19 that had been blunt-end cut. The plasmid DNA was sequenced, and the data showed that the correct DNA sequence had been obtained.

5.3b Reconstitution of nucleosome core particles containing the poly (dA·dT) element

Histone proteins from *Xenopus laevis* were overexpressed in BL21 (DE3) plysS cells and purified using previously published protocols (Luger et al., 1999). The histone proteins were refolding to histone octamers, and reconstituted into nucleosome core particles using either the designed 147bp poly (dA·dT) DNA fragment (A_{16} DNA) or a 146 bp palindromic DNA fragment derived from human α-satellite regions (α-sat DNA) (Luger

et al., 1997). Nucleosomes were reconstituted using a salt-gradient method described previously (Luger et al., 1999). Milligram amounts of nucleosome core particles were subjected to heat shifting (37°C for α-satellite NCPs, 55°C for poly (dA·dT) NCPs) in order to create the free energy minimum position of the DNA around the histone octamer. The nucleosomes were subsequently purified using preparative gel electrophoresis (Luger et al., 1999), and purified NCPs were analyzed using native-PAGE.

5.3c Crystallographic procedures

Crystallization trials utilized both hanging and sitting drop techniques using vapor diffusion methods. A broad salt range was screened initially, with crystals obtained from an optimized salt range of 40 to 70 mM KCl, 68 to 96 mM $MnCl_2$, and 10 mM K-cacodylate pH 6.0 in the initial drop equilibrated against 20 to 35 mM KCl, 34 to 48 mM $MnCl_2$, and 5mM K-cacodylate as the initial well concentration. The optimized protein concentration within the drop was 4mg/ml. For data collection, crystals were harvested and soaked in a 24% methyl-pentane-diol cryo-protectant. Crystals were flash frozen in liquid propane (at -120°C) before transferring to the cryo-stream at -180°C, as previously described (Luger et al., 1997). For initial characterization, crystals were analyzed on our home source X-ray generator. Higher resolution data was obtained at beamline 5.0.2 or 8.2.2 at the Advanced Light Source in Berkeley. Multiple crystals yielded diffraction that was of sufficient quality to be processed using Denzo and Scalepack (Otwinowski and Minor, 1997). Molecular replacement was used to obtain crystal phases with Protein Data Bank entry 1AO1 as the search model. CNS was used to refine the model (Brunger et al., 1997), and the program O was used for model building and to analyze the resulting

$|2F_o - F_c|$ and $|F_o - F_c|$ electron density maps (Jones et al., 1991). Figures were prepared using O (Jones et al., 1991).

5.4 Results

5.4a Plasmid inserts can be amplified with good efficiency

Crystallization of nucleosome core particles requires large amounts of DNA (mg quantities). Obtaining mass quantities of recombinately grown and purified DNA is enhanced if the plasmids contain a number of insert repeats (Richmond et al., 1988). In order to obtain multiple repeats of a designed 147 bp DNA sequence containing the poly (dA·dT) element, I optimized a method to construct plasmids containing multiple direct repeats. In designing the cloning strategy for creating multiple DNA repeats, we flanked the DNA sequence of interest by restriction sites as shown in Figure 5.1A, where A is a unique site (here KpnI) and B and B' are sites for enzymes that are compatible, but non-identical (here Bam HI and Bgl II). Sites for an enzyme that are to be used to excise the fragment from the plasmid are also shown (here EcoRV). Since the final DNA fragment was to be generated by large-scale ligation of two shorter fragments, the HinfI site generates overhangs suitable for high-efficiency ligation. We used HinfI (restriction site GANTC) in order to generate the 147 bp DNA fragment, as this site only allows ligation of the two separate fragments, and not self-ligation of the same fragment. Digestion of the plasmid DNA with A and B creates a vector into which a fragment generated by digestion with A and B' can be ligated, destroying the restriction site at the B-B' junction (Figure 5.1B). Thus, with each cloning step, the number of inserts was doubled. Sixteen inserts were obtained in each plasmid. The following statistics give the experimental

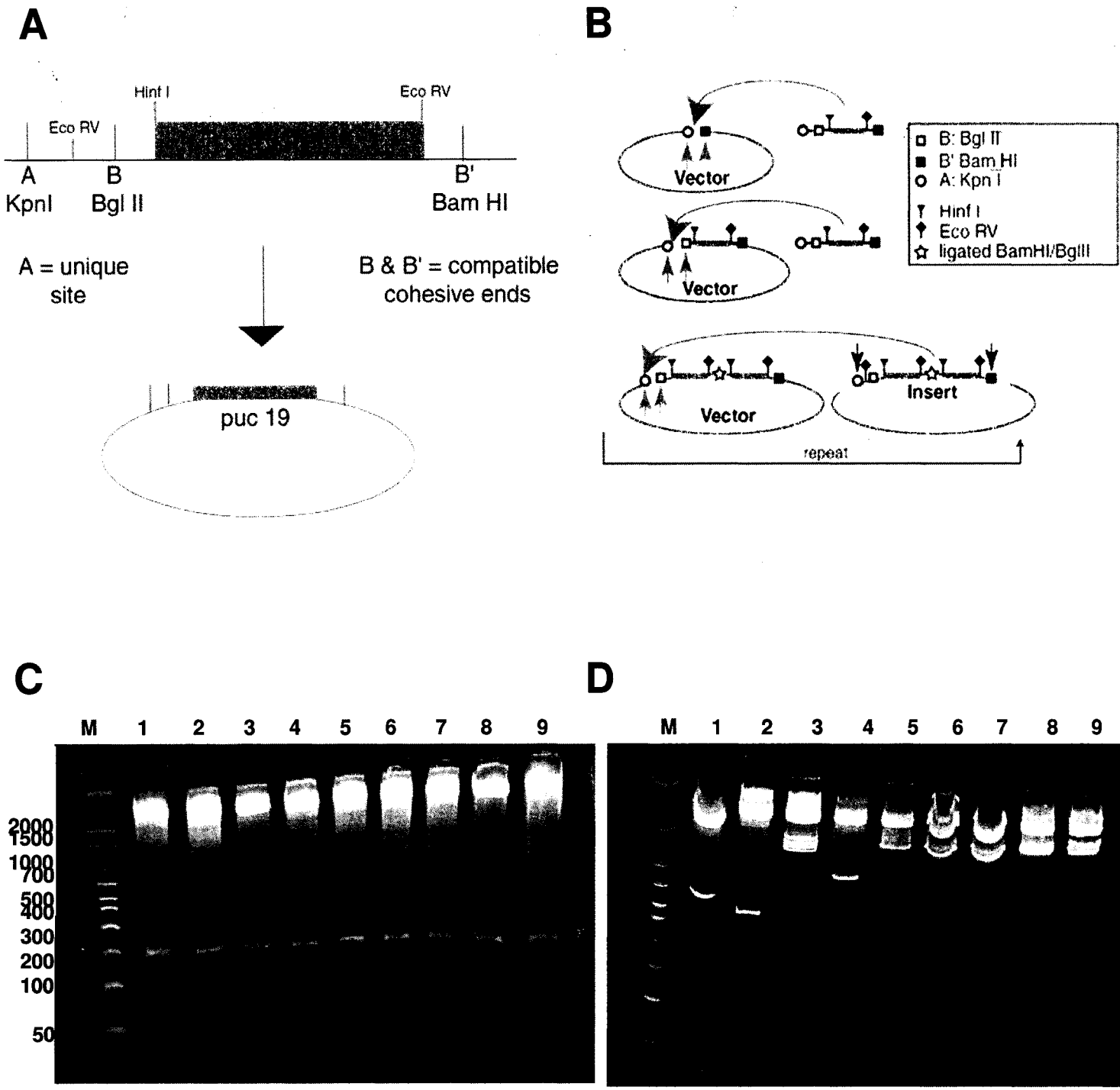

Figure 5.1. Strategy for insert amplification in plasmid DNA.

(A) Strategy for designing inserts for plasmid amplification and subsequent ligation for partially palindromic DNA sequences. Note that the two 'halves' of the final product do not have to be identical if the restriction sit for the final ligation step is chosen judiciously to prevent self-ligation (e.g. HinfI). The size of the designed DNA fragment is approximately 100 bp. **(B)** Cloning and duplication strategy. Sites for restriction enzymes are indicated by symbols (see insert for legend). Figs (A) and (B) are from (Dyer et. al., 2003). **(C)** 10% Native-PAGE gel showing results after the first round of insert amplification. Each transformed bacteria colony (numbered as shown) was grown up and the plasmid DNA was isolated and cut with KpnI/BamHI in order to isolate the insert DNA. As can be seen, 100% of the plasmids contain two inserts. The gel was stained in ethidum bromide. The DNA marker is labeled (shown in bp). The position of the band showing the ligated inserts is marked with a red * **(D)** 10% Native-PAGE gel (stained in ethidum bromide) showing result after four rounds of insert amplification. Plasmids were analyzed as above. The DNA ladder is the same as in (C). Red * indicates the wanted band.

amplification efficiencies found for each doubling cycle: 1 → 2: ~100% efficiency; 2 → 4: ~70% efficiency; 4 → 8: ~60% efficiency; 8 → 16: ~40% efficiency. Figure 5.1C and D gives results for the first doubling cycle for one to two copies, and the final doubling round from eight to sixteen inserts. Eighteen clones were analyzed for each round in order to calculate amplification efficiencies.

5.4b The designed 147bp poly (dA·dT) DNA reconstituted into nucleosomes which yielded diffracting crystals

In the study addressing nucleosomal placement on the Amt1 promoter, a stable nucleosome was mapped within the region extending from approximately -113 to -260 within the Amt1 promoter (Zhu and Thiele, 1996). In this setting, the MRE extends from -186 to -205, and the poly (dA·dT) element is located from -210 to -225 (Figure 5.2A). In the structural context of the nucleosome core particle, the poly (dA·dT) element would map from 36 to 52 base pairs from the DNA 5' end, while the MRE would extend from 66 to 73 bp (Figure 5.2B). Because the α-satellite DNA sequence has been optimized to yield highly diffracting nucleosome core particle crystals, we wanted to deviate from this sequence as little as possible. A small deviation from this sequence will also allow us to see the exact structural changes resulting from the poly (dA·dT) tract and not from other DNA sequence changes. Therefore, these elements were incorporated in a 147 bp α-satellite DNA sequence. 147 bp of DNA was used instead of 146 bp because it has been determined that this is the true amount of DNA bound by a histone octamer, and crystals diffracting to very high resolutions have been obtained using 147 bp of DNA (Davey et al., 2002). Thus, the DNA fragment was constructed to incorporate the poly (dA·dT) element and MRE in the locations stated above with the rest of the DNA sequence being

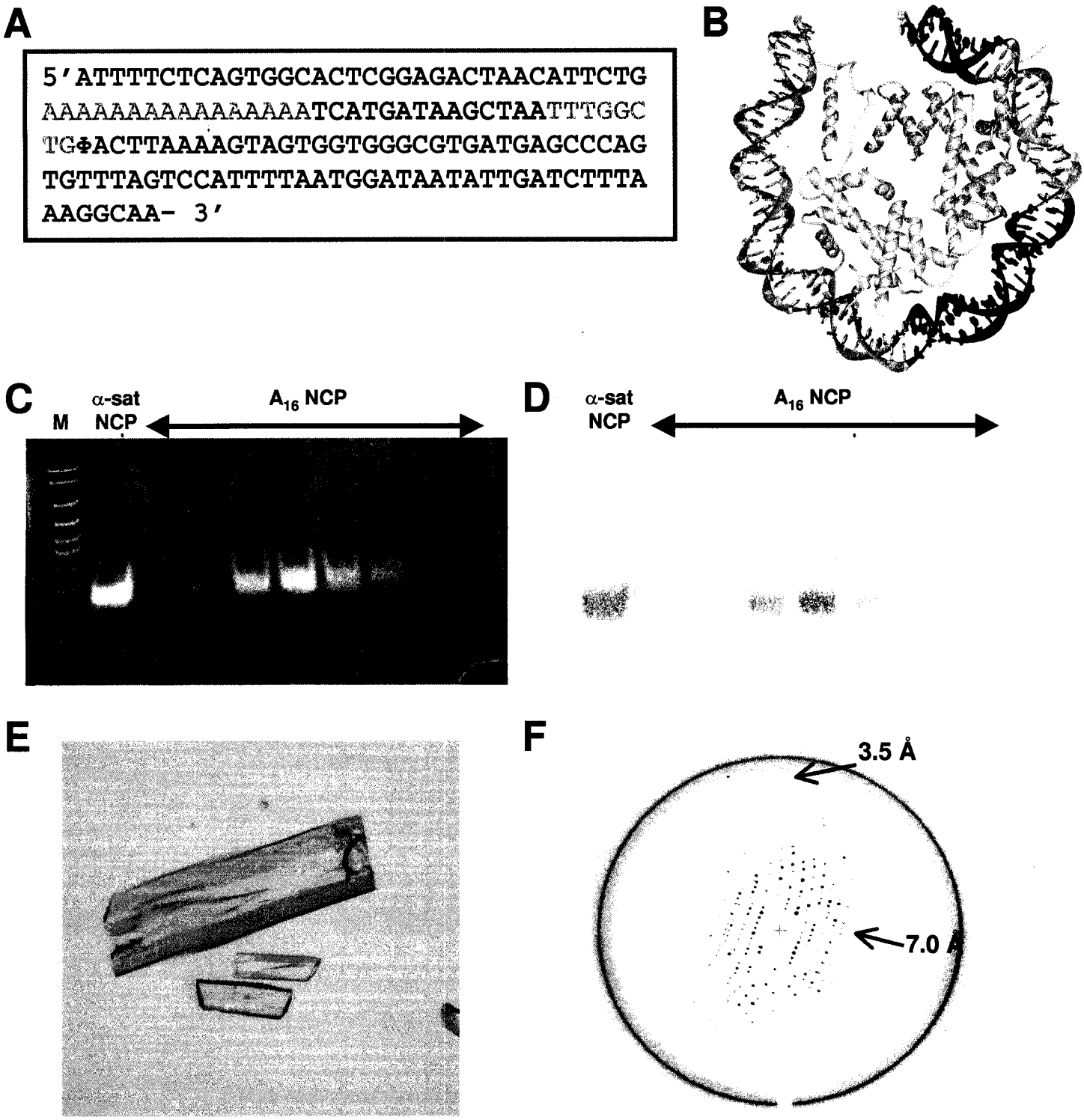

Figure 5.2. A_{16} NCPs form large crystals which give anisotropic diffraction.

(A) DNA sequence of the Amt1 gene promoter in *C. glabrata*. The sequence shown covers the area of the mapped nucleosome on the promoter region. The poly (dA·dT) element is shown in blue and the Amt1 binding site is shown in red. The dyad axis passes through the next base following the green Φ symbol. **(B)** The placement of the mapped poly (dA·dT) element (blue) and Amt1 binding site (red) in the crystal structure of the nucleosome core particle, according to *in vivo* mapping data. Only 73 bp of DNA and associated proteins are shown for clarity. **(C,D)** 5% native-PAGE gel of fractions from the purification of A_{16} NCP over a preparative-electrophoresis cell. α-sat NCP is shown for comparison. The gel was stained in ethidum bromide (B) followed by staining in coomassie blue (C). **(E)** Crystals of A_{16} NCP. The size of the largest crystal is 1.2 mm long by 185 μm wide. **(F)** Diffraction pattern of largest crystal from (D). Very anisotropic diffraction can be seen, with a resolution of 3.5 Å in one dimension, and 7.0 Å in the other.

from the α-satellite DNA fragments used previously by our lab (Suto et al., 2000), (White et al., 2001).

Original plans were to use *Saccharomyces cerevisiae* recombinant histone proteins in the reconstitution of nucleosomes containing the poly (dA·dT) DNA. However, since such fragile and anisotropically-diffracting crystals were obtained using yeast histone proteins, we choose to use *Xenopus laevis* recombinant histones. Reconstitution of purified histones and A_{16} DNA yielded nucleosomes which look identical to nucleosomes from canonical DNA (Figure 5.2 C & D). Purification of the nucleosomes did not deviate from standard published procedures.

Crystallization trials of nucleosomes containing the poly (dA·dT) element resulted in large crystals. A vapor diffusion sitting drop method in which the crystallization drop was placed in 3 μl of oil yielded the largest crystals, with the average crystal being 630 μm long by 220 μm wide (Figure 5.2E). The crystals looked exactly like those of canonical α-satellite NCPs, being a long rod with a center hole down the middle from one end and the other end being solid (Figure 5.2E). Several crystals diffracted to a resolution of ~3.5 Å (Figure 5.2F). However, the diffraction was very anisotropic, with a resolution of ~3.0 to 3.5 Å in one direction and ~6.5 to 7.0 Å in another. Macro-seeding of sitting drops was tried in order to obtain better crystals, but this method failed to yield crystals which diffracted to a better resolution. Varying salt concentration, protein concentration, pH conditions, and crystallization buffers also failed to yield better diffracting crystals.

5.4c The only molecular replacement solution obtained for poly (dA·dT) NCP is with only the octamer as an initial search model

Initial reduction of home source data showed that A_{16} NCPs crystallized in the primitive orthorhombic space group of $P2_12_12_1$ with a unit cell very similar to that of the nucleosome core particle containing canonical DNA. Data was subsequently collected at the synchrotron and indexed and scaled (Table 5.1). Data analysis again showed a primitive orthorhombic space group with similar unit cell dimensions. Molecular replacement using the nucleosome core particle from *Xenopus laevis* as the initial search model (PBD entry 1AOI) was utilized in order to phase the data. Molecular replacement failed, and thus the data was re-indexed in order to see if the data statistics could be improved. Refining parameters such as the profile fitting radius, error density, sigma cutoff, and weak level resulted in some improvement. However, much of the data was being excluded in indexing. As indexing proceeded, more and more spots from crystal diffraction were rejected, and as indexing neared the end, most spots were rejected. This gave poor data completeness. The only apparent reason for this occurrence was that this phenomenon was merely a characteristic of the data, since the spots did not appear to be split or twinned. I tried to use an image from the middle of the data set as an initial indexing frame, but this gave a completely different space group than an image from the first part of the data set. Many crystals were analyzed, and all exhibited these indexing characteristics to one extent or another. Several indexing programs were tried, such as DENZO and HKL 2000, but all gave the same results.

The highest quality of indexed data (Table 5.1) was eventually put through molecular replacement again to see if a solution could be found. Again, no good solution could be found. A simple rigid body refinement from the best solution given also failed to yield a distinguishable model. Molecular replacement was tried using only the histone

Table 5.1. Summary of Crystallographic Analysis - first complete synchrotron data set

Data Collection Statistics					
Space group	a=, b=, c=	Resolution (Å)	Reflections (Total/Unique)	Completeness (%)	R_{sym}[a]
$P2_12_12_1$	105.4, 109.5, 179.9	50 –3.2	104,495 (31,333)	89.0 (77.8)[b]	0.071 (0.323)[c]

[a] $R_{sym} = \Sigma \left| I_h - \langle I_h \rangle \right| / \Sigma I_h$, where $\langle I_h \rangle$ is the mean of measurements for a single hkl.
[b] Value in parentheses is for the highest resolution shell: 3.15 – 3.1 Å.

octamer as a search model (without the DNA present). This resulted in a good solution being found.

5.4d The DNA is not visible in the molecular replacement solution of poly (dA·dT) NCP

$2F_o$-F_c maps of the model using only the histone octamer as the search model showed good density for the histone octamer, but the density in the area of the DNA molecule was highly disordered. The density around the histone octamer was extremely disorganized, and gave no pattern into which the DNA could be built. There were a few areas where some difference density could be seen for a couple of phosphate molecules in a helical pattern, but then nothing could be built after these areas. I determined that the model was "real" since major ion molecules could be seen which are present in all nucleosome structures to date. Since these ions were not present in the initial search model, and therefore, could not be present due to model bias. For example, Figure 5.3A shows the difference density for a water molecule that is conjugated between the two H3 chains at the dyad. The difference density for this manganese can be seen in the model, but it was not present in the search model. Therefore, the data is of sufficient quality as to allow things that are not present in the search model to be seen if they are in a fixed position throughout the crystal lattice.

It was speculated that the reason the density for the DNA could not be seen is because it was not present in the initial search model. In order to determine if this was the case, the data set of the nucleosome core particle from *Saccharomyces cerevisiae* was analyzed by molecular replacement using only the octamer as the initial search model. The yeast NCP data set was of similar quality, and exhibited similar indexing statistics as

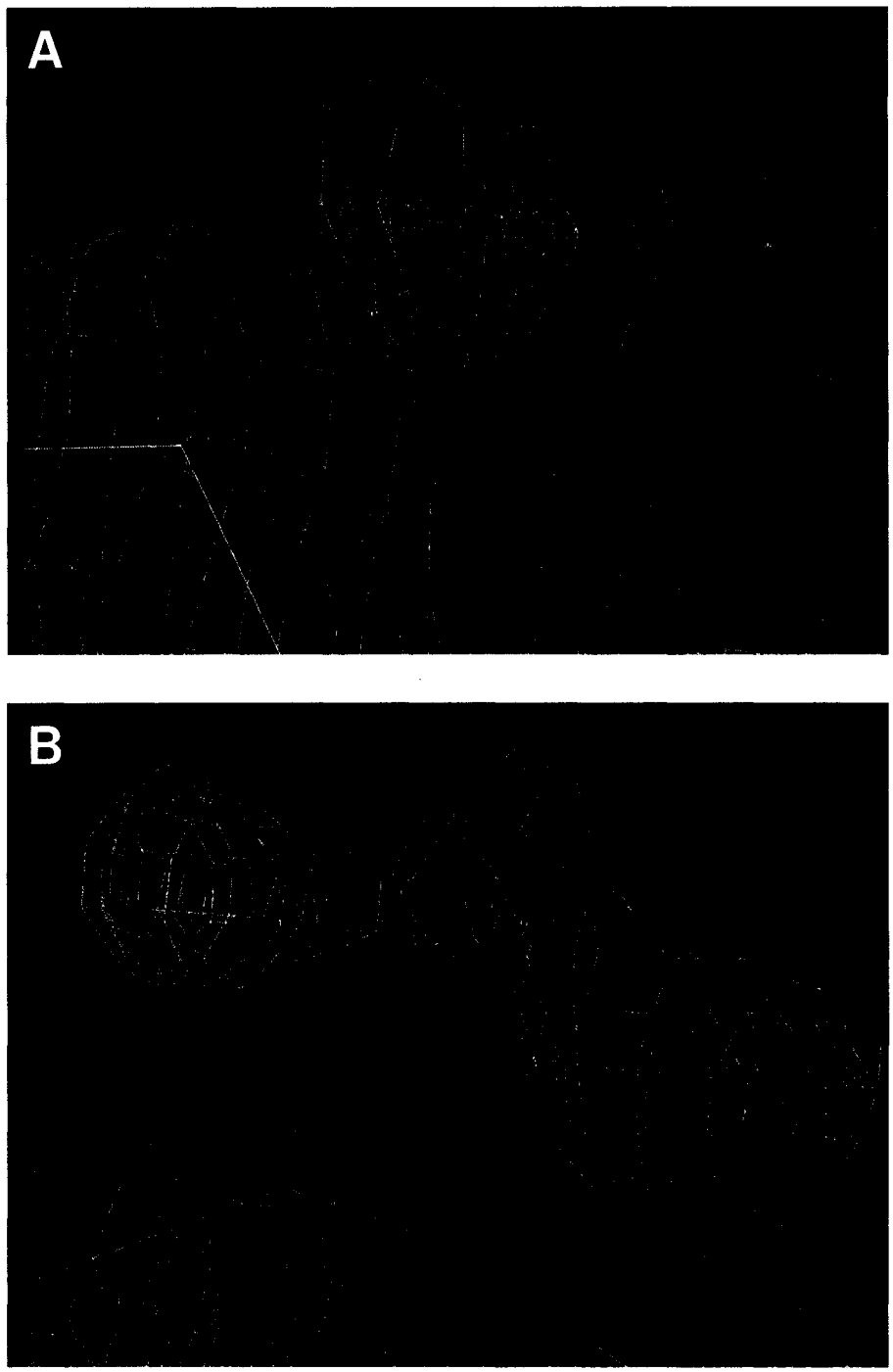

Figure 5.3. The model of the A_{16} NCP is "real" since solvent density can be seen, but no discernable DNA density can be detected.

(A) The density for a water molecule conjugated between the two H3 chains at the dyad axis of the A_{16} NCP model obtained by molecular replacement using the entire structure of the *Xenopus laevis* NCP as a search model. Red density = difference density (F_o - F_c map), and blue density = ($2F_o$ - F_c map), both contoured at 2.5σ. **(B)** Single base pair DNA density in the yeast NCP model obtained by molecular replacement using only the histone octamer as the initial search model. Blue density = difference density of the $2F_o$ - F_c map contoured at 2.0σ. Red density = F_o - F_c map contoured at 2.5σ.

the poly (dA·dT) NCP data set. A good solution was found and maps were subsequently made. Molecular replacement statistics between the two solutions were of similar quality, with the A16 data set having a final R_{free} of .4449, and the yeast data set having a R_{free} of .4017. Model analysis revealed distinct density for the DNA in the yeast model. In fact, density for an entire base pair can readily be found in the yeast NCP model (Figure 5.3B). However, no such density can be seen with poly (dA·dT) DNA. When comparing the two maps in areas just 5' and 3' of the dyad axis (an area where very good DNA density usually occurs), distinct density of the DNA double helix can be seen in the yeast NCP model, but not in the poly (dA·dT) NCP (Figure 5.4). Therefore, the absence of DNA density in the poly (dA·dT) NCP model is not due to the fact that the DNA was absent in the initial search model. On the other hand, it could indicate an inherent lack of order of the poly (dA·dT) DNA within the nucleosome core particle.

5.4e A poly (dA·dT) NCP crystal finally results in good diffraction and data quality

Continued crystal screening finally resulted in a crystal being found that gave good non-anisotropic diffraction to 2.7Å resolution. As can be seen in a diffraction pattern from the crystal in Fig. 5.5A, the crystal did not show such anistropic diffraction. The crystal tray from which this crystal was harvested was seven months old. Therefore, this crystal resulted from very slow growth, probably allowing enough time for a rearrangement of DNA and thus a more efficient packing within the crystal lattice to be obtained. Data from this crystal was collected at the synchrotron, and the data was first analyzed in the P1 space group. Upon data analysis, it became obvious that the crystal belonged to an orthorhombic space group, and there were four nucleosomes per unit cell.

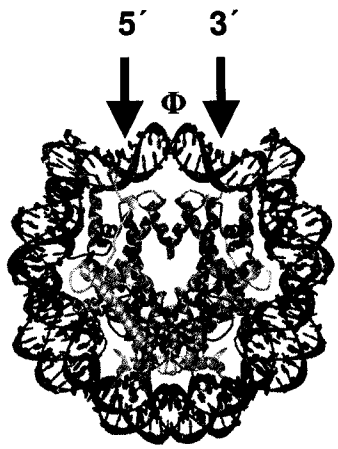

Figure 5.4. The DNA in the molecular replacement solution using only the histone octamer as the search model can be seen in yeast NCP, but not in A_{16} NCP.

A comparison of the two maps of yeast NCP and A_{16} NCP are shown. The left column shows density just 5′ of the dyad, and the right column shows density just 3′ of the dyad. The arrows in the inset of the crystal structure of the yeast nucleosome core particle shows approximate areas of density shown (the dyad axis is denoted by Φ). The top row is the density from the A_{16} NCP, and the bottom row is the density from yeast NCP. The blue density is the $2F_o - F_c$ map at 2.0 σ. The red density is the $F_o - F_c$ map at 2.5σ.

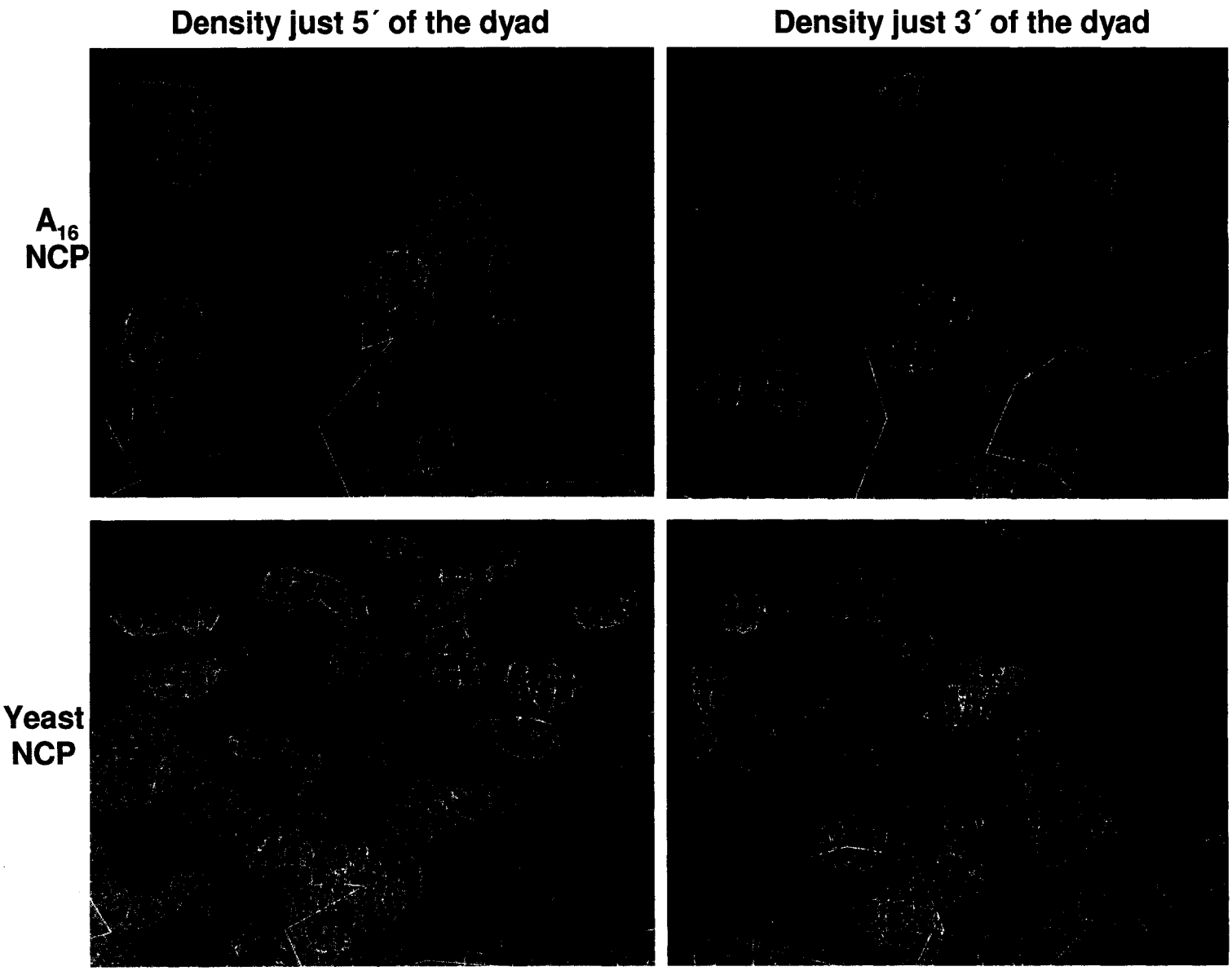

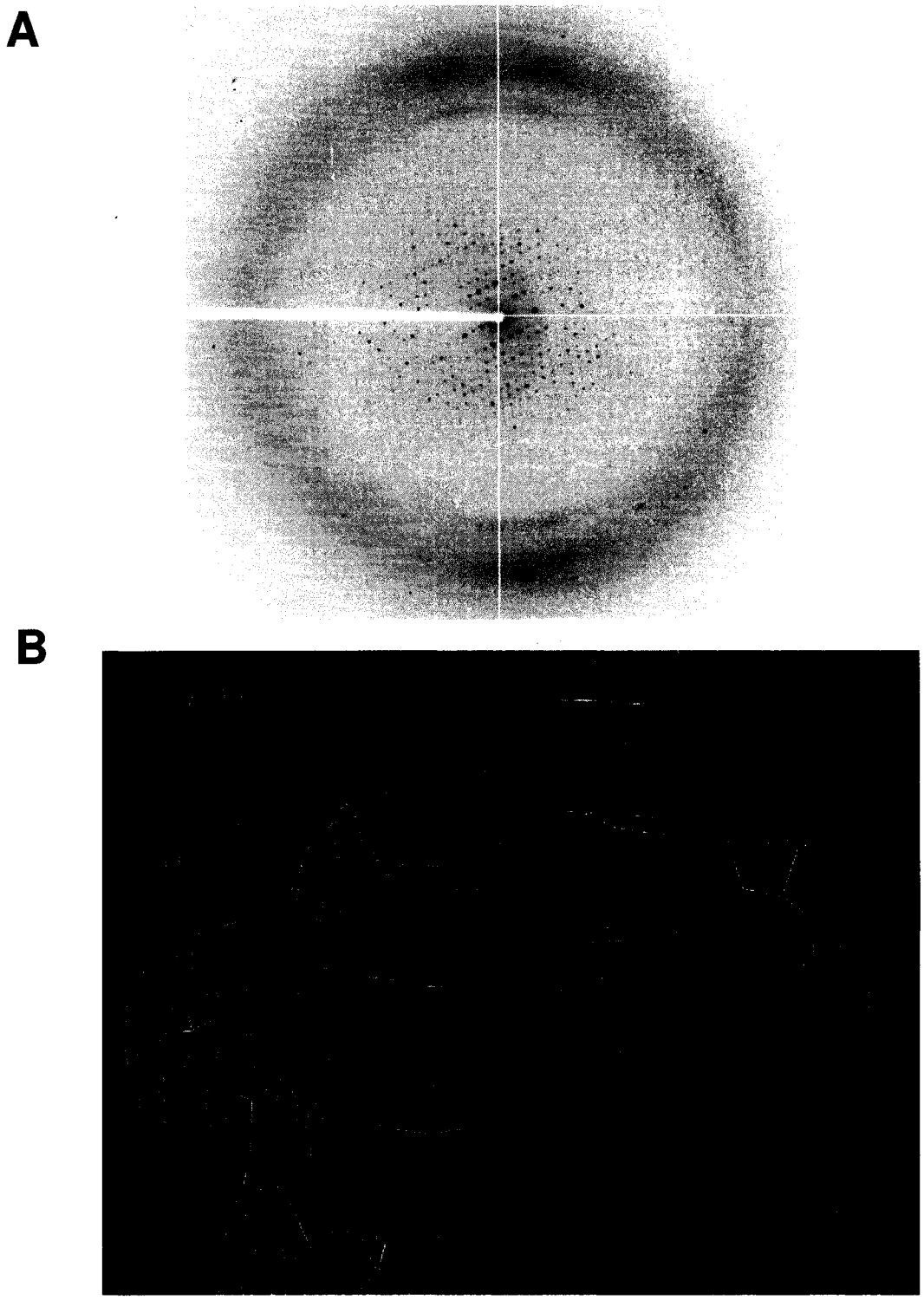

Figure 5.5 Crystal diffraction and density of poly (dA·dT) NCP

(A) Diffraction pattern of the best diffraction poly (dA·dT) NCP crystal. The crystal diffracted to a resolution of 2.7 Å. **(B)** $2F_o - F_c$ map at contoured at 1.0 σ showing density for the DNA for the most current synchrotron data set.

Table 5.2. Summary of Crystallographic Analysis - most current synchrotron data set

Data Collection Statistics					
Space group	a=, b=, c=	Resolution (Å)	Reflections (Total/Unique)	Completeness (%)	R_{sym} [a]
$P2_12_12_1$	104.9, 109.6, 177.9	50 – 2.7	328,308 (51579)	89.3 (53.4)[b]	0.064 (0.329)[c]

[a] $R_{sym} = \Sigma | I_h - \langle I_h \rangle | / \Sigma I_h$, where $\langle I_h \rangle$ is the mean of measurements for a single hkl.
[b] Value in parentheses is for the highest resolution shell: 2.80 – 2.70 Å.

The data was re-indexed in the primitive orthorombic space group of $P2_12_12_1$, which yielded good data quality and completeness (Table 5.2). Molecular replacement using the entire crystal structure of the nucleosome core particle from *Xenopus laevis* as the initial search model resulted in a solution being found. $2F_o$-F_c maps of the model revealed nice density for the DNA and histone octamer (Fig. 5.5B). Initial analysis of the maps show that the DNA is mostly ordered, but does contain some regions where the density seems to be different than the original DNA placement in the initial search model. Several rounds of structure refinement will need to be performed, as well as the calculation of simulated annealing omit maps for the DNA molecule, before a definite statement can be made about the structure of the DNA in the molecule since model bias will need to be eliminated before such conclusions can be drawn.

5.5 Discussion

Access of transcription factors to their respective binding sites is dependent on many factors. The placement of nucleosomes tends to preclude factor binding to cis-acting regulatory sites. Therefore, the cell must find ways of opening up binding sites in order to initiate gene transcription. It is thought that one mechanism by which promoter regions are made more accessible to DNA binding factors is the incorporation of rigid DNA sequences that either preclude nucleosome formation on promoters or create areas of localized DNA distortion within nucleosomal DNA. This distortion then allows more facile binding to sites encompassed with nucleosomes. *In vivo* and *in vitro* digestion studies have shown that rigid DNA sequences can allow greater digestion of nucleosomal DNA (Shimizu et al., 2000), (Brown and Fox, 1998), (Zhu and Thiele, 1996). However,

no structural studies have been completed which looked directly at rigid nucleosomal DNA sequences.

In order to directly address this hypothesis, I have attempted to solve the crystal structure of a nucleosome core particle containing a 16 bp poly (dA·dT) element. The nucleosomes reconstituted well and purification followed standard procedures. This shows that nucleosomes will readily form on poly (dA·dT) elements and thus rigid DNA elements of this size do not act to preclude nucleosome core particle formation within genes solely based on their structural properties (see chapter 4). Crystallization conditions which yielded diffractable crystals were very similar to previous conditions found for nucleosome core particle structures (Luger et al., 1997), (White et al., 2001). The crystals also had the same morphology as *Xenopus laevis* nucleosomes containing "regular" DNA (Luger, 1997). However, diffraction of the crystals of nucleosomes containing poly (dA·dT) DNA proved to be very anisotropic. Indexing of the diffraction data showed "drifting" space groups, since a different space group would be obtained for various diffraction patterns throughout the data set. This suggests that there was an inherent disorder within the crystal lattice. When a data set was finally obtained that gave fairly good indexing results, phasing by molecular replacement using the nucleosome core particle structure from *Xenopus laevis* as the search model failed to find a solution. Only when the DNA was removed from the initial search model completely was a solution found. This solution showed no discernable density present for the DNA in the model. These findings could suggest that the nucleosomal DNA within the crystal lattice is highly disordered. This conclusion supports the hypothesis that poly (dA·dT)

elements create regions of nucleosomal DNA distortion which are propagated to many areas throughout the nucleosomal DNA molecule.

Continued crystal screening resulted in a crystal that yielded nice diffraction data which did not demonstrate the anisotropy found for previous data sets. Data indexing resulted in good statistics being obtained with a single space group being found. Molecular replacement found a solution that resulted in good density for both the protein octamer and the DNA molecule. Because the crystal was obtained from a tray that had been set up seven months earlier, the DNA within the nucleosome probably had time to reach an equilibrium position in relation to the histone octamer. If this is indeed the case, this could have allowed better diffraction data to be obtained without so much disorder within the DNA molecule. Initial maps of the model show areas in which the modeled DNA does not fit into the present density. This suggests that areas of localized DNA differences do exist in the poly (dA·dT) NCP as compared to the α-satellite NCP. However, the initial model is always subject to search model bias, and therefore several rounds of model refinement, as well as the calculation of simulated annealing omit maps, will have to be performed before any definite conclusions can be made about the structure.

In conclusion, the structural data obtained thus far suggests that poly (dA·dT) elements could act to create disorder within nucleosomal DNA. Our current findings could suggest that rigid DNA sequences of moderate length within promoter regions probably do not act to preclude nucleosome core particle formation, but rather act to make nucleosomal DNA binding sites more accessible to transcription factors. However, the current model from the most recent data set will need to be refined and the structure

analyzed before any definite statements can be made. This analysis will confirm or reject our hypothesis that poly (dA·dT) sequence elements create localized disorderment within nucleosomal DNA which could result in easier access of transcription factors to their respective binding sites in promoter regions.

5.6 Acknowledgements

I would like to thank Yunhe Bao for help with the analysis of the last data set collected. This work was supported by NIH grant GM61909.

Chapter 6

Contributions to other Publications

The following are references and very brief explanations of the contributions I made to other scientific publications of which I was a co-author.

1. **Suto, R.K., Edayathumangalam, R.S., White, C.L., Melander, C., Gottesfeld, J.M., Dervan, P.B., and Luger, K.** 2003. Crystal Structures of Nucleosome Core Particles in Complex with Minor Groove DNA-binding ligands. J. Mol. Biol. **326**(2): 371-380.

The crystal structures of three nucleosome core particles in complex with site-specific DNA-binding ligands, the pyrrole-imidazole polyamides, were determined. While the structure of the histone octamer and its interaction with the DNA remain unaffected by ligand-binding, nucleosomal DNA undergoes significant structural changes at the ligand-binding sites and in adjacent regions to accommodate the ligands. The findings suggest that twist diffusion occurs over long distances through tightly bound

nucleosomal DNA. I completed the initial binding studies of the pyrrole-imidazole polyamides to the nucleosome core particles.

2. **Muthurajan, U.M., Bao, Y., Forsberg, J., Edayathumangalam, R.S., Dyer, P.N., White, C.L., and Luger, K.** 2003. Crystallographic and Biochemical Studies of Nucleosome Core Particles Containing Histone Sin Mutants. *Submitted to The EMBO Journal.*

Eleven crystal structures and biochemical properties of nucleosome core particles containing individual point mutations in the structured regions of histones H3 and H4 were solved. All of the mutated residues are located at the two protein-DNA interfaces flanking the nucleosomal dyad. We find that even non-conservative mutations of these residues have only moderate effects on global nucleosome structure. Rather, local protein-DNA interactions are disrupted and weakened in a subtle and complex manner. The number of lost protein-DNA interactions correlates directly with an increased propensity of the histone octamer to reposition with respect to the DNA, and with an overall destabilization of the nucleosome. I expressed, purified, assembled octamers, reconstituted nucleosomes, and collected initial X-ray diffraction data sets on two of the histone mutants - H4 R45H and H4 R45A.

3. In addition, I expressed and purified yeast core histones, and refolded yeast histone octamer for a research project conducted by Dr. Craig Peterson.

Chapter 7

Future Considerations

The results I have obtained during the course of my thesis work support the hypothesis that the yeast nucleosome core particle is structurally different and less stable than that from higher eukaryotic organisms (chapers 2 and 3). These findings support previous data showing that yeast maintain a more open higher order chromatin structure. The more open structure could be due to a decreased nucleosome stability or more direct effects on higher order packing. All of the research presented here employs a mononucleosome. Therefore, it would be of interest to study the yeast nucleosome in the context nucleosomal arrays. One could then ask whether the decreased stability of the yeast nucleosome core particle would result in a difference in the compaction of the yeast nucleosomal array, such as is suggested by the packing of yeast nucleosomes within the crystal lattice. Core histone post-translational modifications also affect chromatin folding in yeast. Therefore, it would be of interest to ubiquitinate the carboxy terminal Lysine 123 of histone H2B to determine the effect on the formation of yeast nucleosomal arrays.

Also, transcription assays comparing yeast nucleosomal array templates compared to that of *Xenopus laevis* would shed light on the role of nucleosome stability in transcription elongation.

The data I have presented helps explain how yeast, a unicellular eukaryotic organism, is able to keep a large part of its genes constitutively transcribed, as well as how yeast can mount such a rapid transcriptional response to environmental stress. However, all of my data collected thus far has been gathered *in vitro*. The next step would be to study the stability of the *Saccharomyces cerevisiae* nucleosome core particle *in vivo*. The yeast histone L1 loop sequences could be replaced with that of *Xenopus laevis* in histones H2A and H2B. This can easily by done using the plasmid shuffle technique in a yeast strain in which the histone genes have been knocked out. If there are phenotypic consequences to having the *X. laevis* histone L1 loop in H2A and H2B, perhaps creating more stable nucleosomes and a more closed chromatin structure, then the exact sequence found in the *S. cerevisiae* L1 loop could appear to be necessary for proper gene regulation in yeast.

Experimental evidence outlined here suggests that rigid DNA sequences, such as poly (dA·dT) tracts, tend to create disorder within nucleosomal DNA (chapters 4 and 5). However, this hypothesis can only be substantiated by determining the crystal structure of a nucleosome containing a poly (dA·dT) tract. Data has been collected and indexed on a crystal that produced good diffraction and data statistics (chapter 5). Molecular replacement resulted in an initial model being obtained. This model now needs to be refined in order to eliminate model bias and thus give a true structure of the 16 bp poly (dA·dT) element within the nucleosome. Analysis of the model will hopefully reveal the

exact structural changes this rigid element imparts on nucleosomal DNA. This could verify the role of these elements in promoter regions, and thus their function in transcriptional activation.

In this report, I have shown that transcription factor binding to DNA encompassed within a nucleosome core particle can cause breathing of the DNA ends, but does not cause dissociation of the underlying histone octamer. The histone dimer and tetramer remains intact upon factor binding. However, the specific structural changes that transcription factor binding imparts on the DNA and to the DNA - octamer interface remains to be elucidated. These changes could be more completely understood by solving the crystal structure of a nucleosome core particle with a transcription factor bound to the DNA molecule. The Amt1 system I have developed would be an ideal platform for one to determine this structure. However, several problems would have to be overcome. In particular, we need to be able to obtain a complex in which each nucleosome is bound by a single Amt1 protein. I can only obtain such a complex using very small Amt1 and nucleosomal concentrations. When greater concentrations are used, such as would have to be used in setting up crystals, I get supershifting of the nucleosomal complex. This suggests that under higher concentrations, multiple Amt1 proteins are binding to the nucleosomal DNA. This problem has precluded our ability to obtain diffracting crystals, since each protein complex within a crystal lattice must be identical in order to obtain a crystal packing that would yield good data quality. Conditions and concentrations would need to be optimized in order to obtain a nucleosome : Amt1 ratio of 1:1 for each complex formed. Also, I have shown that upon Amt1 binding, the ends of the DNA become dissociated from the octamer core. Because

the crystal packing of nucleosomes is dependent on the direct interaction of the DNA ends between neighboring nucleosomes, a different crystal packing would surely be required in order for Amt1-NCP crystals to be obtained. However, if these problems can be overcome and conditions found to produce crystals, the crystal structure of a transcription factor bound to a nucleosome core particle would surely provide a wealth of information on transcriptional activation within a chromatin context, and reveal the importance of the interactions of transcription factors with nucleosomes in order to achieve activated transcription, as well as proper DNA replication and repair.

7.1 References:

Aalfs, J. D., and Kingston, R. E. (2000). What does 'chromatin remodeling' mean? Trends Biochem Sci *25*, 548-55.

Adams, C. R., and Kamakaka, R. T. (1999). Chromatin assembly: biochemical identities and genetic redundancy. Curr Opin Genet Dev *9*, 185-90.

Alexeev, D. G., Lipanov, A. A., and Skuratovskii, I. (1987). Poly(dA).poly(dT) is a B-type double helix with a distinctively narrow minor groove. Nature *325*, 821-3.

Allegra, P., Sterner, R., Clayton, D. F., and Allfrey, V. G. (1987). Affinity chromatographic purification of nucleosomes containing transcriptionally active DNA sequences. J Mol Biol *196*, 379-88.

Anderson, J. D., and Widom, J. (2000). Sequence and position-dependence of the equilibrium accessibility of nucleosomal DNA target sites. J Mol Biol *296*, 979-87.

Angelov, D., Vitolo, J. M., Mutskov, V., Dimitrov, S., and Hayes, J. J. (2001). Preferential interaction of the core histone tail domains with linker DNA. Proc Natl Acad Sci U S A *98*, 6599-604.

Arents, G., and Moudrianakis, E. N. (1995). The histone fold: a ubiquitous architectural motif utilized in DNA compaction and protein dimerization. Proc Natl Acad Sci U S A *92*, 11170-4.

Banères, J. L., Martin, A., and Parello, J. (1997). The N Tails of Histones H3 and H4 Adopt a Highly Structured Conformation in the Nucleosome. J Mol Biol *273*, 503-508.

Bannister, A. J., Schneider, R., and Kouzarides, T. (2002). Histone methylation: dynamic or static? Cell *109*, 801-6.

Baxevanis, A. D., and Landsman, D. (1998). Histone Sequence Database: new histone fold family members. Nucleic Acids Res *26*, 372-5.

Bazett-Jones, D. P., Cote, J., Landel, C. C., Peterson, C. L., and Workman, J. L. (1999). The SWI/SNF complex creates loop domains in DNA and polynucleosome arrays and can disrupt DNA-histone contacts within these domains. Mol Cell Biol *19*, 1470-8.

Beato, M., and Eisfeld, K. (1997). Transcription factor access to chromatin. NAR *25*, 3559-3563.

Boyer, L. A., Shao, X., Ebright, R. H., and Peterson, C. L. (2000). Roles of the histone H2A-H2B dimers and the (H3-H4)(2) tetramer in nucleosome remodeling by the SWI-SNF complex. J Biol Chem *275*, 11545-52.

Bram, S. (1975). A double coil chromatin sub-unit model. Biochimie *57*, 1301-6.

Breslauer, K. J. (1991). A thermodynamic perspective of DNA bending. Current Opinion in Structural Biology *1*, 416-422.

Brown, P. M., and Fox, K. R. (1998). DNA triple-helix formation on nucleosome-bound poly(dA).poly(dT) tracts. Biochem J *333*, 259-67.

Brunger, A. T., Adams, P. D., and Rice, L. M. (1997). New applications of simulated annealing in X-ray crystallography and solution NMR. Structure *5*, 325-336.

Carruthers, L. M., Bednar, J., Woodcock, C. L., and Hansen, J. C. (1998). Linker histones stabilize the intrinsic salt-dependent folding of nucleosomal arrays: mechanistic ramifications for higher-order chromatin folding. Biochemistry *37*, 14776-87.

Carruthers, L. M., and Hansen, J. C. (2000). The core histone N termini function independently of linker histones during chromatin condensation. J Biol Chem *275*, 37285-90.

Cheung, P., Allis, C. D., and Sassone-Corsi, P. (2000). Signaling to chromatin through histone modifications. Cell *103*, 263-71.

Chiarugi, A. (2002). Poly(ADP-ribose) polymerase: killer or conspirator? The 'suicide hypothesis' revisited. Trends Pharmacol Sci *23*, 122-9.

Cirillo, L. A., Lin, F. R., Cuesta, I., Friedman, D., Jarnik, M., and Zaret, K. S. (2002). Opening of Compacted Chromatin by Early Developmental Transcription Factors HNF3 (FoxA) and GATA-4. Mol Cell *9*, 279-89.

Coll, M., Frederick, C. A., Wang, A. H., and Rich, A. (1987). A bifurcated hydrogen-bonded conformation in the d(A.T) base pairs of the DNA dodecamer d(CGCAAATTTGCG) and its complex with distamycin. Proc Natl Acad Sci U S A *84*, 8385-9.

Cote, J., Quinn, J., Workman, J. L., and Peterson, C. L. (1994). Stimulation of GAL4 derivative binding to nucleosomal DNA by the yeast SWI/SNF complex. Science *265*, 53-60.

Cotton, R. W., Hamkalo, B. A. (1981). Nucleosome dissociation at physiological ionic strengths. Nucleic Acids Research *9*, 445-457.

Davey, C. A., Sargent, D. F., Luger, K., Maeder, A. W., and Richmond, T. J. (2002). Solvent mediated interactions in the structure of the nucleosome core particle at 1.9 a resolution. J Mol Biol *319*, 1097-113.

Dechering, K. J., Cuelenaere, K., Konings, R. N., and Leunissen, J. A. (1998). Distinct frequency-distributions of homopolymeric DNA tracts in different genomes. Nucleic Acids Res *26*, 4056-62.

Deckert, J., and Struhl, K. (2001). Histone Acetylation at promoters is differentially affected by specific activators and repressors. Molec. Cell. Biol. *21*, 2726-2735.

Dickerson, R. E., Drew, H. R., Conner, B. N., Wing, R. M., Fratini, A. V., and Kopka, M. L. (1982). The anatomy of A-, B-, and Z-DNA. Science *216*, 475-85.

Dorigo, B., Schalch, T., Bystricky, K., Richmond, T.J. (2003). Chromatin fiber folding: requirement for the histone H4 N-terminal tail. Journal of Molecular Biology *327*, 85-96.

Durrin, L. K., Mann, R. K., Kayne, P. S., and Grunstein, M. (1991). Yeast histone H4 N-terminal sequence is required for promoter activation in vivo. Cell *65*, 1023-31.

Eissenberg JC, W. L. (2003). Heterochromatin, position effects, and the genetic dissection of chromatin. Prog Nucleic Acid Res Mol Biol *74*, 275-99.

Escher, D., and Schaffner, W. (1997). Gene activation at a distance and telomeric silencing are not affected by yeast histone H1. Mol Gen Genet *256*, 456-61.

Esnouf, R. M. (1999). Further Additions to Molscript Version 1.4, including reading and contouring of electron density maps. Acta Cryst. D *55*, 838-940.

Fan, J. Y., Gordon, F., Luger, K., Hansen, J. C., and Tremethick, D. J. (2002). The essential histone variant H2A.Z regulates the equilibrium between different chromatin conformational states. Nat Struct Biol *19*, 172-176.

Farrell, R. A., Thorvaldsen, J. L., and Winge, D. R. (1996). Identification of the Zn(II) site in the copper-responsive yeast transcription factor, AMT1: a conserved Zn module. Biochemistry *35*, 1571-1580.

Fassler, J. S., and Winston, F. (1988). Isolation and analysis of a novel class of suppressor of Ty insertion mutations in Saccharomyces cerevisiae. Genetics *118*, 203-12.

Ferrin, T. E., Huang, C. C., Jarvis, L. E., and Langridge, R. (1988). The MIDAS Display System. J. Mol. Graphics *6*, 13-27.

Filetici, P., Aranda, C., Gonzalez, A., and Ballario, P. (1998). GCN5, a yeast transcriptional coactivator, induces chromatin reconfiguration of HIS3 promoter in vivo. Biochem Biophys Res Commun *242*, 84-7.

Gao, J., and Benyajati, C. (1998). Specific local histone-DNA sequence contacts facilitate high-affinity, non-cooperative nucleosome binding of both adf-1 and GAGA factor. Nucleic Acids Res *26*, 5394-401.

Garvie, C. W., and Wolberger, C. (2001). Recognition of specific DNA sequences. Mol Cell *8*, 937-46.

Gerchman, S. E., and Ramakrishnan, V. (1987). Chromatin higher-order structure studied by neutron scattering and scanning transmission electron microscopy. Proc Natl Acad Sci U S A *84*, 7802-6.

Glowczewski, L., Yang, P., Kalashnikova, T., Santisteban, M. S., and Smith, M. M. (2000). Histone-histone interactions and centromere function. Mol Cell Biol *20*, 5700-11.

Gottesfeld, J. M., and Luger, K. (2001). Energetics and Affinity of the Histone Octamer for Defined DNA Sequences. Biochemistry *40*, 10927-10933.

Gottesfeld, J. M., Melander, C., Suto, R. K., Raviol, H., Luger, K., and Dervan, P. B. (2001). Sequence-specific recognition of DNA in the nucleosome by pyrrole- imidazole polyamides. J Mol Biol *309*, 625-39.

Graden, J. A., Posewitz, M. C., Simon, J. R., George, G. N., Pickering, I. J., and Winge, D. R. (1996). Presence of a copper(I)-thiolate regulatory domain in the copper-activated transcription factor Amt1. Biochemistry *35*, 14583-14589.

Gregory, P. D. (2001). Transcription and chromatin converge: lessons from yeast genetics. Curr Opin Genet Dev *11*, 142-7.

Grunstein, M. (1997). Histone acetylation in chromatin structure and transcription. Nature *389*, 349-352.

Grunstein, M. (1997). Molecular model for telomeric heterochromatin in yeast. Curr Opin Cell Biol *9*, 383-7.

Grunstein, M., Hecht, A., Fisher Adams, G., Wan, J., Mann, R. K., Strahl Bolsinger, S., Laroche, T., and Gasser, S. (1995). The regulation of euchromatin and heterochromatin by histones in yeast. J Cell Sci Suppl *19*, 29-36.

Guo, X. W., Th'ng, J. P., Swank, R. A., Anderson, H. J., Tudan, C., Bradbury, E. M., and Roberge, M. (1995). Chromosome condensation induced by fostriecin does not require p34cdc2 kinase activity and histone H1 hyperphosphorylation, but is associated with enhanced histone H2A and H3 phosphorylation. Embo J *14*, 976-85.

Hansen, J. C. (2002). CONFORMATIONAL DYNAMICS OF THE CHROMATIN FIBER IN SOLUTION: Determinants, Mechanisms, and Functions. Annu Rev Biophys Biomol Struct *31*, 361-92.

Hansen, J. C., and Ausio, J. (1992). Chromatin dynamics and the modulation of genetic activity. Trends Biochem Sci *17*, 187-91.

Hansen, J. C., Ausio, J., Stanik, V. H., and van Holde, K. E. (1989). Homogeneous reconstituted oligonucleosomes, evidence for salt-dependent folding in the absence of histone H1. Biochemistry *28*, 9129-36.

Hansen, J. C., Tse, C., and Wolffe, A. P. (1998). Structure and function of the core histone N-termini: more than meets the eye. Biochemistry *37*, 17637-41.

Hansen, J. C., and Wolffe, A. P. (1994). A role for histones H2A/H2B in chromatin folding and transcriptional repression. Proc Natl Acad Sci U S A *91*, 2339-43.

Harp, J. M., Hanson, B. L., Timm, D. E., and Bunick, G. J. (2000). Asymmetries in the nucleosome core particle at 2.5 A resolution. Acta Crystallogr D Biol Crystallogr *56 Pt 12*, 1513-34.

Hartzog, G. A., and Winston, F. (1997). Nucleosomes and transcription: recent lessons from genetics. Curr Opin Genet Dev *7*, 192-8.

Hayes, J. J., Bashkin, J., Tullius, T. D., and Wolffe, A. P. (1991). The histone core exerts a dominant constraint on the structure of DNA in a nucleosome. Biochemistry *30*, 8434-40.

Hebbes, T. R., Clayton, A. L., Thorne, A. W., and Crane-Robinson, C. (1994). Core histone hyperacetylation co-maps with generalized DNase I sensitivity in the chicken beta-globin chromosomal domain. Embo J *13*, 1823-30.

Hirschhorn, J. N., Bortvin, A. L., Ricupero Hovasse, S. L., and Winston, F. (1995). A new class of histone H2A mutations in Saccharomyces cerevisiae causes specific transcriptional defects in vivo. Mol Cell Biol *15*, 1999-2009.

Horz, W., and Zachau, H. G. (1980). Deoxyribonuclease II as a probe for chromatin structure. I. Location of cleavage sites. J Mol Biol *144*, 305-27.

Howman, E. V., Fowler, K. J., Newson, A. J., Redward, S., MacDonald, A. C., Kalitsis, P., and Choo, K. H. (2000). Early disruption of centromeric chromatin organization in centromere protein A (Cenpa) null mice. Proc Natl Acad Sci U S A *97*, 1148-53.

Hsu, J. Y., Sun, Z. W., Li, X., Reuben, M., Tatchell, K., Bishop, D. K., Grushcow, J. M., Brame, C. J., Caldwell, J. A., Hunt, D. F., Lin, R., Smith, M. M., and Allis, C. D. (2000).

Mitotic phosphorylation of histone H3 is governed by Ipl1/aurora kinase and Glc7/PP1 phosphatase in budding yeast and nematodes. Cell *102*, 279-91.

Huletsky, A., de Murcia, G., Muller, S., Hengartner, M., Menard, L., Lamarre, D., and Poirier, G. G. (1989). The effect of poly(ADP-ribosyl)ation on native and H1-depleted chromatin. A role of poly(ADP-ribosyl)ation on core nucleosome structure. J Biol Chem *264*, 8878-86.

Hymes, J., and Wolf, B. (1999). Human biotinidase isn't just for recycling biotin. J Nutr *129*, 485S-489S.

Imbalzano, A. N., Kwon, H., Green, M. R., and Kingston, R. E. (1994). Facilitated binding of TATA-binding protein to nucleosomal DNA [see comments]. Nature *370*, 481-5.

Jackson, J. D., and Gorovsky, M. A. (2000). Histone H2A.Z has a conserved function that is distinct from that of the major H2A sequence variants [In Process Citation]. Nucleic Acids Res *28*, 3811-6.

Jason, L. J., Moore, S. C., Lewis, J. D., Lindsey, G., and Ausio, J. (2002). Histone ubiquitination: a tagging tail unfolds? Bioessays *24*, 166-74.

Jenuwein, T., and Allis, C. D. (2001). Translating the histone code. Science *293*, 1074-80.

Jeppesen, P., and Turner, B. M. (1993). The inactive X chromosome in female mammals is distinguished by a lack of histone H4 acetylation, a cytogenetic marker for gene expression. Cell *74*, 281-9.

Jones, T. A., Zou, J. Y., Cowan, S. W., and Kjelgaard, M. (1991). Improved methods for building protein models in electron density maps and the location of errors in these models. Acta Cryst *A47*, 110-119.

Koch, K. A., and Thiele, D. J. (1996). Autoactivation by a Candida glabrata copper metalloregulatory transcription factor requires critical minor groove interactions. Mol Cell Biol *16*, 724-734.

Koch, K. A., and Thiele, D. J. (1999). Functional analysis of a homopolymeric (dA-dT) element that provides nucleosomal access to yeast and mammalian transcription factors. J Biol Chem *274*, 23752-60.

Kraulis, P. (1991). MOLSCRIPT: a program to produce both detailed and schematic plots of protein structures. J. Appl Cryst *24*, 946-950.

Kruger, W., Peterson, C. L., Sil, A., Coburn, C., Arents, G., Moudrianakis, E. N., and Herskowitz, I. (1995). Amino acid substitutions in the structured domains of histones H3 and H4 partially relieve the requirement of the yeast SWI/SNF complex for transcription. Genes Dev *9*, 2770-9.

Kunkel, G. R., and Martinson, H. G. (1981). Nucleosomes will not form on double-stranded RNa or over poly(dA).poly(dT) tracts in recombinant DNA. Nucleic Acids Res *9*, 6869-88.

Kuo, M. H., Brownell, J. E., Sobel, R. E., Ranalli, T. A., Cook, R. G., Edmondson, D. G., Roth, S. Y., and Allis, C. D. (1996). Transcription-linked acetylation by Gcn5p of histones H3 and H4 at specific lysines. Nature *383*, 269-72.

Kurumizaka, H., and Wolffe, A. P. (1997). Sin mutations of histone H3: influence on nucleosome core structure and function. Mol Cell Biol *17*, 6953-6969.

Landsman, D. (1996). Histone H1 in Saccharomyces cerevisiae: a double mystery solved? Trends Biochem Sci *21*, 287-8.

Langst, G., Bonte, E. J., Corona, D. F., and Becker, P. B. (1999). Nucleosome movement by CHRAC and ISWI without disruption or trans- displacement of the histone octamer. Cell *97*, 843-52.

Lascaris, R. F., Groot, E., Hoen, P. B., Mager, W. H., and Planta, R. J. (2000). Different roles for abf1p and a T-rich promoter element in nucleosome organization of the yeast RPS28A gene. Nucleic Acids Res *28*, 1390-6.

Laskowski, R., MacArthur, M., Moss, D., and Thornton, J. (1993). PROCHECK: a program to evaluate stereochemical quality of protein structures. J. Appl. Crystallogr. *26*, 283-291.

Lee, K. M., Sif, S., Kingston, R. E., Hayes, J. J. (1999). hSWI/SNF disrupts interactions between the H2A N-terminal tail and nucleosomal DNA. Biochemistry *38*, 8423-9.

Lee, K. P., Baxter, H. J., Guillemette, J. G., Lawford, H. G., and Lewis, P. N. (1982). Structural studies on yeast nucleosomes. Can J Biochem *60*, 379-88.

LeRoy, G., Orphanides, G., Lane, W. S., and Reinberg, D. (1998). Requirement of RSF and FACT for transcription of chromatin templates in vitro [see comments]. Science *282*, 1900-4.

Li, B., Adams, C. C., and Workman, J. L. (1994). Nucleosome binding by the constitutive transcription factor Sp1. J Biol Chem *269*, 7756-63.

Li, Q., and Wrange, O. (1995). Accessibility of a glucocorticoid response element in a nucleosome depends on its rotational positioning. Mol Cell Biol *15*, 4375-84.

Li, W., Nagaraja, S., Delcuve, G. P., Hendzel, M. J., and Davie, J. R. (1993). Effects of histone acetylation, ubiquitination and variants on nucleosome stability. Biochem J *296*, 737-44.

Li, W., Nagaraja, S., Delcuve, G. P., Hendzel, M. J., and Davie, J. R. (1993). Effects of histone acetylation, ubiquitination and variants on nucleosome stability. Biochem J *296*, 737-44.

Ling, X., Harkness, T. A., Schultz, M. C., Fisher Adams, G., and Grunstein, M. (1996). Yeast histone H3 and H4 amino termini are important for nucleosome assembly in vivo and in vitro: redundant and position-independent functions in assembly but not in gene regulation. Genes Dev *10*, 686-99.

Liu, X. D., and Thiele, D. J. (1997). Yeast metallothionein gene expression in response to metals and oxidative stress. Methods *11*, 289-99.

Lohr, D., and Hereford, L. (1979). Yeast chromatin is uniformly digested by DNase-I. Proc Natl Acad Sci U S A *76*, 4285-8.

Lohr, D., and Ide, G. (1979). Comparison on the structure and transcriptional capability of growing phase and stationary yeast chromatin: a model for reversible gene activation. Nucleic Acids Res *6*, 1909-27.

Lorch, Y., Zhang, M., and Kornberg, R. D. (1999). Histone octamer transfer by a chromatin-remodeling complex. Cell *96*, 389-92.

Losa, R., Omari, S., and Thoma, F. (1990). Poly(dA).poly(dT) rich sequences are not sufficient to exclude nucleosome formation in a constitutive yeast promoter. Nucleic Acids Res *18*, 3495-3502.

Louters, L., and Chalkley, R. (1985). Exchange of histones H1, H2A, and H2B in vivo. Biochemistry *24*, 3080-5.

Luger, K., Maeder, A. W., Richmond, R. K., Sargent, D. F., and Richmond, T. J. (1997). X-ray structure of the nucleosome core particle at 2.8 Å resolution. Nature *389*, 251-259.

Luger, K., Maeder, A. W., Sargent, D. F., and Richmond, T. J. (2000). The atomic structure of the nucleosome core particle. *Journal of Biomolecular Structure & Dynamics 11*, 185 - 189.

Luger, K., Rechsteiner, T. J., Flaus, A. J., Waye, M. M., and Richmond, T. J. (1997). Characterization of nucleosome core particles containing histone proteins made in bacteria. J Mol Biol *272*, 301-11.

Luger, K., Rechsteiner, T. J., and Richmond, T. J. (1999). Preparation of nucleosome core particle from recombinant histones. Methods Enzymol *304*, 3-19.

Luger, K., and Richmond, T. J. (1998). DNA binding within the nucleosome core. Current Opinion in Structural Biology *8*, 33-40.

Luger, K., and Richmond, T. J. (1998). The histone tails of the nucleosome. Curr Opin Genet Dev *8*, 140-146.

Mai, X., Chou, S., and Struhl, K. (2000). Preferential accessibility of the yeast his3 promoter is determined by a general property of the DNA sequence, not by specific elements. Mol Cell Biol *20*, 6668-76.

Moore, S. C., and Ausio, J. (1997). Major role of the histones H3-H4 in the folding of the chromatin fiber. BBRC *230*, 136-139.

Moreira, J. M., Horz, W., and Holmberg, S. (2002). Neither Reb1p nor poly(dA*T) elements are responsible for the highly specific chromatin organization at the ILV1 promoter. J Biol Chem *277*, 3202-9.

Morse, R. H., Pederson, D. S., Dean, A., and Simpson, R. T. (1987). Yeast nucleosomes allow thermal untwisting of DNA. Nucleic Acids Res *15*, 10311-30.

Muthurajan, U. M., Park, Y. J., Edayathumangalam, R. S., Suto, R. K., Chakravarthy, S., Dyer, P. N., and Luger, K. (2003). Structure and dynamics of nucleosomal DNA. Biopolymers *68*, 547-56.

Nelson, H. C., Finch, J. T., Luisi, B. F., and Klug, A. (1987). The structure of an oligo(dA).oligo(dT) tract and its biological implications. Nature *330*, 221-6.

Otwinowski, Z., and Minor, W. (1997). Processing of X-ray diffraction data collected in oscillation mode, Volume 276, Macromolecular Crystallography, part A, C. W. Carter and R. M. Sweet, eds. (New York: Academic Press).

Patterton, H. G., Landel, C. C., Landsman, D., Peterson, C. L., and Simpson, R. T. (1998). The biochemical and phenotypic characterization of hho1p, the putative linker histone H1 of saccharomyces cerevisiae. J Biol Chem *273*, 7268-7276.

Peck, L. J., and Wang, J. C. (1981). Sequence dependence of the helical repeat of DNA in solution. Nature *292*, 375-8.

Perez-Martin, J. (1999). Chromatin and transcription in Saccharomyces cerevisiae. FEMS Microbiol Rev *23*, 503-23.

Pineiro, M., Puerta, C., and Palacian, E. (1991). Yeast nucleosomal particles: structural and transcriptional properties. Biochemistry *30*, 5805-10.

Pinto, I., and Winston, F. (2000). Histone H2A is required for normal centromere function in Saccharomyces cerevisiae. Embo J *19*, 1598-612.

Polach, K. J., and Widom, J. (1995). Mechanism of protein access to specific DNA sequences in chromatin: a dynamic equilibrium model for gene regulation. J Mol Biol *254*, 130-49.

Polach, K. J., and Widom, J. (1996). A model for the cooperative binding of eukaryotic regulatory proteins to nucleosomal target sites. J Mol Biol *258*, 800-12.

Prior, C. P., Cantor, C. R., Johnson, E. M., Littau, V. C., and Allfrey, V. G. (1983). Reversible changes in nucleosome structure and histone H3 accessibility in transcriptionally active and inactive states of rDNA chromatin. Cell *34*, 1033-42.

Prunell, A. (1982). Nucleosome reconstitution on plasmid-inserted poly(dA) . poly(dT). .

Puhl, H. L., and Behe, M. J. (1995). Poly(dA).poly(dT) forms very stable nucleosomes at higher temperatures. J Mol Biol *245*, 559-67.

Puhl, H. L., Gudibande, S. R., and Behe, M. J. (1991). Poly[d(A.T)] and other synthetic polydeoxynucleotides containing oligoadenosine tracts form nucleosomes easily. J Mol Biol *222*, 1149-60.

Puig, S., Matallana, E., and Perez-Ortin, J. E. (1999). Stochastic nucleosome positioning in a yeast chromatin region is not dependent on histone H1. Curr Microbiol *39*, 168-72.

Ravindra, A., Weiss, K., and Simpson, R. T. (1999). High-resolution structural analysis of chromatin at specific loci: Saccharomyces cerevisiae silent mating-type locus HMRa. Mol Cell Biol *19*, 7944-50.

Recht, J., and Osley, M. A. (1999). Mutations in both the structured domain and N-terminus of histone H2B bypass the requirement for Swi-Snf in yeast. Embo J *18*, 229-240.

Rhodes, D. (1979). Nucleosome cores reconstituted from poly (dA-dT) and the octamer of histones. Nucleic Acids Res *6*, 1805-16.

Rice, J. C., Allis, C.D. (2001). Code of Silence. Nature *414*, 258-61.

Richmond, T. J., Davey, C.A. (2003). The structure of DNA in the nucleosome core. Nature *423*, 145-150.

Richmond, T. J., Searles, M. A., and Simpson, R. T. (1988). Crystals of a nucleosome core particle containing defined sequence DNA. J Mol Biol *199*, 161-70.

Robzyk, K., Recht, J., and Osley, M. A. (2000). Rad6-dependent ubiquitination of histone H2B in yeast. Science *287*, 501-4.

Robzyk, K., Recht, J., and Osley, M. A. (2000). Rad6-dependent ubiquitination of histone H2B in yeast. Science *287*, 501-4.

Rubbi, L., Camilloni, G., Caserta, M., Di Mauro, E., and Venditti, S. (1997). Chromatin structure of the Saccharomyces cerevisiae DNA topoisomerase I promoter in different growth phases. Biochem J *328*, 401-7.

Samatey, F. A., Imada, K., Nagashima, S., Vonderviszt, F., Kumasaka, T., Yamamoto, M., and Namba, K. (2001). Structure of the bacterial flagellar protofilament and implications for a switch for supercoiling. Nature *410*, 331-337.

Santisteban, M. S., Arents, G., Moudrianakis, E. N., and Smith, M. M. (1997). Histone octamer function in vivo: mutations in the dimer-tetramer interfaces disrupt both gene activation and repression. Embo J *16*, 2493-506.

Santisteban, M. S., Kalashnikova, T., and Smith, M. M. (2000). Histone H2A.Z regulats transcription and is partially redundant with nucleosome remodeling complexes. Cell *103*, 411-22.

Satchwell, S. C., Drew, H. R., and Travers, A. A. (1986). Sequence periodicities in chicken nucleosome core DNA. J Mol Biol *191*, 659-75.

Schieferstein, U., and Thoma, F. (1996). Modulation of cyclobutane pyrimidine dimer formation in a positioned nucleosome containing poly(dA.dT) tracts. Biochemistry *35*, 7705-14.

Seigneurin-Berny, D., Verdel, A., Curtet, S., Lemercier, C., Garin, J., Rousseaux, S., and Khochbin, S. (2001). Identification of components of the murine histone deacetylase 6 complex: link between acetylation and ubiquitination signaling pathways. Mol Cell Biol *21*, 8035-44.

Shen, C. H., and Clark, D. J. (2001). DNA sequence plays a major role in determining nucleosome positions in yeast CUP1 chromatin. J Biol Chem *276*, 35209-16.

Shim, E. Y., Woodcock, C., and Zaret, K. S. (1998). Nucleosome positioning by the winged helix transcription factor HNF3. Genes and Development *12*, 5-10.

Shimizu, M., Mori, T., Sakurai, T., and Shindo, H. (2000). Destabilization of nucleosomes by an unusual DNA conformation adopted by poly(dA) small middle dotpoly(dT) tracts in vivo. Embo J *19*, 3358-65.

Simpson, R. T., and Kunzler, P. (1979). Cromatin and core particles formed from the inner histones and synthetic polydeoxyribonucleotides of defined sequence. Nucleic Acids Res *6*, 1387-415.

Steger, D. J., and Workman, J. L. (1997). Stable co-occupancy of transcription factors and histones at the HIV-1 enhancer. Embo J *16*, 2463-72.

Strahl, B. D., and Allis, C. D. (2000). The language of covalent histone modifications. Nature *403*, 41-5.

Strahl, B. D., Ohba, R., Cook, R. G., and Allis, C. D. (1999). Methylation of histone H3 at lysine 4 is highly conserved and correlates with transcriptionally active nuclei in Tetrahymena. Proc Natl Acad Sci U S A *96*, 14967-72.

Struhl, K. (1998). Histone acetylation and transcriptional regulatory mechanisms. Genes Dev *12*, 599-606.

Struhl, K. (1985). Naturally occurring poly(dA-dT) sequences are upstream promoter elements for constitutive transcription in yeast. Proc Natl Acad Sci U S A *82*, 8419-23.

Sun, Z. W., and Allis, C. D. (2002). Ubiquitination of histone H2B regulates H3 methylation and gene silencing in yeast. Nature *418*, 104-8.

Suter, B., Schnappauf, G., and Thoma, F. (2000). Poly(dA.dT) sequences exist as rigid DNA structures in nucleosome-free yeast promoters in vivo. Nucleic Acids Res *28*, 4083-9.

Suto, R. K., Clarkson, M. J., Tremethick, D. J., and Luger, K. (2000). Crystal structure of a nucleosome core particle containing the variant histone H2A.Z. Nat Struct Biol *7*, 1121-1124.

Suto, R. K., Edayathumangalam, R. S., White, C. L., Melander, C., Gottesfeld, J. M., Dervan, P. B., and Luger, K. (2003). Crystal Structures of Nucleosome Core Particles in Complex with Minor Groove DNA-binding Ligands. J Mol Biol *326*, 371-80.

Tachibana, M., Sugimoto, K., Nozaki, M., Ueda, J., Ohta, T., Ohki, M., Fukuda, M., Takeda, N., Niida, H., Kato, H., and Shinkai, Y. (2002). G9a histone methyltransferase plays a dominant role in euchromatic histone H3 lysine 9 methylation and is essential for early embryogenesis. Genes Dev *16*, 1779-91.

Tanaka, S., Livingstone-Zatchej, M., and Thoma, F. (1996). Chromatin structure of the yeast URA3 gene at high resolution provides insight into structure and positioning of nucleosomes in the chromosomal context. J Mol Biol *257*, 919-34.

Tanny, J. C., Dowd, G. J., Huang, J., Hilz, H., and Moazed, D. (1999). An enzymatic activity in the yeast Sir2 protein that is essential for gene silencing. Cell *99*, 735-45.

Thorvaldsen, J. L., Sewell, A. K., Tanner, A. M., Peltier, J. M., Pickering, I. J., George, G. N., and Winge, D. R. (1994). Mixed Cu+ and Zn2+ coordination in the DNA-binding domain of the AMT1 transcription factor from Candida glabrata. Biochemistry *33*, 9566-9577.

Tse, C., and Hansen, J. C. (1997). Hybrid trypsinized nucleosomal arrays: identification of multiple functional roles of the H2A/H2B and H3/H4 N-termini in chromatin fiber compaction. Biochemistry *36*, 11381-11388.

Turner, R. B., Smith, D. L., Zawrotny, M. E., Summers, M. F., Posewitz, M. C., and Winge, D. R. (1998). Solution structure of a zinc domain conserved in yeast copper-regulated transcription factors. Nat Struct Biol *5*, 551-5.

Ushinsky, S. C., Bussey, H., Ahmed, A. A., Wang, Y., Friesen, J., Williams, B. A., and Storms, R. K. (1997). Histone H1 in Saccharomyces cerevisiae. Yeast *13*, 151-61.

Van Holde, K. E. (1988). Chromatin, A. Rich, ed. (New York: Springer-Verlag).

Vaquero, A., Loyola, A., and Reinberg, D. (2003). The Constantly Changing Face of Chromatin. Sage Ke *14*, 1-16.

Varga-Weisz, P. D., and Becker, P. B. (1998). Chromatin-remodeling factors: machines that regulate? Curr Opin Cell Biol *10*, 346-53.

Vignali, M., and Workman, J. L. (1998). Location and function of linker histones [news]. Nat Struct Biol *5*, 1025-8.

Vogelauer, M., Wu, J., Suka, N., and Grunstein, M. (2000). Global histone acetylation and deacetylation in yeast. Nature *408*, 495-8.

Wada-Kiyama, Y., Kuwabara, K., Sakuma, Y., Onishi, Y., Trifonov, E. N., and Kiyama, R. (1999). Localization of curved DNA and its association with nucleosome phasing in the promoter region of the human estrogen receptor alpha gene. FASB letters *444*, 117-24.

Wade, P. A. (2001). Transcriptional control at regulatory checkpoints by histone deacetylases: molecular connections between cancer and chromatin. Hum Mol Genet *10*, 693-8.

Wallis, J. W., Hereford, L., and Grunstein, M. (1980). Histone H2B genes of yeast encode two different proteins. Cell *22*, 799-805.

Wang, X., Moore, S. C., Laszckzak, M., and Ausio, J. (2000). Acetylation increases the alpha-helical content of the histone tails of the nucleosome. J Biol Chem *275*, 35013-20.

Wechser, M. A., Kladde, M. P., Alfieri, J. A., and Peterson, C. L. (1997). Effects of Sin- versions of histone H4 on yeast chromatin structure and function. Embo J *16*, 2086-95.

Wechsler, D. S., Papoulas, O., Dang, C. V., and Kingston, R. E. (1994). Differential binding of c-Myc and Max to nucleosomal DNA. Mol Cell Biol *14*, 4097-107.

White, C. L., Suto, R. K., and Luger, K. (2001). Structure of the yeast nucleosome core particle reveals fundamental changes in internucleosome interactions. Embo J *20*, 5207-18.

Widom, J. (2001). Role of DNA sequence in nucleosome stability and dynamics. Q Rev Biophys *34*, 269-324.

Widom, J. (1998). Structure, Dynamics, and function of chromatin in vitro. Annu. Rev. Biophys. *27*, 285-387.

Winter, E., and Varshavsky, A. (1989). A DNA binding protein that recognizes oligo(dA).oligo(dT) tracts. Embo J *8*, 1867-77.

Wolffe, A. (1998). Chromatin: Structure and Function, third edition Edition: Academic Press).

Workman, J. L., and Kingston, R. E. (1998). Alteration of nucleosome structure as a mechanism of transcriptional regulation. Annu Rev Biochem *67*, 545-79.

Wyrick, J. J., Holstege, F. C., Jennings, E. G., Causton, H. C., Shore, D., Grunstein, M., Lander, E. S., and Young, R. A. (1999). Chromosomal landscape of nucleosome-dependent gene expression and silencing in yeast. Nature *402*, 418-21.

Yager, T. D., van Holde, K. E. (1984). Dynamics and equilibria of nucleosomes at elevated ionic strength. Journal of Biological Chemistry *259*.

Yang, W., Wang, H., and Fliegel, L. (1996). Regulation of Na+/H+ exchanger gene expression. Role of a novel poly(dA.dT) element in regulation of the NHE1 promoter. J Biol Chem *271*, 20444-9.

Zhang, Y., Reinberg, D. (2001). Transcription regulation by histone methylation: interplay between different covalent modifications of the core histone tails. Genes Dev. *15*, 2343-2360.

Zhang, Y., LeRoy, G., Seelig, H. P., Lane, W. S., and Reinberg, D. (1998). The dermatomyositis-specific autoantigen Mi2 is a component of a complex containing histone deacetylase and nucleosome remodeling activities [In Process Citation]. Cell *95*, 279-89.

Zheng, C., and Hayes, J. J. (2003). Intra- and inter-nucleosomal protein-DNA interactions of the core histone tail domains in a model system. J Biol Chem *15*, 15.

Zhou, P., Szczypka, M. S., Sosinowski, T., and Thiele, D. J. (1992). Expression of a yeast metallothionein gene family is activated by a single metalloregulatory transcription factor. Mol Cell Biol *12*, 3766-75.

Zhou, P., and Thiele, D. J. (1993). Copper and gene regulation in yeast. Biofactors *4*, 105-15.

Zhu, Z., and Thiele, D. J. (1996). A specialized nucleosome modulates transcription factor access to a C. glabrata metal responsive promoter. Cell *87*, 459-70.